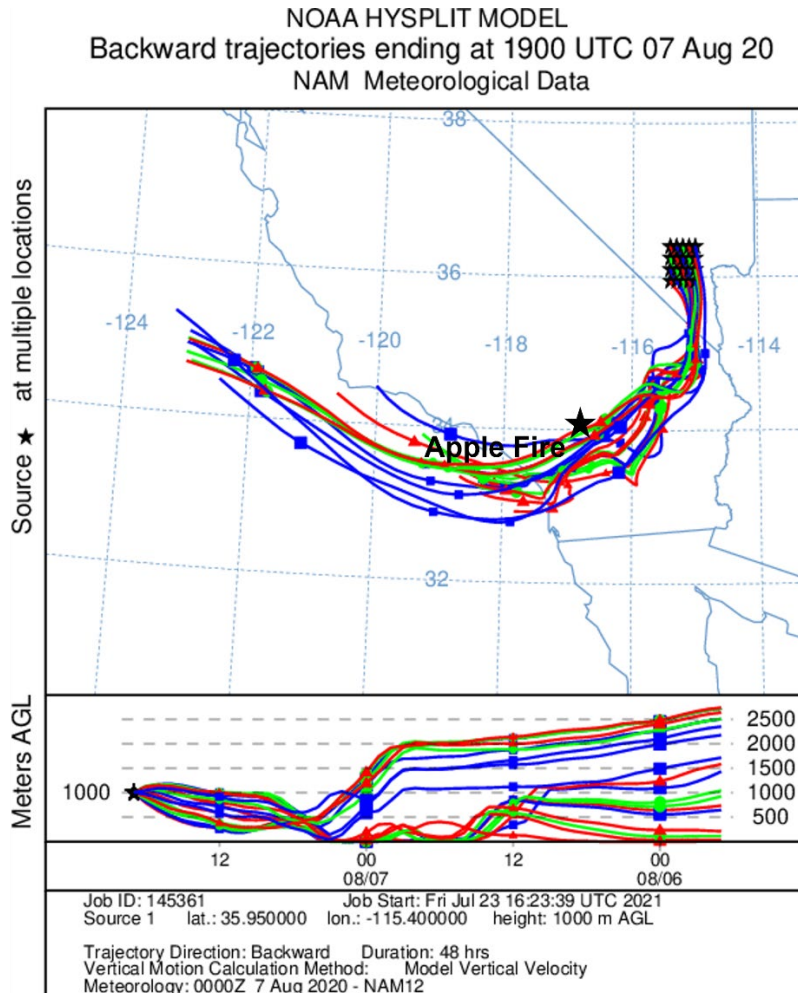


Exceptional Event Demonstration for Ozone Exceedances in Clark County, Nevada – August 7, 2020



Final Report Prepared for

U.S. EPA Region 9
San Francisco, CA

September 2021

This document contains blank pages to accommodate two-sided printing.



Exceptional Event Demonstration for Ozone Exceedances in Clark County, Nevada – August 7, 2020

Prepared by

Steve Brown, PhD
Crystal McClure, PhD
Cari Gostic
David Miller, PhD
Nathan Pavlovic
Charles Scarborough
Ningxin Wang, PhD

Sonoma Technology
1450 N. McDowell Blvd., Suite 200
Petaluma, CA 94954
Ph 707.665.9900 | F 707.665.9800
sonomatech.com

Prepared for

Clark County Department of Environment
and Sustainability
Division of Air Quality
4701 W. Russell Road, Suite 200
Las Vegas, NV 89118
Ph 702.455.3206
www.clarkcountynv.gov

Final Report
STI-920053-7477

September 1, 2021

Cover graphic illustrates the transport from the Apple Fire to Clark County, Nevada. See Section 3.1.3 for more information.

Contents

Contents.....	iii
Figures	iv
Tables.....	vii
Executive Summary.....	1
1. Overview.....	1-1
1.1 Introduction.....	1-1
1.2 Exceptional Event Rule Summary.....	1-3
1.3 Demonstration Outline.....	1-4
1.4 Conceptual Model.....	1-7
2. Historical and Non-Event Model.....	2-1
2.1 Regional Description.....	2-1
2.2 Overview of Monitoring Network.....	2-3
2.3 Characteristics of Non-Event Historical Ozone Formation.....	2-6
3. Clear Causal Relationship Analyses	3-1
3.1 Tier 1 Analyses.....	3-1
3.1.1 Comparison of Event with Historical Data	3-1
3.1.2 Ozone, Fire, and Smoke Maps.....	3-4
3.1.3 HYSPLIT Trajectories	3-12
3.1.4 Media Coverage and Ground Images.....	3-24
3.2 Tier 2 Analyses.....	3-26
3.2.1 Key Factor #1: Q/d Analysis.....	3-26
3.2.2 Key Factor #2: Comparison of Event Concentrations with Non-Event Concentrations.....	3-32
3.2.3 Satellite Retrievals of Pollutant Concentrations.....	3-35
3.2.4 Supporting Pollutant Trends and Diurnal Patterns	3-39
3.3 Tier 3 Analyses.....	3-47
3.3.1 Total Column & Meteorological Conditions	3-47
3.3.2 Matching Day Analysis	3-53
3.3.3 GAM Statistical Modeling.....	3-58
3.4 Clear Causal Relationship Conclusions.....	3-78
4. Natural Event Unlikely to Recur.....	4-1
5. Not Reasonably Controllable or Preventable	5-1
6. Public Comment.....	6-1
7. Conclusions and Recommendations	7-1
8. References.....	8-1

Figures

- 2-1. Regional topography around Clark County, with an inset showing the county boundaries and the air quality monitoring sites analyzed in this report.....2-2
- 2-2. Clark County topography, with an inset showing air quality monitoring sites that measure ozone in the Clark County area.....2-3
- 2-3. Time series of 2015-2020 ozone concentrations at the Walter Johnson site.....2-7
- 2-4. Time series of 2015-2020 ozone concentrations at the Joe Neal site.....2-8
- 2-5. Time series of 2015-2020 ozone concentrations at the Indian Springs site.....2-9
- 2-6. Seasonality of 2015-2020 ozone concentrations from the Walter Johnson site.....2-10
- 2-7. Seasonality of 2015-2020 ozone concentrations from the Joe Neal site.....2-11
- 2-8. Seasonality of 2015-2020 ozone concentrations from the Indian Springs site.....2-12
- 2-9. Ozone time series at all monitoring sites.....2-13
- 3-1. Time series of 2020 MDA8 ozone concentrations from the Walter Johnson site.....3-1
- 3-2. Time series of 2020 MDA8 ozone concentrations from the Joe Neal site.....3-2
- 3-3. Time series of 2020 MDA8 ozone concentrations from the Indian Springs site.....3-2
- 3-4. Maps showing the daily ozone AQI for the August 7 event and the three days before the event.....3-4
- 3-5. Maps showing the daily PM_{2.5} AQI levels for the August 7 event and the three days before the event.....3-5
- 3-6. Daily HMS Smoke for August 4 to August 7, 2020.....3-7
- 3-7. Daily HMS Smoke over the southwestern U.S. for August 4 to August 7, 2020.....3-8
- 3-8. Visible satellite imagery over southern California, Nevada, and Arizona on August 4, 2020.3-9
- 3-9. Visible satellite imagery over southern California, Nevada, and Arizona on August 5, 2020.3-10
- 3-10. Visible satellite imagery over southern California, Nevada, and Arizona on August 6, 2020....3-11
- 3-11. Visible satellite imagery over southern California, Nevada, and Arizona on August 7, 2020.3-12
- 3-12. HYSPLIT back trajectories with HMS smoke from downtown Las Vegas, ending on August 7, 2020.3-16
- 3-13. HYSPLIT back trajectories with HMS smoke on August 6 (grey) and August 7 (orange) from downtown Las Vegas, ending on August 7, 2020.....3-17
- 3-14. High-resolution HYSPLIT back trajectories from downtown Las Vegas.....3-18
- 3-15. High-resolution HYSPLIT back trajectories from the Indian Springs site.....3-19

3-16. 48-hour, NAM HYSPLIT back trajectory matrix initiated on August 7 at 19:00 UTC (11:00 a.m. local time) from downtown Las Vegas at 500 m and 1,000 m above ground level..... 3-20

3-17. 48-hour, NAM frequency HYSPLIT back trajectories initiated on August 7 at 19:00 UTC (11:00 a.m. local time) from downtown Las Vegas at 500 m above ground level..... 3-21

3-18. 48-hour, NAM frequency HYSPLIT back trajectories initiated for August 6 from downtown Las Vegas at 500 m above ground level..... 3-22

3-19. 32-hour, NAM forward HYSPLIT trajectory matrix initiated on August 6 at 22:00 UTC (August 6 2:00 p.m. local time) from the Apple Fire at 500 m, 750 m, and 1000 m, and 1500 m above ground level..... 3-23

3-20 A Facebook post added by the Clark County Department of Environment and Sustainability on August 5, 2020, reporting lingering impacts of smoke from the Apple Fire on ozone levels in the Las Vegas area..... 3-24

3-21. Clark County visibility images from August 7, 2020..... 3-25

3-22. Visibility images taken from webcams set up in Clark County on a clear day (May 21, 2020)..... 3-26

3-23. Large fires burning on August 7, 2020, in the vicinity of Clark County are shown in red..... 3-28

3-24. Q/d analysis. 24-hour back trajectories are shown as solid or dotted lines..... 3-31

3-25. MAIAC MODIS Aqua/Terra combined AOD retrievals for the three days before the EE, during the EE on August 7, and the day after the EE. 3-37

3-26. A zoomed-in view over Clark County and the Apple Fire of the MAIAC MODIS Aqua/Terra combined AOD retrieval two days before the EE and during the EE on August 7, 2020. 3-38

3-27. Hourly concentrations of ozone, PM_{2.5}, NO_x, and TNMOC..... 3-40

3-28. August 7 diurnal profile of ozone and PM_{2.5} (solid), and the five-year seasonal (May-Sept.) average (dotted) at sites in exceedance on August 7, 2020..... 3-41

3-29. Diurnal profile of ozone (red) and PM_{2.5} (blue) concentrations at the Walter Johnson site, including concentrations on August 7 (solid) and the seasonal (May-Sept.) average (dotted)..... 3-42

3-30. Diurnal profile of ozone (red) and PM_{2.5} (blue) concentrations at the Joe Neal site, including concentrations on August 7 (solid) and the seasonal (May-Sept.) average (dotted)..... 3-43

3-31. Ozone (red) and CO (green) concentrations for the Joe Neal site on August 7..... 3-44

3-32. Ozone and NO₂ concentrations during the August 7 EE at Joe Neal. 3-45

3-33. Daily upper-level meteorological maps for the three days leading up to the EE and during the August 7 EE..... 3-48

3-34. Time series of mixing heights taken from the Jerome Mack site (NCore site) for two weeks before and after the August 7 EE day..... 3-49

3-35. Daily surface meteorological maps for the three days leading up to the EE and during the August 7 EE..... 3-50

3-36. Skew-T diagrams from August 4 and 5, 2020, in Las Vegas, Nevada. 3-51

3-37. Skew-T diagrams from August 6 and 7, 2020 (local time), in Las Vegas, Nevada..... 3-52

3-38. Clusters for 2014-2020 back trajectories..... 3-60

3-39. Exceptional event vs. non-exceptional event residuals. 3-65

3-40. Daily GAM residuals for 2014-2020 vs GAM Fit (Predicted) MDA8 Ozone values..... 3-68

3-41. Histogram of GAM residuals at all modeled Clark County monitoring sites..... 3-69

3-42. GAM cluster residual results for 18:00 UTC..... 3-70

3-43. GAM cluster residual results for 22:00 UTC..... 3-71

3-44. Observed MDA8 ozone vs. GAM fit ozone by year..... 3-72

3-45. April–May Interannual GAM Response. 3-73

3-46. GAM MDA8 Fit versus Observed MDA8 ozone data from 2014 through 2020 for the EE
affected sites on August 7, 2020. 3-74

3-47. GAM time series showing observed MDA8 ozone for two weeks before and after the
August 7 EE (solid lines)..... 3-77

Tables

1-1. August 7, 2020, EE information..... 1-2

1-2. Proposed Clark County 2018 EEs..... 1-2

1-3. Proposed Clark County 2020 EEs..... 1-3

1-4. Tier 1, 2, and 3 EE analysis requirements for evaluating wildfire impacts on ozone exceedances. 1-4

1-5. Locations of Tier 1, 2, and 3 elements in this report..... 1-5

2-1. Clark County monitoring site data..... 2-5

3-1. Ozone season non-event comparison..... 3-3

3-2. HYSPLIT run configurations for each analysis type, including meteorology data set, time period of run, starting location(s), trajectory time length, starting height(s), starting time(s), vertical motion methodology, and top of model height. 3-14

3-3. Fire data for the Apple Fire associated with the August 7 EE..... 3-29

3-4. Daily growth, emissions, and Q/d for the Apple Fire..... 3-32

3-5. Six-year percentile ozone.. 3-33

3-6. Six-year, ozone-season percentile ozone. The August 7 EE ozone concentration at each site is calculated as a percentile of the last six years' ozone season (May-September) with and without other 2018 and 2020 EEs included in the historical record..... 3-33

3-7. Site-specific ozone design values for the Walter Johnson monitoring site. 3-34

3-8. Site-specific ozone design values for the Joe Neal monitoring site..... 3-34

3-9. Site-specific ozone design values for the Indian Springs monitoring site. 3-34

3-10. Two-week non-event comparison..... 3-35

3-11. Levoglucosan concentrations at monitoring sites around Clark County, Nevada, before and after the August 7 ozone event. 3-46

3-12. Local meteorological parameters and their data sources..... 3-54

3-13. Percentile rank of meteorological parameters on May 6, 2020, compared to the 30-day period surrounding August 7 over seven years (July 23 through August 22, 2014-2020). 3-56

3-14. Top 14 matching meteorological days to August 7, 2020. 3-57

3-15. GAM variable results..... 3-62

3-16. Overall 2014-2020 GAM median residuals and 95% confidence interval range in square brackets for each site modeled..... 3-64

3-17. GAM high ozone, non-smoke case study results. 3-67

3-18. August 7 GAM results and residuals for each site..... 3-76

3-19. Results for each tier analysis for the August 7 EE..... 3-79

Executive Summary

On August 7, 2020, Clark County experienced an atypical episode of elevated ambient ozone. During this episode, the 2015 8-hr ozone National Ambient Air Quality Standards (NAAQS) threshold was exceeded at the Walter Johnson, Joe Neal, and Indian Springs monitoring sites. The exceedance at the Walter Johnson and Joe Neal sites could lead to an ozone nonattainment designation for the Clark County area. Air trajectory analysis and air quality modeling results show that emissions from a wildfire burning in southern California contributed to the transport to and formation of ozone in Clark County. The U.S. Environmental Protection Agency (EPA) Exceptional Event Rule (U.S. Environmental Protection Agency, 2016) allows air agencies to omit air quality data from the design value calculation if it can be demonstrated that the measurement in question was caused by an exceptional event. This report describes analyses that help to establish a clear causal relationship between wildfire smoke and the August 7, 2020, ozone exceedances at all three monitoring sites.

The analyses we conducted provide evidence supportive of wildfire smoke and impacts on ozone concentrations in Clark County. We show that (1) smoke was transported from a wildfire in southern California to the surface in the Clark County area in the hours leading up to the exceedance date and on the exceedance date; (2) wildfire smoke impacted the typical diurnal profiles of ground-level pollution measurements, including PM_{2.5}, CO, and NO₂, in the Clark County area on August 6-7; (3) byproducts and tracers of wildfire combustion were present and elevated at the surface in the Clark County area on August 7, the day of the ozone exceedance; and (4) meteorological regression modeling and similar meteorological day analysis show that ozone observations on August 7 were unusual in the historical record given the meteorological conditions. Sources of evidence used in these analyses include (1) air quality monitor data to show that supporting pollutant trends at the surface were influenced by wildfire smoke; (2) air trajectory analysis to show transport of smoke-laden air to the Clark County area; (3) media coverage of wildfires and smoke impacts; and (4) meteorological regression modeling and meteorologically similar day analysis.

EPA guidance for exceptional event demonstrations (U.S. Environmental Protection Agency, 2016) provides a three-tiered approach. Depending on the complexity of the event, increasingly involved information may be required to demonstrate a causal relationship between wildfire smoke and an exceedance. Here, we provide the results of analyses conducted to address Tier 1, Tier 2, and Tier 3 exceptional event demonstration requirements.

These analyses show that smoke was transported from a wildfire in southern California to the Clark County area over the hours leading up to the August 7 ozone exceedance. Combined with additional evidence, such as meteorological regression modeling and meteorologically similar day analysis, our results provide key evidence to support smoke impacts on ozone concentrations in Clark County on August 7, 2020.

1. Overview

1.1 Introduction

The 2020 wildfire season in California was unprecedented, with five of the six largest wildfires in California history occurring in either August or September 2020 (https://www.fire.ca.gov/media/11416/top20_acres.pdf). Smoke emissions from California wildfires can affect downwind areas, including Clark County, Nevada. This was the case on August 7, 2020, as smoke emissions from the rapidly growing Apple Fire in southern California reached Clark County. On this date, 3 of the 14 ozone (O₃) monitoring locations around Clark County recorded an exceedance of the 2015 National Ambient Air Quality Standard (NAAQS) for 8-hour ozone (0.070 ppm).

Emissions from wildfires can affect concentrations of ozone downwind by direct transport of both ozone and precursor gases (i.e., nitrogen oxides [NO_x] and volatile organic compounds [VOCs]). Each mechanism can cause an enhancement in the overall ozone concentration and/or the amount of ozone that could be produced. For example, in an area where NO_x concentrations are high, such as an urban area like Las Vegas, Nevada, the transport of VOCs from wildfire emissions can enhance the amount of ozone that can be produced, potentially driving concentrations above the ozone standard. According to U.S. Environmental Protection Agency's (EPA) exceptional event (EE) guidance (U.S. Environmental Protection Agency, 2016), EEs such as wildfires that affect ozone concentrations can be subject to exclusion from calculations of NAAQS attainment if a clear causal relationship can be established between a specific event and the monitoring exceedance.

This report describes the clear causal relationship between the Apple Fire in southern California and the exceedance of the maximum daily 8-hour ozone average (MDA8) at the three monitoring sites in Clark County on August 7, 2020. The evidence in this report includes all three tiers of analysis required by EPA's EE guidance: for Tier 1, ground and satellite-based measurement of smoke emissions, transport of smoke from the Apple Fire to Clark County, and media coverage of the smoke event in Clark County; for Tier 2, emission vs. distance analysis, ground and satellite analysis of smoke-related pollutants, and comparison of event and non-event concentrations; and for Tier 3, vertical column analyses and Generalized Additive Statistical Modeling (GAM) of the event. The wildfire that affected ozone concentrations in Clark County could not be reasonably controlled or prevented because it was caused by accidental ignition and is unlikely to recur. [Table 1-1](#) lists the sites affected during the August 7 event, as well as their locations and MDA8 ozone concentrations.

Table 1-1. August 7, 2020, EE information. All monitoring sites in Clark County that exceeded the 2015 NAAQS standard on August 7, 2020, are listed along with AQS Site Codes, location information, and MDA8 ozone concentrations.

AQS Site Code	Site Name	Latitude (degrees N)	Longitude (degrees W)	MDA8 Ozone Concentration (ppb)
320030071	Walter Johnson	36.170	-115.263	71
320030075	Joe Neal	36.271	-115.238	72
320037772	Indian Springs	36.569	-115.677	72

Concurrent with this document, Clark County is submitting documentation for other ozone EEs in 2018 and 2020 that were caused by wildfires and stratospheric intrusions. These events are mentioned throughout this report and are referred to as “proposed 2018 and 2020 EEs,” recognizing that discussion with EPA is still pending. All proposed EEs for Clark County in 2018 and 2020 are listed in [Tables 1-2 and 1-3](#). Wherever possible, we calculated statistics to provide context that both includes and excludes the proposed EEs from 2018 and 2020.

Table 1-2. Proposed Clark County 2018 EEs. For each site and date combination where the 2015 NAAQS standard was exceeded, the MDA8 ozone concentration is shown in parts per billion (ppb). Blank cells indicate that there was no exceedance on that site/date combination.

Date	Paul Meyer	Walter Johnson	Green Valley	Jerome Mack	Joe Neal	Palo Verde	Jean	Indian Springs	Apex	Boulder City
6/19/2018	72	72	77	75						
6/20/2018	71	74			72					
6/23/2018	72	76	75	72	72	71	77	73		
6/27/2018	75	76	78	76	72	72	81	78	74	72
7/14/2018	72		78	78						
7/15/2018		71	73	73	78					
7/16/2018	75	79	71	73	80	75				
7/17/2018	74	77				74				
7/25/2018	71	72	72							
7/26/2018	72	75	77	77					71	
7/27/2018	72	74			76					
7/30/2018			73	72						
7/31/2018		73			73					
8/6/2018	79	77	74	71	76	72			74	
8/7/2018	73	74	72	71	74				71	

Table 1-3. Proposed Clark County 2020 EEs. For each site and date combination where the 2015 NAAQS standard was exceeded, the MDA8 ozone concentration is shown in ppb. Blank cells indicate that there was no exceedance on that site/date combination.

Date	Walter Johnson	Paul Meyer	Joe Neal	Jerome Mack	Green Valley	Boulder City	Jean	Indian Springs	Apex
5/6/2020	78	77	76	73	72		75		76
5/9/2020	71	74							
5/28/2020	71	76							
6/22/2020	73	74	78						
6/26/2020		73							
8/3/2020	82	78	81		72	72	73	71	
8/7/2020	71		72					72	
8/18/2020	82	79	78						
8/19/2020	74	74	73		71				
8/20/2020			71						
8/21/2020		71							
9/2/2020	75	73							
9/26/2020	71		75						

1.2 Exceptional Event Rule Summary

The “EPA Guidance on the Preparation of Exceptional Events Demonstration for Wildfire Events that May Influence Ozone Concentrations” (U.S. Environmental Protection Agency, 2016) describes a three-tier analysis approach to determine a “clear causal relationship” for EEs demonstrations from an air agency. A summary of analysis requirements for each tier is listed in [Table 1-4](#), and in the list below.

- Tier 1 analyses can be used when ozone exceedances are clearly influenced by a wildfire in areas of typically low ozone concentrations, are associated with ozone concentrations higher than non-event-related values, or occur outside of an area’s usual ozone season.
- Tier 2 analyses are appropriate for wildfire emission cases where the impacts of the wildfire on ozone levels are less clear and require more supportive documentation than Tier 1 analyses.
- If a more complicated relationship between the wildfire and the ozone exceedance is observed, Tier 3 analyses with additional supportive documentation—such as statistical modeling of the ozone event, vertical profile analysis of smoke in the column, and meteorological analysis—should be used.

In this work, we conduct all the recommended Tier 1, Tier 2 and Tier 3 analyses.

Table 1-4. Tier 1, 2, and 3 EE analysis requirements for evaluating wildfire impacts on ozone exceedances.

Tier	Requirements
1	<ul style="list-style-type: none"> • Comparison of fire-influenced exceedance with historical concentrations • Key factor: Evidence that fire and monitor meet one of the following criteria: <ul style="list-style-type: none"> – Seasonality differs from typical season, or – Ozone concentrations are 5-10 ppb higher than non-event-related concentrations • Evidence of transport of fire emissions to monitor: <ul style="list-style-type: none"> – Trajectories of fire emissions (reaching ground level) – Satellite images and supporting evidence from surface measurements – Media coverage and photographic evidence of smoke
2	<ul style="list-style-type: none"> • All Tier 1 requirements • Key Factor #1: Fire emissions and distance of fires • Key Factor #2: Comparison of the event-related ozone concentration, with non-event-related high ozone concentrations (high percentile rank over five years/seasons) <ul style="list-style-type: none"> – Annual and seasonal comparison • Evidence that fire emissions affected the monitor (at least one of the following): <ul style="list-style-type: none"> – Visibility impacts – Changes in supporting measurements – Satellite enhancements of fire-related species (i.e., NO_x, carbon dioxide (CO), aerosol optical depth (AOD), etc.) – Fire-related enhancement ratios and/or tracer species – Differences in spatial/temporal patterns
3	<ul style="list-style-type: none"> • All Tier 2 requirements • Evidence of fire emissions effects on monitor: <ul style="list-style-type: none"> – Multiple analyses from those listed for Tier 2 • Evidence of fire emissions transport to the monitor: <ul style="list-style-type: none"> – Trajectory or satellite plume analysis, and – Additional discussion of meteorological conditions • Additional evidence such as: <ul style="list-style-type: none"> – Comparison to ozone concentrations on matching (meteorologically similar) days – Statistical regression modeling – Photochemical modeling of smoke contributions to ozone concentrations

1.3 Demonstration Outline

As discussed in Section 1.2, the “clear causal relationship” analyses involve first comparing the exceedance ozone concentrations to historical values, providing evidence that the event and monitors meet the tier’s key factors, providing evidence of the transport of wildfire emissions to the

monitors, and additional analyses such as ground-level measurements and various forms of modeling depending on the complexity of the event. [Table 1-5](#) summarizes the key factors and additional supporting evidence of the tiered approach and shows the corresponding sections in this report for each analysis.

Table 1-5. Locations of Tier 1, 2, and 3 elements in this report.

Tier	Element	Section of This Report (Analysis Type)
Tier 1	Key Factor: seasonality differs from typical season and/or ozone concentrations are 5-10 ppb higher than non-event-related concentrations	Section 3.1.1 (comparison of event with historical data)
	Evidence of transport of fire emissions to monitor	Sections 3.1.2 (maps of ozone, particulate matter with a diameter less than 2.5 micrometers (PM _{2.5}), fire, smoke, visible satellite imagery), and 3.1.3 (Hybrid Single-Particle Lagrangian Integrated Trajectory [HYSPLIT] trajectories)
	Media coverage and photographic evidence of smoke	Section 3.1.4 (Media coverage and Images)
Tier 2	Key Factor #1: fire emissions and distance of fires	Section 3.2.1 (analysis of the relationship between fire emissions and distance [Q/d])
	Key Factor #2: comparison of event concentrations with non-event-related high ozone concentrations	Section 3.2.2 (comparison of event concentrations with non-event concentrations)
	Evidence that the fire emissions affected the monitor	Sections 3.2.3 (Satellite Retrievals of Pollutant Concentrations) and 3.2.4 (changes in supporting measurements, differences in spatial/temporal patterns, and tracer measurements)
Tier 3	Evidence of fire emissions transport to the monitor	Section 3.3.1 (trajectory or satellite plume analysis, additional discussion of meteorological conditions, comparison to ozone concentrations on matching [meteorologically similar] days)
	Meteorologically similar matching day analysis	Section 3.3.2 (methodology and analysis for meteorologically similar days)
	Additional evidence	Section 3.3.3 (statistical regression modeling)

Tier 1 analyses are shown in Section 3.1. The key factor of Tier 1 analyses is the ozone concentration's uniqueness when compared to the typical seasonality and/or levels of ozone exceedance. The EPA guidance suggests providing a time series plot of 12 months of ozone concentrations overlaying more than five years of monitored data and describing how typical seasonality differs from ozone in the demonstration (U.S. Environmental Protection Agency, 2016). In addition, trajectory analysis—produced by the Hybrid Single-Particle Lagrangian Integrated Trajectory (HYSPLIT) model, together with satellite plume imagery and ground-level measurements of plume components (e.g., PM_{2.5}, CO, or organic and elemental carbon)—should be used to provide evidence of wildfire emissions being transported to the monitoring sites. We demonstrate the Tier 1 analysis results for the August 7, 2020, event in Section 3.1. We address the key factors in Section 3.1.1, provide evidence of wildfire smoke transport to the Clark County monitoring sites in Sections 3.1.2 and 3.1.3, and discuss the media coverage and show ground images in Section 3.1.4.

Tier 2 analyses are shown in Section 3.2. The two key factors for Tier 2 analyses are (1) fire emissions and distance of fires to the impacted monitoring sites, and (2) comparison of event-related ozone concentrations with non-event-related high ozone values. We address the first factor in Section 3.2.1 by determining the emissions divided by distance (Q/d) relationship and address the second factor in Section 3.2.2 by comparing the five-year percentiles and yearly rank-order analysis of ozone concentrations. The Tier 2 analyses also require evidence of wildfire smoke transport to affected monitoring sites; we provide this evidence in Section 3.2.3 through satellite measurements of pollutant concentrations. In Section 3.2.4, we discuss supporting pollutant trends and diurnal patterns of PM_{2.5}, CO, NO_x, and total non-methane organic compounds (TNMOC) compared with ozone concentrations and wildfire tracer measurements.

Tier 3 analyses are shown in Section 3.3. We investigated total column information and event-related meteorological conditions (Section 3.3.1), analyzed meteorologically similar days to find typical ozone concentrations for the exceptional event's specific meteorological conditions (Section 3.3.2), and developed a Generalized Additive Statistical Model (GAM) to estimate the wildfire's contribution to ozone concentrations (Section 3.3.3).

Following the EPA's EE guidance, we performed Tier 1, Tier 2, and Tier 3 analyses to show the "clear causal relationship" between the Apple Fire in southern California and the exceedance event in Clark County on August 7, 2020. Focusing on the characterization of the meteorology, smoke, transport, and air quality on the days leading up to the event, we conducted the following specific analyses (results of these analyses are presented in Section 3):

- Developed time series plots that show the August 7 ozone concentrations at each affected monitoring site in historical context for 2020 and the past five years
- Compiled maps of (1) ozone and PM_{2.5} concentrations in the area, (2) smoke plumes, and (3) fire locations from satellite data
- Showed the transport patterns via HYSPLIT modeling, and identified where the back trajectory air mass intersected with smoke plumes or passed over or near fires

- Discussed media coverage of the August 7 event and showed ground images
- Quantified total fire emissions and calculated emissions/distance ratio (Q/d) for the fire
- Performed statistical analysis to compare event ozone concentrations to non-event concentrations
- Provided maps showing satellite retrievals of NO_x, AOD, and CO
- Developed plots to show diurnal patterns of ozone and supporting pollutants such as PM_{2.5}, CO, NO_x, and TNMOC
- Examined wildfire tracer species and their background concentrations vs. event concentrations
- Assessed vertical transport of smoke using satellite-observed aerosol vertical profiles and ceilometer mixing height retrievals
- Performed meteorologically similar matching ozone day analysis to assess typical concentrations of ozone given meteorological parameters
- Created a GAM model of MDA8 ozone concentrations to assess the enhancement of ozone concentrations due to wildfire influence

1.4 Conceptual Model

The conceptual model for the exceptional event that led to the ozone exceedances at the Walter Johnson, Joe Neal, and Indian Springs monitoring sites on August 7, 2020, is outlined in Table 1-5. Table 1-5 provides the analysis techniques performed and evidence for each Tier. This establishes a weight of evidence for the clear causal relationship between the wildfire emissions in southern California and the August 7 exceptional ozone event. We assert that wildfire emissions on August 6 from the Apple Fire in southern California led to enhanced ozone concentrations in Clark County on August 7 and the MDA8 ozone exceedances at the Walter Johnson, Joe Neal, and Indian Springs sites. In support of this assertion, the key points of evidence for the conceptual model are summarized below.

1. The August 7 ozone exceedance occurred during a typical ozone season, but event concentrations at the Walter Johnson, Joe Neal, and Indian Springs exceedance sites were significantly higher than non-event concentrations. Ozone concentrations at all exceedance sites showed a high percentile rank when compared with the ozone seasons over the past six years.
2. HMS smoke and fire detections and aerosol optical depth observations show a consistent picture of wildfire emission plumes from the Apple Fire extending northeastward and impacting Clark County on August 6 and 7.
3. Back and forward trajectories from the near-surface boundary layer at the exceedance sites

at the time of maximum ozone concentration show consistent transport patterns passing over the HMS smoke plumes and region of enhanced aerosol optical depth originating from the Apple Fire. The combination of trajectories intersecting the fire location and the associated smoke plumes and a deep mixed layer over Clark County favoring vertical mixing demonstrate that wildfire emissions were transported to the surface in Clark County by August 6, 2020, the day prior to the exceedance event.

4. Meteorological conditions on August 7 did not favor enhanced local ozone production when compared with meteorologically similar ozone season days. Average MDA8 ozone across similar days was well below the ozone NAAQS and at least 10 ppb lower than the August 7 ozone exceedances.
5. GAM model predictions of MDA8 ozone on August 7 are all well below the 70-ppb ozone NAAQS for each EE-affected site. Using the 75th-95th quantile of positive residuals (observed MDA8 ozone minus GAM-predicted MDA8 ozone), we find a minimum wildfire effect on ozone of 1-13 ppb in Clark County from an atypical source; in this case, the Apple Fire in southern California.
6. Abnormal, coincident surface PM_{2.5}, CO, NO₂, and TNMOC concentration enhancements overnight prior to the exceedance event with typical PM₁₀:PM_{2.5} ratios, and August 7 enhancements of the wildfire tracer levoglucosan above background ozone season levels at two sites indicate the presence of wildfire emissions of ozone precursors at the surface in Clark County coincident with the wildfire plume arrival on August 6 and 7.

2. Historical and Non-Event Model

2.1 Regional Description

Clark County is located in the southern portion of Nevada and borders California and Arizona. Clark County includes the City of Las Vegas, which has a population of approximately 2 million and is one of the fastest growing metropolitan areas in the United States (U.S. Census Bureau, 2010). Las Vegas is located in a 1,600 km² desert valley basin at 500 to 900 m above sea level (Langford et al., 2015). It is surrounded by the Spring Mountains to the west (3,000 m elevation) and the Sheep Mountain Range to the north (2,500 m elevation), and three mountain ranges to the south. The valley floor slopes downward from west to east, which influences surface wind, temperature, precipitation, and runoff patterns. The Cajon Pass and I-15 corridor to the east is an important atmospheric transport pathway from the Los Angeles Basin into the Las Vegas Valley (Langford et al., 2015). [Figures 2-1 and 2-2](#) show the topography of the Clark County area and surrounding areas.

The Las Vegas Valley climatology features abundant sunshine and hot summertime temperatures, with average summer month high temperatures of 34-40°C. Because of the mountain barriers to moisture inflow, the region experiences dry conditions year-round (~107 mm annual precipitation, 22% of which occurs during the summer monsoon season in July through September). The urban heat island effect in Las Vegas during the summer leads to large temperature gradients within the valley, with generally cooler temperatures on the eastern side. During the summer season, monsoon moisture brings high humidity and thunderstorms to the region, typically in July and August (National Weather Service Forecast Office, 2020). Winds in the Las Vegas basin tend to be out of the southwest (from Los Angeles) during the spring and summer; winds in the fall and winter tend to be out of the northwest, with air transported between the neighboring mountain ranges and along the valley.

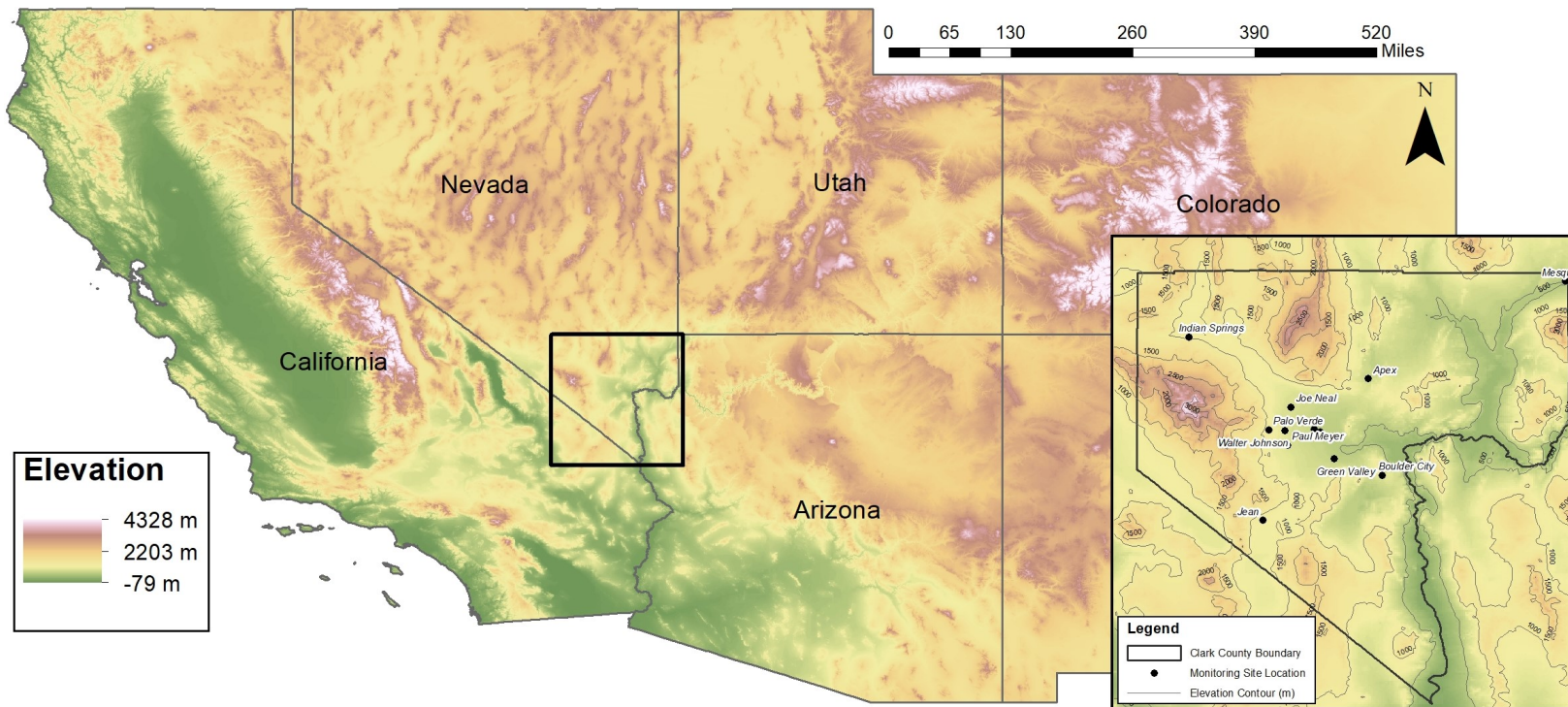


Figure 2-1. Regional topography around Clark County, with an inset showing the county boundaries and the air quality monitoring sites analyzed in this report.

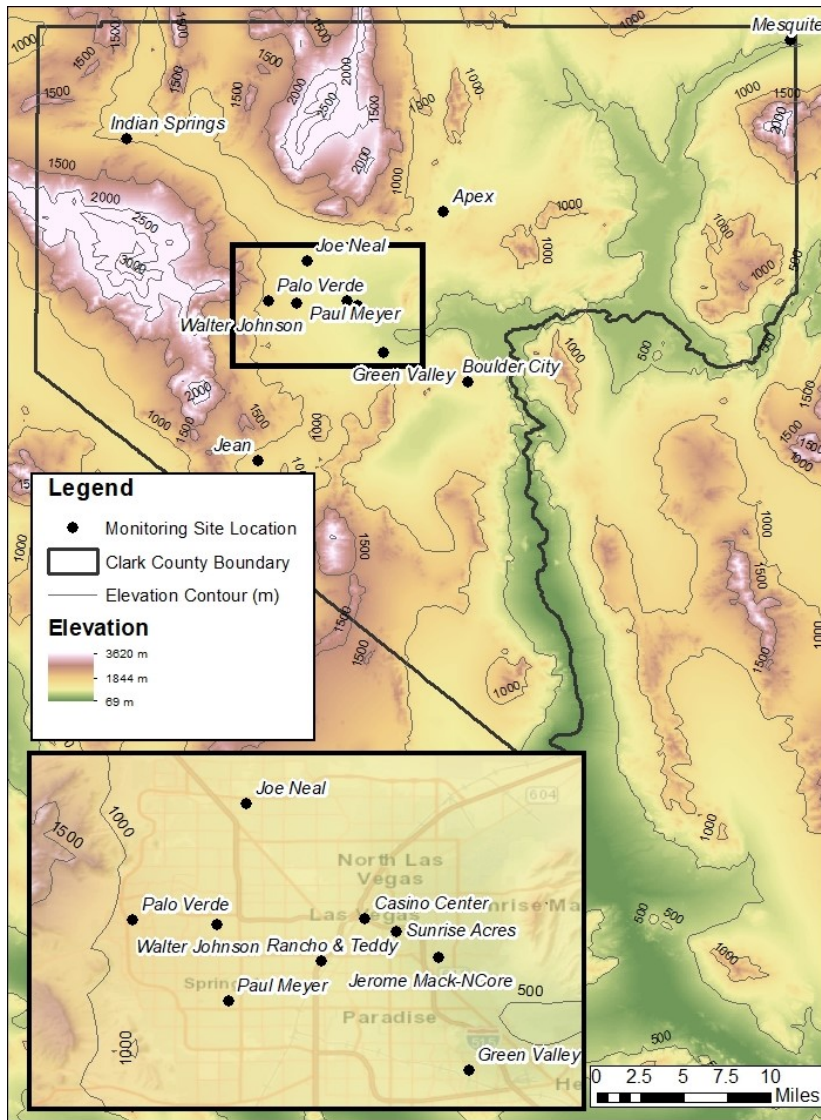


Figure 2-2. Clark County topography, with an inset showing air quality monitoring sites that measure ozone in the Clark County area.

2.2 Overview of Monitoring Network

The Clark County Department of Environment and Sustainability, Division of Air Quality (DAQ), operated 14 ambient air monitoring sites in the region during 2020 (shown in Figure 2-2). These sites measure hourly OZONE, PM_{2.5}, particulate matter with a diameter less than 10 micrometers (PM₁₀), NO_x, TNMOC, and CO concentrations along with meteorological parameters. Table 2-1 presents the monitoring data coverage across time and space for criteria pollutants and surface meteorological parameters (barometric pressure, temperature, wind speed, and direction), as well as mixing height.

We examined ozone and other criteria pollutants at 11 sites around Clark County to investigate the high ozone event observed on August 7, 2020. DAQ's ambient air monitoring network meets the monitoring requirements for criteria pollutants pursuant to Title 40, Part 58, of the Code of Federal Regulations (CFR), Appendix D (Code of Federal Regulations, 1997). Data are quality-assured in accordance with 40 CFR 58 and submitted to the EPA's Air Quality System (AQS). The spatial distribution of the monitoring sites characterizes the regional air quality in Las Vegas, as well as air quality upwind and downwind of the urban valley region (Figure 2-2). The Jean monitoring site along the I-15 corridor is generally upwind such that it captures atmospheric transport into the region and is least impacted by local sources.

Table 2-1. Clark County monitoring site data. The available date ranges of all parameters and monitoring sites used in this report are shown for Clark County, Nevada. Casino Center and RT are near-road sites that are not used for the exceptional event analysis.

Site	AQS Sitecode	O ₃	PM _{2.5}	CO	NO	NO ₂	TNMOC	Temp.	Wind Speed	Wind Direction	Barom. Pressure	Mixing Height
Apex	320030022	2014-2020						2014-2020	2014-2020	2014-2020		
Boulder City	320030601	2014-2020									2014-2016	
Green Valley	320030298	2015-2020	2014-2020	2020				2016-2020	2014-2020	2014-2020	2014-2016	
Indian Springs	320037772	2014-2020										
Jean	320031019	2014-2020	2014-2020					2014-2020	2014-2020	2014-2020	2014-2016	
Jerome Mack	320030540	2014-2020	2014-2020	2015-2020 ^{1,2}	2015-2020	2015-2020	2020	2014-2020	2014-2020	2014-2020	2014-2020	2020
Joe Neal	320030075	2020	2018-2020	2019-2020		2015-2020		2014-2020	2014-2020	2014-2020	2014-2016	
Mesquite	320030023	2014-2020						2014-2020	2014-2020	2014-2020		
Palo Verde	320030073	2014-2020	2020					2014-2020	2014-2020	2014-2020	2014-2016	
Paul Meyer	320030043	2014-2020	2017-2020					2014-2020	2014-2020	2014-2020	2014-2016	
Walter Johnson	320030071	2014-2020	2020					2015-2020	2015-2020	2015-2020	2014-2016	

¹CO data invalid at Jerome Mack on Sep. 2, 2020

²CO data invalid at Jerome Mack Apr. 28, 2020 – May 20, 2020

2.3 Characteristics of Non-Event Historical Ozone Formation

During the ozone season (April–September) in Clark County, ozone concentrations are typically influenced by local formation, transport into the region, and on occasion by EEs such as wildfires and stratospheric intrusions. Transport from upwind source regions (e.g., the Los Angeles Basin, Mojave Desert, Asia) occurs with southwesterly winds, and southerly transport dominates the later portion of the season due to the summer monsoon (Langford et al., 2015; Zhang et al., 2020). Local precursor emissions in Clark County include mobile NO_x and VOCs sources, natural gas fueled power generation NO_x sources, and biogenic VOC emissions. Based on 2017 Las Vegas emission inventories, on a typical ozone season weekday, there are 98 tons of NO_x emissions per day and 238 tons of VOC emissions per day (Clark County Department of Environment and Sustainability, 2020). On-road mobile sources comprise 40% of NO_x emissions and total mobile emissions comprise 88% of total NO_x emissions during the ozone season. In contrast, 52% of VOC emissions originate from biogenic sources within Clark County. Local emissions and/or precursors transported into the region contribute to ozone formation within Clark County (Langford et al., 2015; Clark County Department of Air Quality, 2019).

In this demonstration, we discuss the impacts of wildfire smoke on ozone concentrations in Clark County on August 7, 2020. In order to fully discern the effect of wildfire smoke on ozone concentrations in Clark County on this date, we examine the historical ozone record for all affected sites (see Table 1-1 in Section 1). *Non-event days* refer to all days other than the August 7 event. Because percentile rankings are sensitive to including the relatively large number of potential EE days during 2018 and 2020, we also provide statistics *excluding potential EE days* (i.e., without including the 2018 and 2020 potential EE days as defined in Tables 1-2 and 1-3 in Section 1). The 8-hour ozone design value (DV) is the three-year running average of the fourth-highest MDA8 ozone concentration (U.S. Environmental Protection Agency, 2015). Within Clark County, Las Vegas is classified as an EPA Region 9 marginal nonattainment region, with a 73 ppb ozone DV for 2017–2019 (U.S. Environmental Protection Agency, 2020). Ozone EE days are identified as days with significant wildfire or stratospheric intrusion influence in addition to an MDA8 concentration greater than 70 ppb. By this criterion, 15 possible EE days in 2018 and 13 possible EE days in 2020 were identified, with no EE days in 2019 identified.

The August 7, 2020, EE occurred late in the ozone season under hot, dry air, upper-level high pressure and surface low-pressure meteorological conditions. These conditions favor subsidence and enhanced vertical mixing of wildfire smoke-influenced ozone and precursors to ground level (see Section 3.3.1). Compared with a non-event conceptual model of local precursor emissions contributing to ozone formation at ground level under similar conditions, the August 7 conditions indicate additional transport of wildfire-influenced air parcels via southwesterly winds aloft.

Figures 2-3 through 2-8 depict the six-year historical record and seasonality of MDA8 ozone concentrations at each EE affected monitoring site, along with the 99th percentile and NAAQS standard ozone concentrations. August 7 ranks in the top 1% for daily maximum ozone concentration in the six-year historical record at the Indian Springs site. August 7 also ranks in the top 5% for MDA8 ozone during the ozone season at the Walter Johnson and Joe Neal sites.

Figure 2-9 depicts a two-week ozone diurnal cycle of 1-hour ozone, beginning one week before the August 7 event and ending one week after. On August 7, daily maximum 1-hour ozone concentrations were the second highest during this two-week period at each of the three EE affected sites (see Table 1-1).

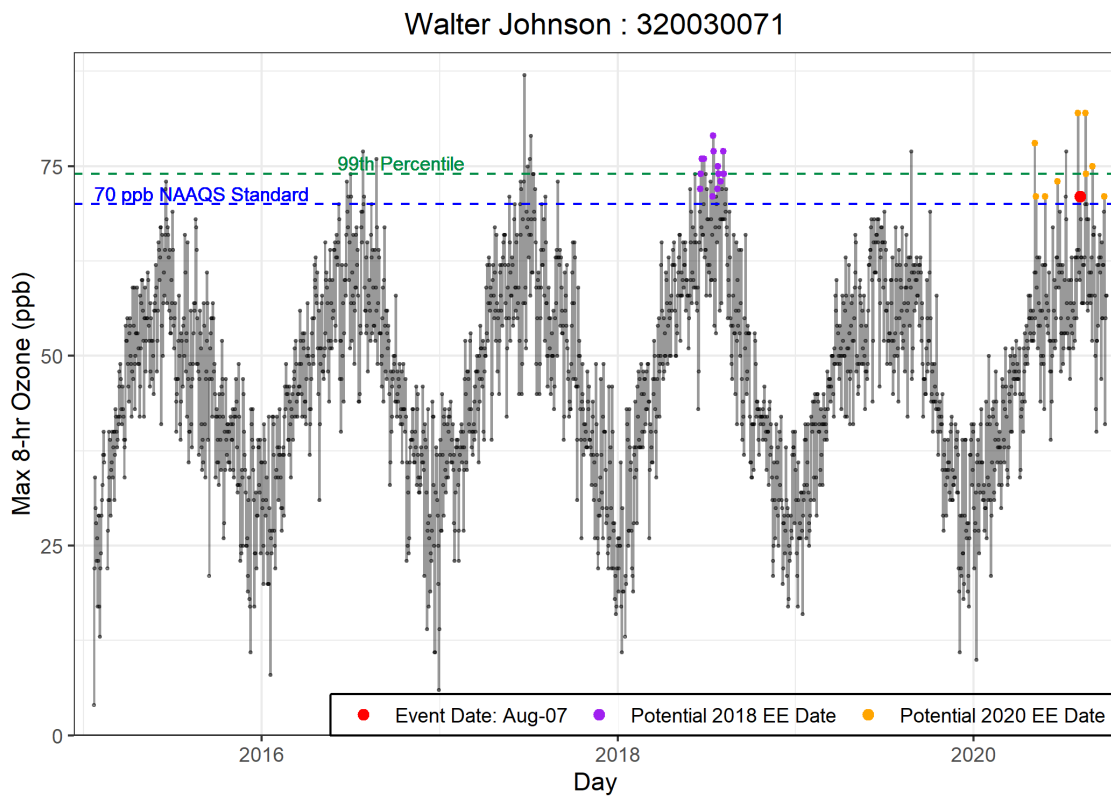


Figure 2-3. Time series of 2015-2020 ozone concentrations at the Walter Johnson site. August 7, 2020, is shown in red.

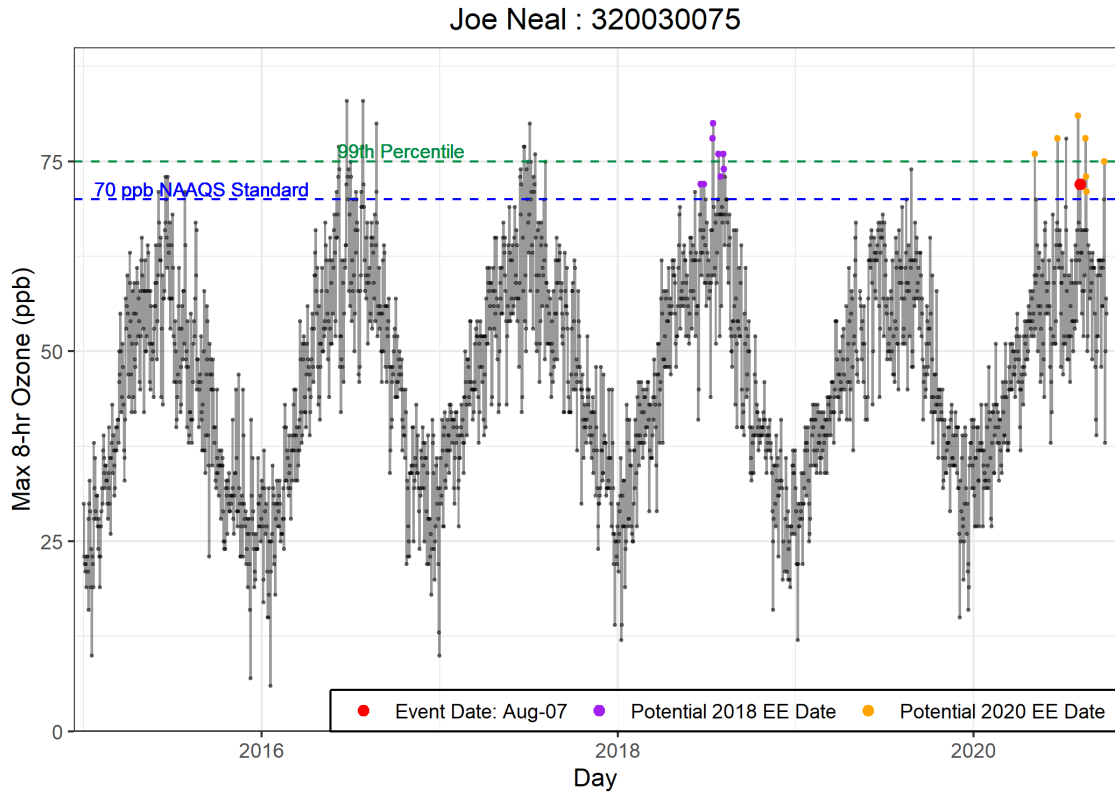


Figure 2-4. Time series of 2015-2020 ozone concentrations at the Joe Neal site. August 7, 2020, is shown in red.

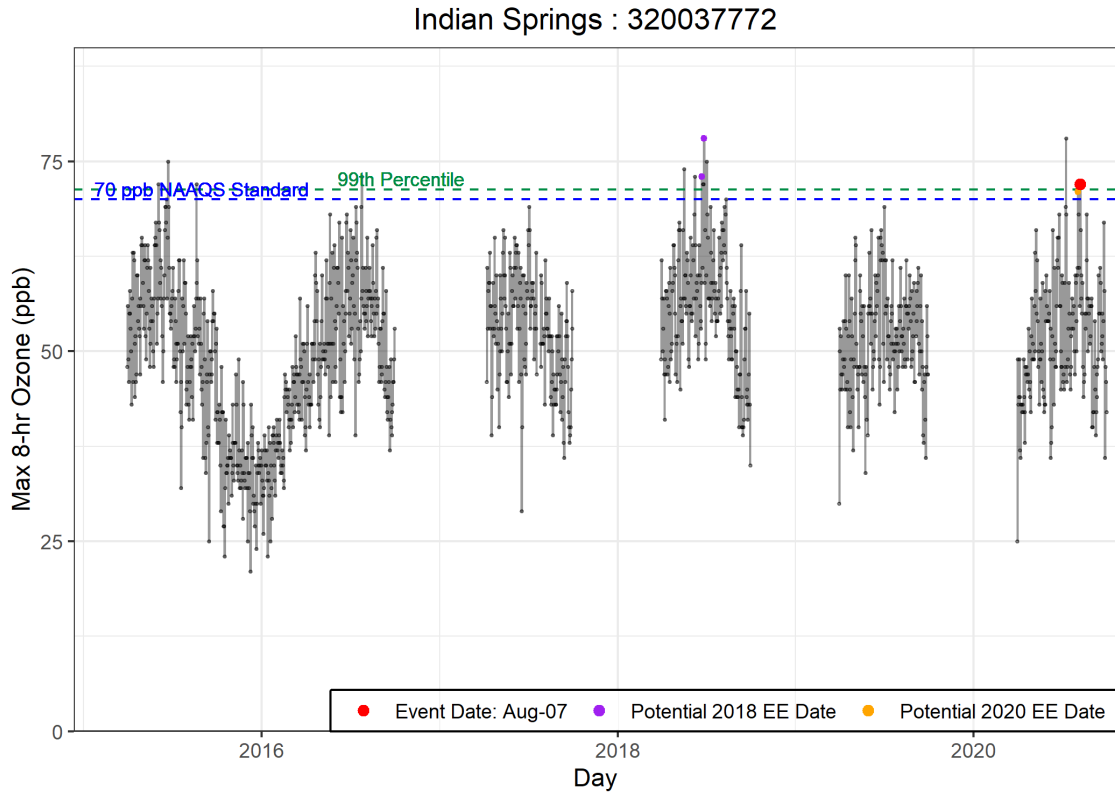


Figure 2-5. Time series of 2015-2020 ozone concentrations at the Indian Springs site. August 7, 2020, is shown in red.

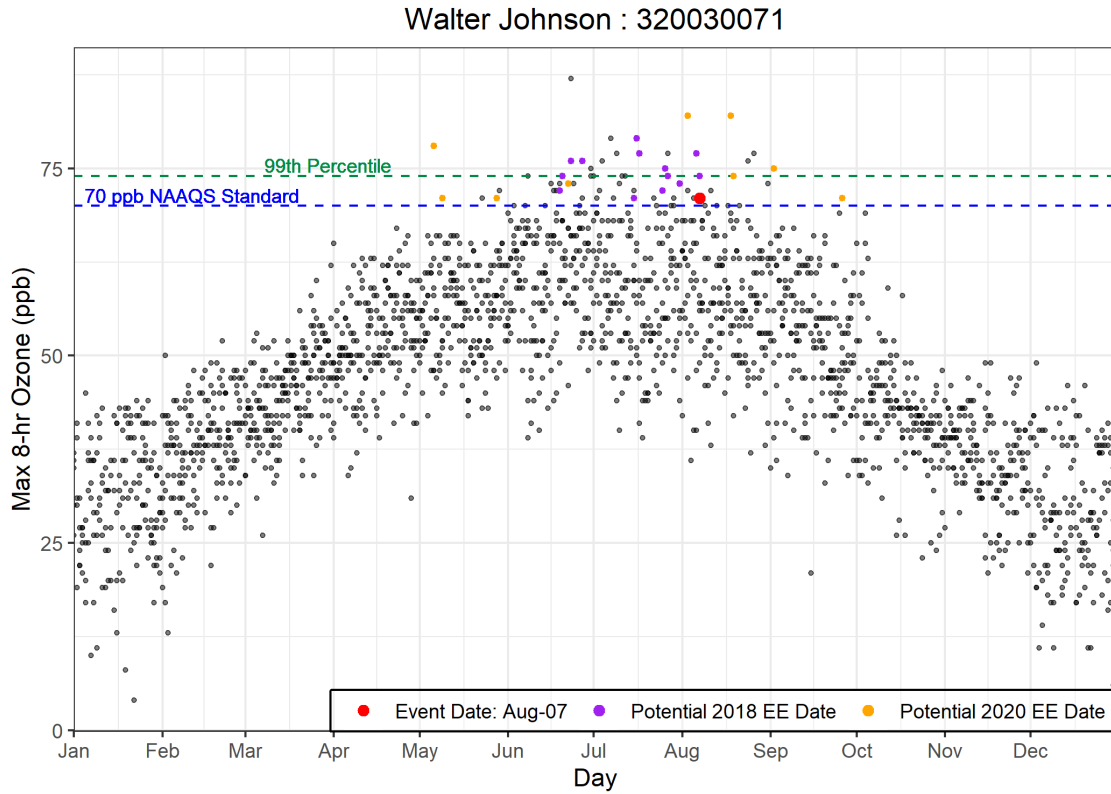


Figure 2-6. Seasonality of 2015-2020 ozone concentrations from the Walter Johnson site. August 7, 2020, is shown in red.

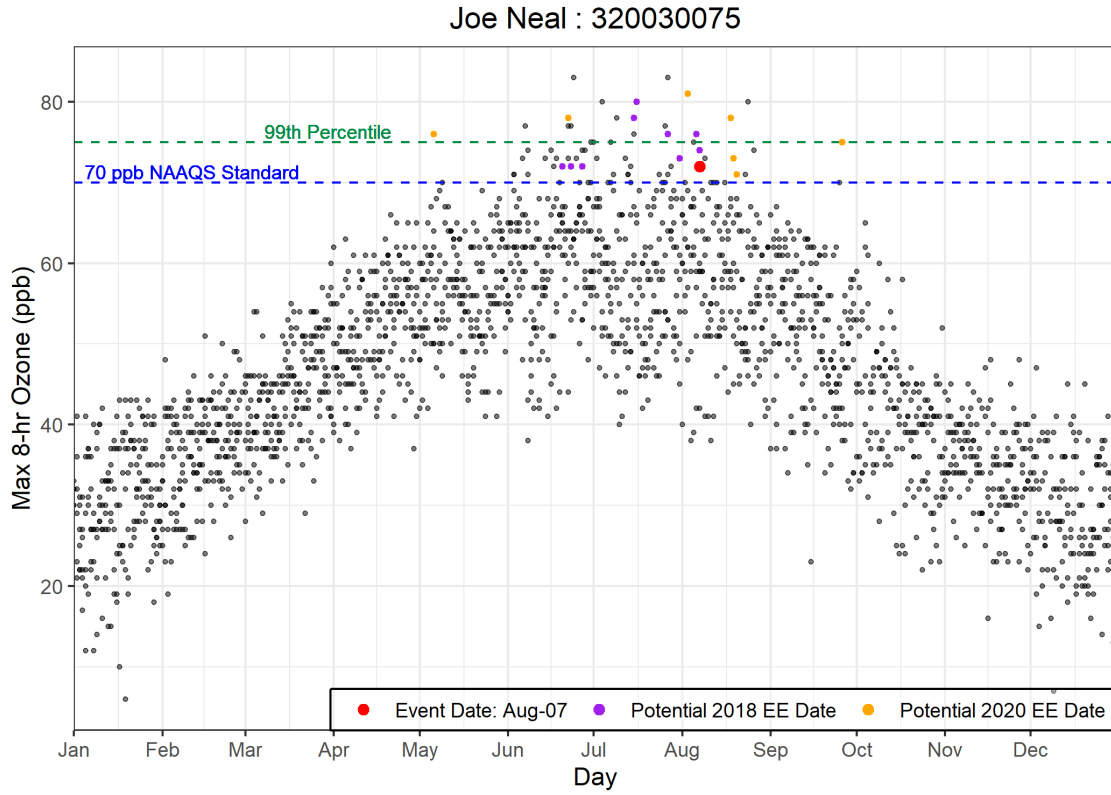


Figure 2-7. Seasonality of 2015-2020 ozone concentrations from the Joe Neal site. August 7, 2020, is shown in red.

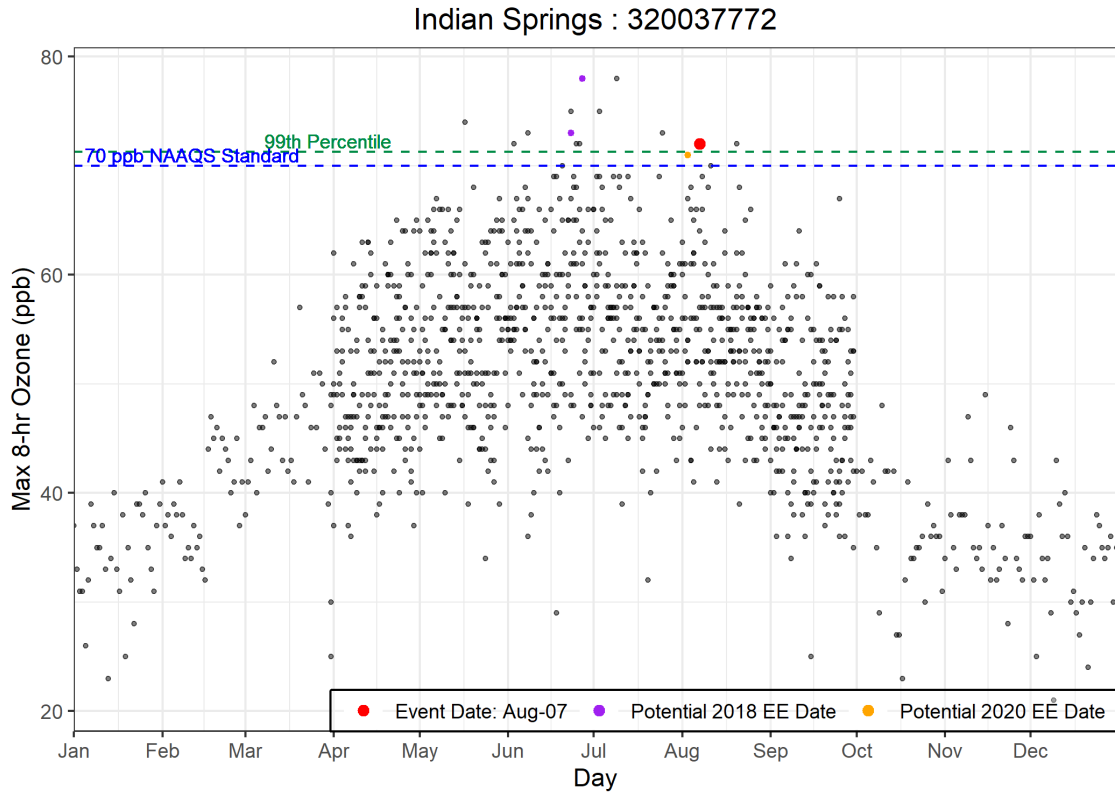


Figure 2-8. Seasonality of 2015-2020 ozone concentrations from the Indian Springs site. August 7, 2020, is shown in red.

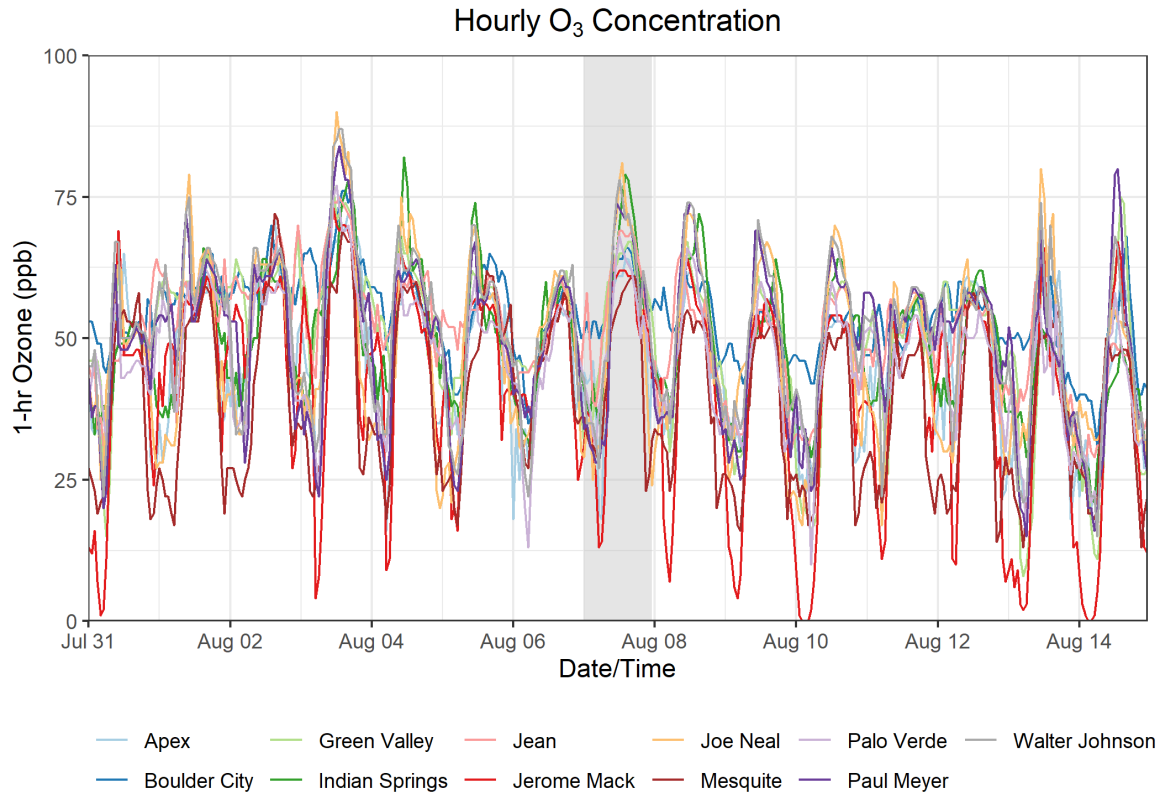


Figure 2-9. Ozone time series at all monitoring sites. Time series of hourly ozone concentrations at monitoring sites in Clark County for one week before and after the August 7 event are shown. August 7, 2020, is shaded for reference.

3. Clear Causal Relationship Analyses

3.1 Tier 1 Analyses

3.1.1 Comparison of Event with Historical Data

To address the Tier 1 EE criterion of comparison with historical ozone concentrations, we compared the August 7 EE ozone concentrations at each site with the 2020 ozone record, focusing mainly on the ozone season when highest ozone concentrations occur. **Figures 3-1 through 3-3** depict the 2020 daily maximum ozone record at each monitoring site, along with the 99th percentile of previous 5-year MDA8 ozone and NAAQS criteria ozone concentrations. During 2020, August 7 ranks in the top 1% (and second highest overall) for daily maximum ozone concentration in the past five years at the Indian Springs monitoring site. For the Las Vegas Valley sites that were affected by the EE (the Walter Johnson and Joe Neal sites), the August 7 EE was in the top 5% of MDA8 ozone concentrations in the past five years and this EE event occurred between additional EEs on August 3 and August 18-21. When compared with daily ozone rankings on August 7 over the six-year ozone record (Figures 2-6 through 2-8), the 2020 rankings indicate that August 7, 2020, was a high ozone event.

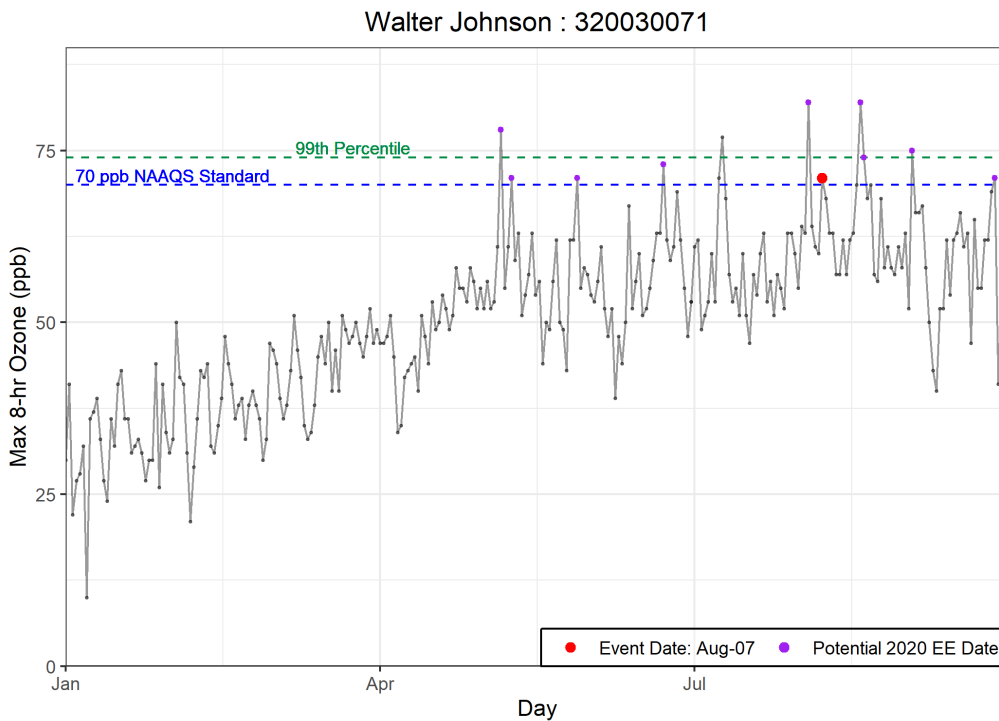


Figure 3-1. Time series of 2020 MDA8 ozone concentrations from the Walter Johnson site. August 7, 2020, is shown in red.

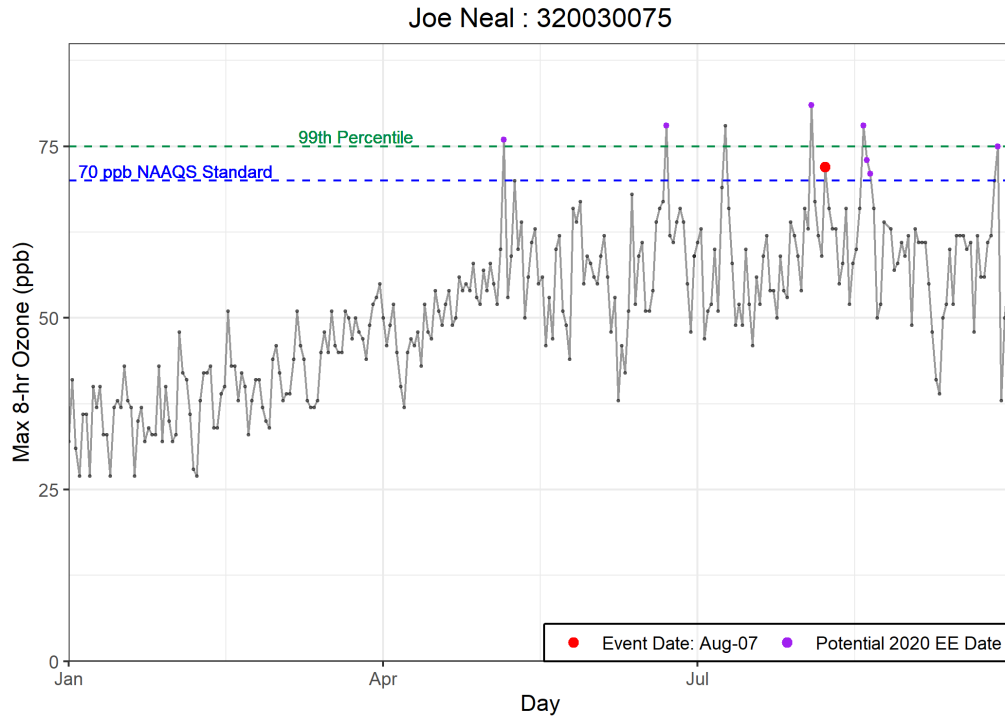


Figure 3-2. Time series of 2020 MDA8 ozone concentrations from the Joe Neal site. August 7, 2020, is shown in red.

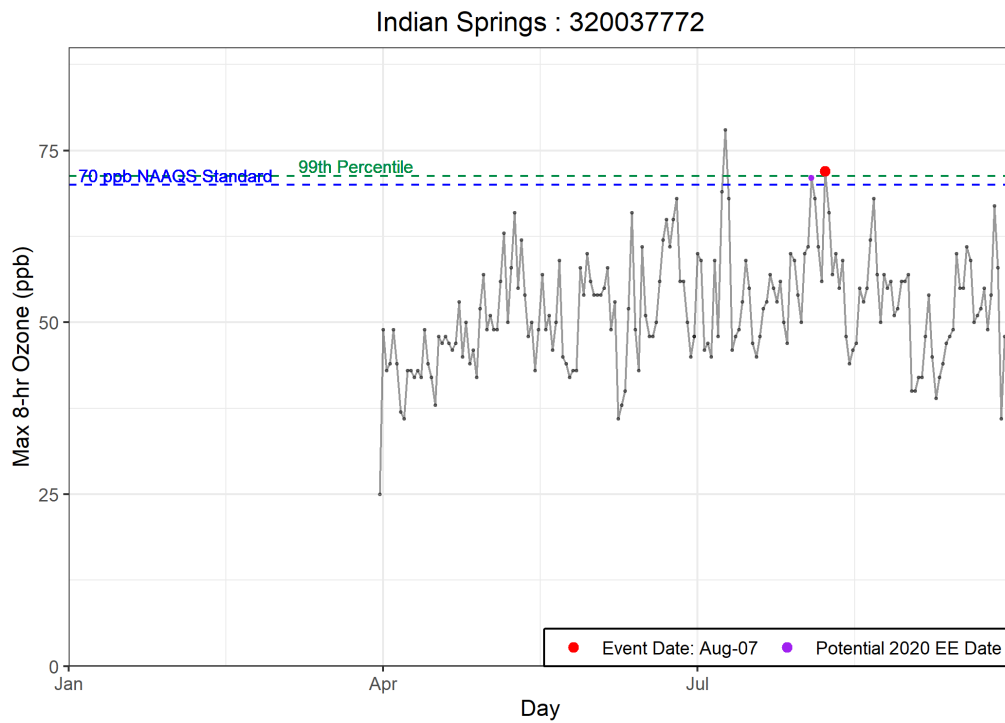


Figure 3-3. Time series of 2020 MDA8 ozone concentrations from the Indian Springs site. August 7, 2020, is shown in red.

The August 7, 2020, ozone exceedance occurred during the typical ozone season, but MDA8 ozone concentrations on August 7 were the second highest compared with daily ozone concentrations excluding potential EE days (Figures 3-1 through 3-3). **Table 3-1** provides historical monitoring site statistics for each affected site on August 7, 2020. The statistics shown are for May through September from 2015-2019; we do not exclude the dates with proposed 2018 EE ozone concentrations. The MDA8 ozone concentrations on August 7 were more than 10 ppb above the mean and median ozone concentrations for the historical ozone season at all EE affected sites. The Indian Springs site exhibited ozone concentrations 6 ppb above the 95th percentile of ozone concentrations when compared with historical ozone season non-event days, while the other EE affected sites were equal to the 95th percentile of non-event day historical ozone concentrations. Because August 7 is during the normal ozone season and MDA8 ozone concentration at two of three EE affected sites could not be clearly distinguished from the 95th percentile ozone concentration during the non-event historical ozone season, the August 7 event does not satisfy the key factor for a Tier 1 EE. A Tier 2 comparison of the event-related ozone concentrations with non-event-related high ozone concentrations (greater than 99th percentile over five years, or top four highest daily ozone measurements) are described in Section 3.2.2.

Table 3-1. Ozone season non-event comparison. MDA8 ozone concentrations at each affected site on August 7, 2020, are shown in the top row. Five-year (2015-2019) average MDA8 ozone statistics for the May through September ozone season are shown for each affected site around Clark County to compare with the event ozone concentrations.

	Indian Springs 320037772	Joe Neal 320030075	Walter Johnson 320030071
Aug. 7	72	72	71
Mean	54	57	57
Median	54	57	57
Mode	56	62	57
St. Dev	8	9	9
Minimum	25	23	21
95 %ile	66	72	71
99 %ile	72	78	77
Maximum	78	83	87
Range	53	60	66
Count	911	912	917

3.1.2 Ozone, Fire, and Smoke Maps

Ozone and PM_{2.5} Maps

We produced maps of ozone Air Quality Index (AQI) levels, PM_{2.5} AQI levels, active fire and smoke detections from satellites, and visible satellite imagery that show the transport of smoke from California to Las Vegas on August 7, 2020. These maps also show that high ozone concentrations occurred across multiple states, corresponding with the presence of wildfire smoke.

From August 4 through August 7, moderate and unhealthy ground-level ozone concentrations (indicated by the yellow, orange, and red areas in [Figure 3-4](#)) were detected in the western United States, especially in California, Nevada, and Utah. On August 4, high ozone concentrations (i.e., the orange and red areas) are seen from southern California to central Colorado, and elevated ozone covers southern California, southern Nevada, much of Arizona, Utah, and Colorado. In the following two days, the elevated ozone seemed to dissipate over Arizona, but still covered southern Nevada. On the day of the event (August 7), areas of high concentrations of ozone (indicated by the orange areas) were observed in southern California and southern Nevada.

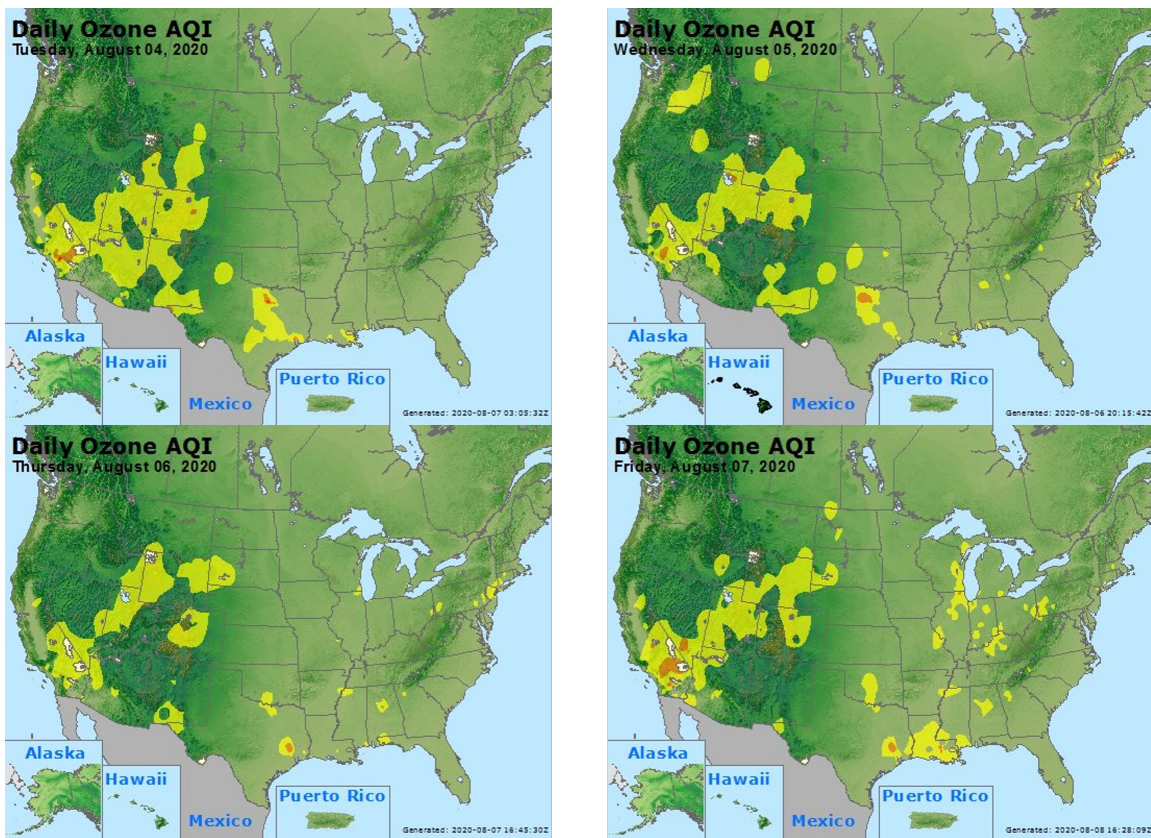


Figure 3-4. Maps showing the daily ozone AQI for the August 7 event and the three days before the event.

A similar pattern of pollutant distribution in southern California is seen in the AQI plots for PM_{2.5} levels (Figure 3-5). On August 4, elevated PM_{2.5} concentrations (indicated by the yellow areas) covered southern California, Utah, and eastern Colorado. In the following three days, although much of the PM_{2.5} had dissipated over Utah and Colorado, southern California saw continued elevated concentrations. Although elevated PM_{2.5} AQI levels were not observed over Nevada on the day of the event (August 7), evidence in Sections 3.1.2 through 3.2.4 still show that a wildfire smoke plume was transported from the California Apple Fire to Clark County, Nevada.

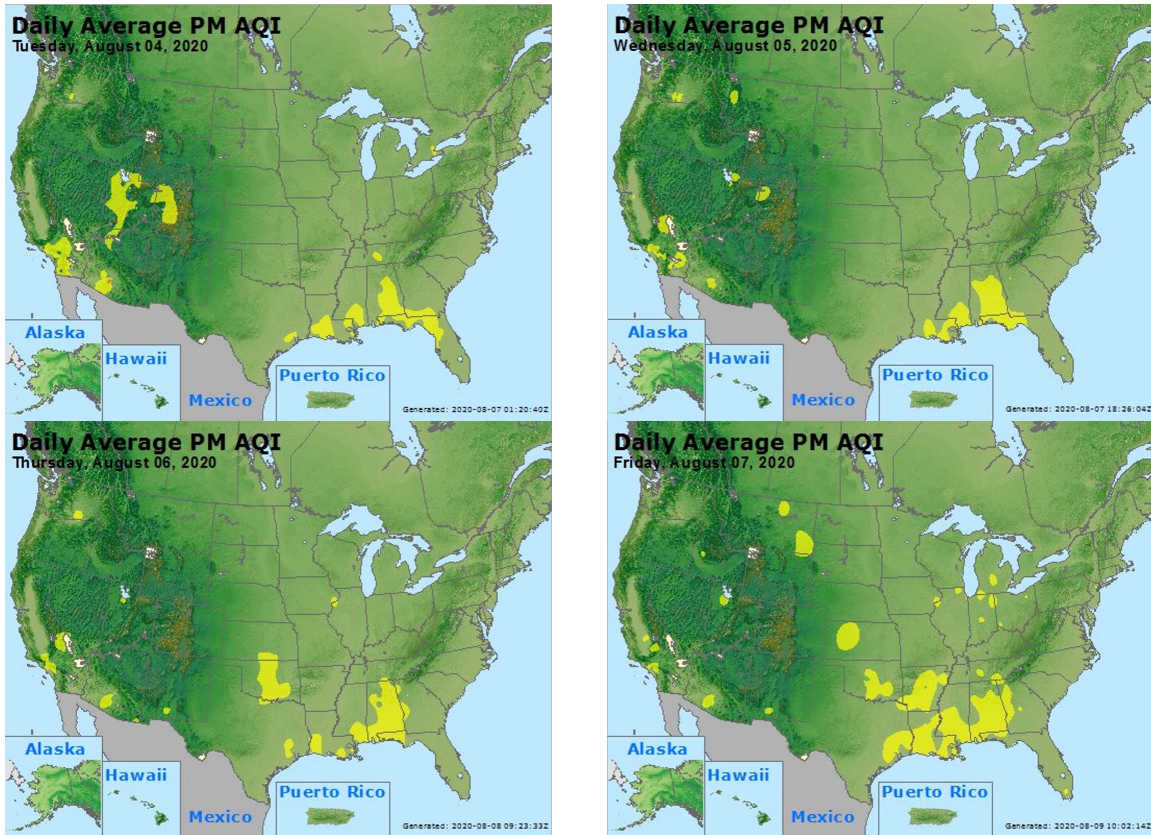


Figure 3-5. Maps showing the daily PM_{2.5} AQI levels for the August 7 event and the three days before the event.

HMS Fire Detection Maps

According to EPA’s guidance on Tier 1 analysis requirements (U.S. Environmental Protection Agency, 2016), the National Oceanic and Atmospheric Administration (NOAA) Hazard Mapping System (HMS) Fire and Smoke Product can be used to demonstrate the transport of fire emissions to impacted monitors. The HMS Fire and Smoke Product consists of

1. A daily fire detection product derived from three satellite data products¹ to spatially and temporally map fire locations at 1 km grid resolution, and
2. A daily smoke product derived from visible satellite imagery² that consists of polygons showing regions impacted by smoke.

The HMS smoke plume data is based on measurements from several environmental satellites, and is reviewed by trained NOAA analysts to identify cases where smoke is dispersed by transport. The NOAA Satellite and Information Service website (ospo.noaa.gov/Products/land/hms.html) allows users to download real-time and archived HMS fire detection and smoke products.

Figure 3-6 shows the HMS smoke plume and fire detection data for August 4 to August 7, 2020. **Figure 3-7** shows HMS smoke and fire detections over the southwestern United States, including southern California where the Apple Fire burned, during this same period. As the daily plots indicate, there was concentrated fire activity along the West Coast and in the southeast United States. While several scattered fires can be observed in Nevada, more fires occurred in the surrounding states during those days, especially in California. On August 4, the daily plots show smoke plumes forming from southern California fires and moving eastward across multiple states, including southern Nevada, Arizona, Utah, and Colorado. On August 5, much of the southwestern United States was covered in smoke, with concentrated plumes originating from the Apple Fire (in Riverside County, California) travelling northeast and covering southern Nevada, Utah, and Colorado. The following day saw sporadic plume coverage, usually concentrated near the fire locations. On the day of the event (i.e., August 7), a concentrated plume emitted from the Apple Fire reached Clark County directly. This is consistent with the increased ozone concentrations observed in Clark County, as shown above in the AQI plot (Figure 3-4).

The HMS smoke plume data for the days leading up to August 7 were obtained and combined with HYSPLIT back trajectories on high ozone concentration days to identify intersections and assess potential smoke impacts (Section 3.1.3). The following sections provide further evidence of smoke transport, based on HYSPLIT trajectories and satellite data, that traveled from the southern California fires (specifically the Apple Fire in Riverside County) to the Clark County area.

¹ The HMS fire detection product is developed using data from the Moderate Resolution Imaging Spectroradiometer (MODIS), the Geostationary Operational Environmental Satellite system (GOES), the Advanced Very High Resolution Radiometer (AVHRR), and the Visible Infrared Imaging Radiometer Suite (VIIRS) satellite instruments.

² The HMS smoke product is derived from GOES-EAST and GOES-WEST visible satellite imagery.

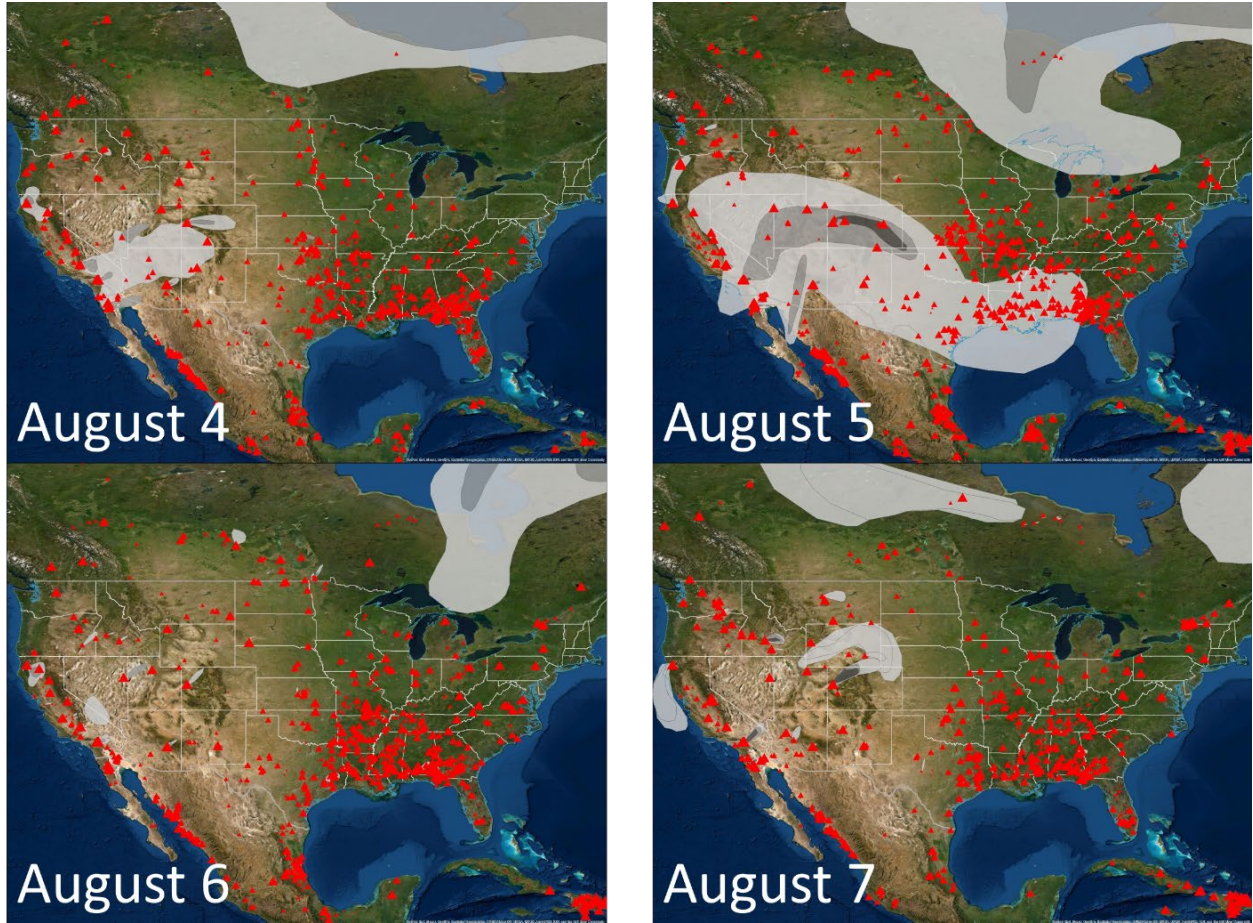


Figure 3-6. Daily HMS Smoke for August 4 to August 7, 2020.

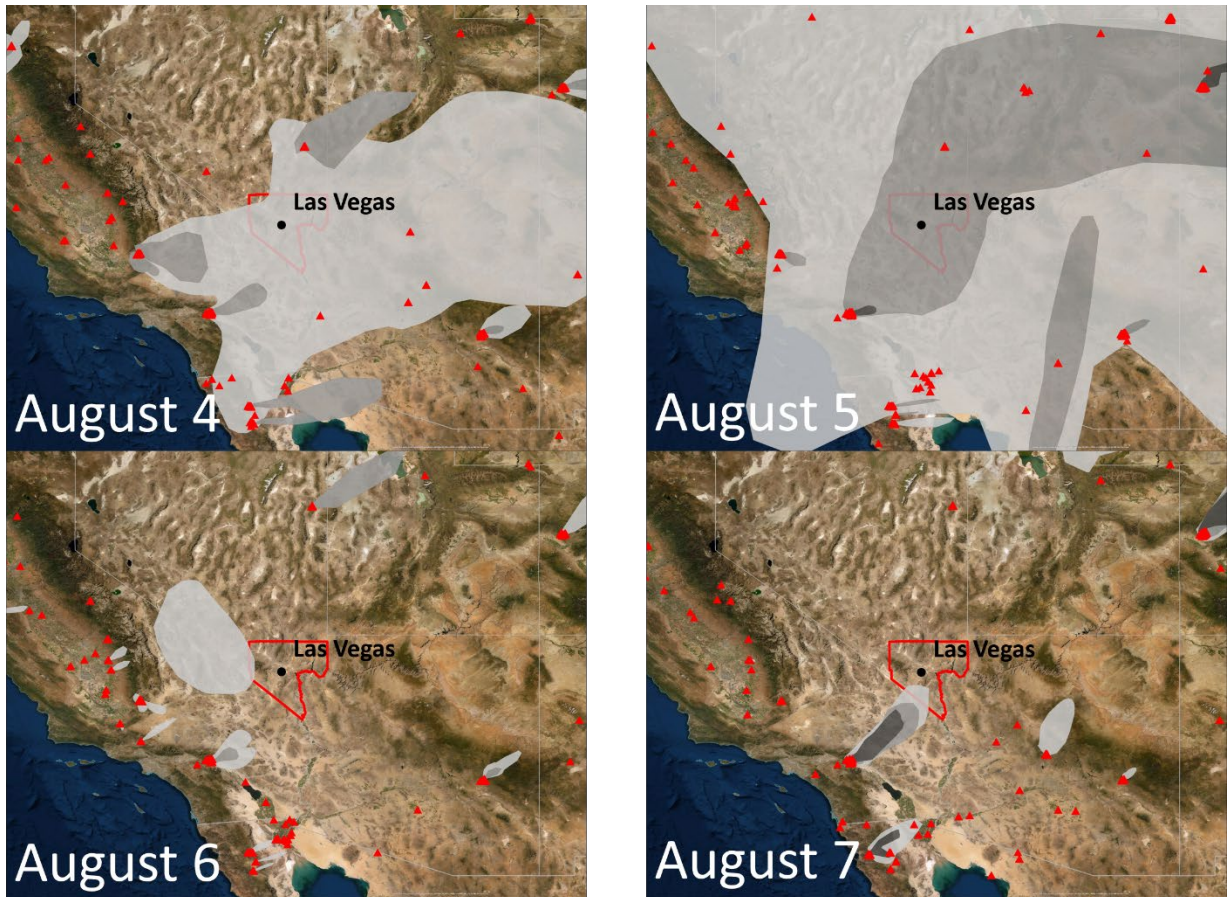


Figure 3-7. Daily HMS Smoke over the southwestern U.S. for August 4 to August 7, 2020.

Visible Satellite Imagery

Visible satellite imagery from the MODIS Aqua and Terra satellites shows transport of smoke from the Apple Fire burning in Riverside County in California northeastward, between August 4 and August 7 (Figures 3-8 through 3-11). This is consistent with the HMS smoke maps above. Smoke plumes from the Apple Fire were transported northeastward, covering southern Nevada (including Las Vegas). The transport of this smoke coincides with the increase in high ozone concentrations in Las Vegas, as shown in Figure 3-4. In addition, the transport of smoke northeastward from southern California is consistent with transport patterns observed in the HYSPLIT trajectory analysis presented in Section 3.1.3, as well as the satellite and ground-based measurements of smoke-associated species presented in Sections 3.2.3 and 3.2.4.

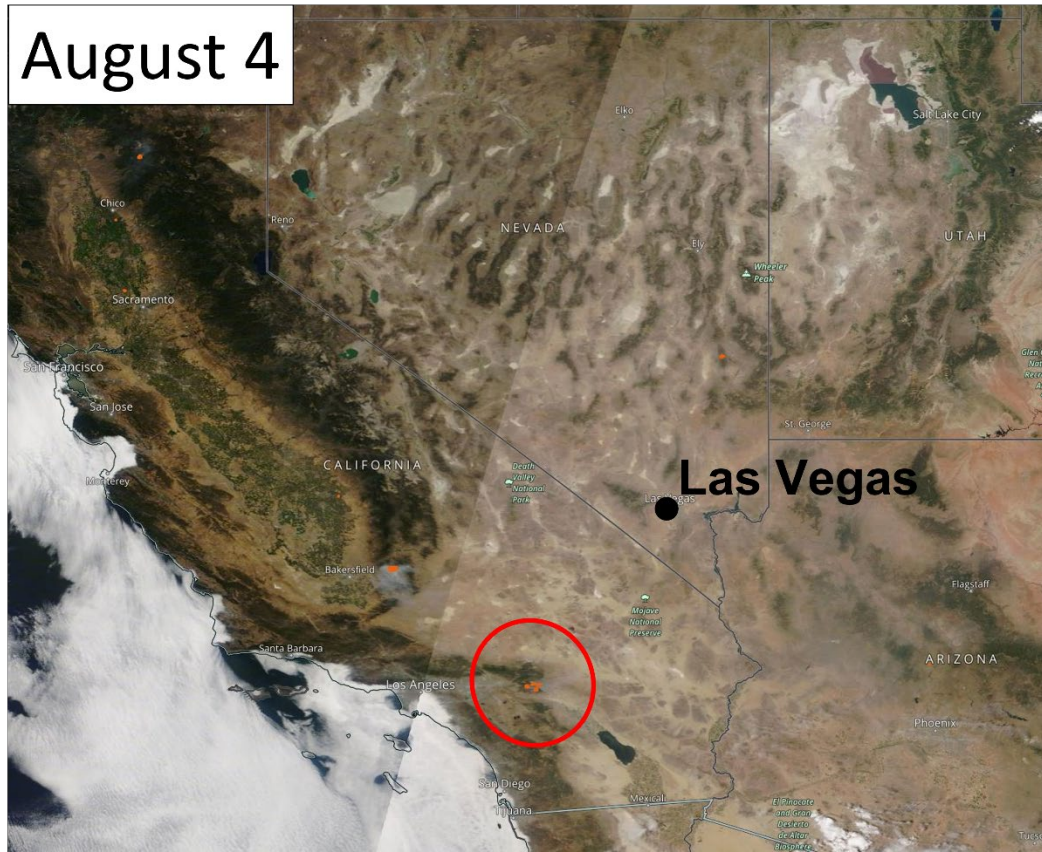


Figure 3-8. Visible satellite imagery over southern California, Nevada, and Arizona on August 4, 2020. Source: NASA Worldview. The red circle identifies the Apple Fire in southern California.

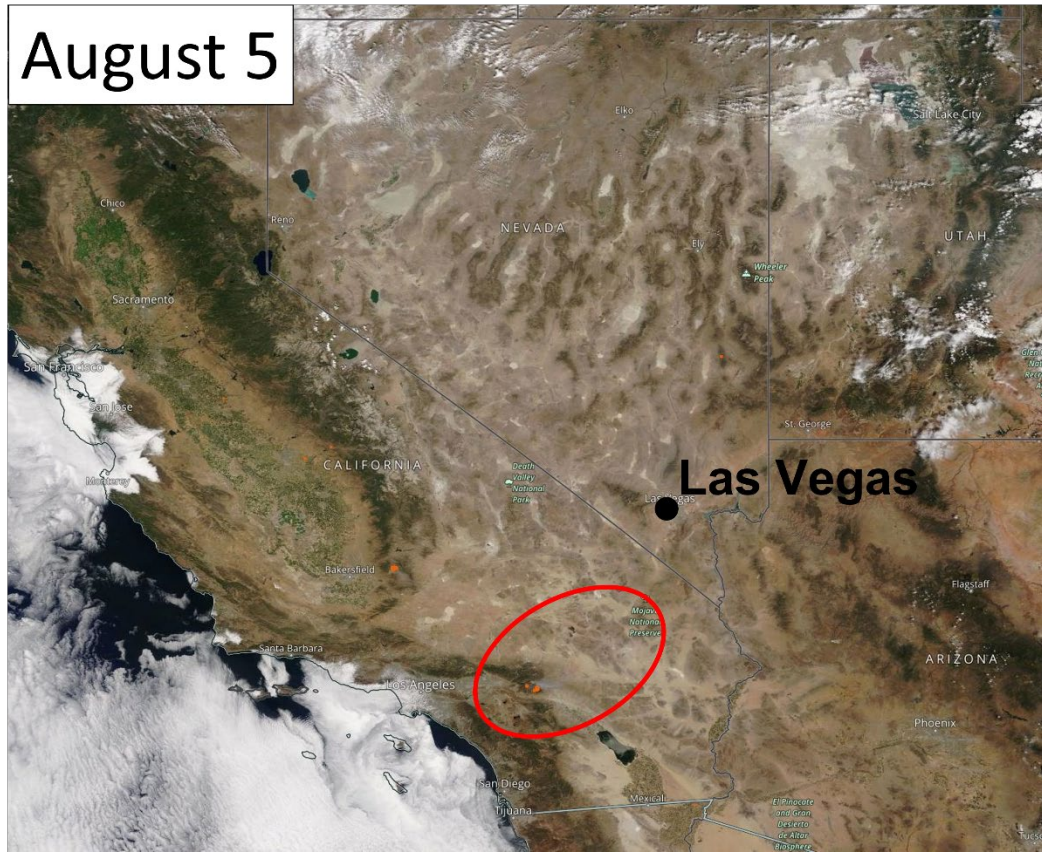


Figure 3-9. Visible satellite imagery over southern California, Nevada, and Arizona on August 5, 2020. Source: NASA Worldview. The red circle identifies the Apple Fire and associate smoke from this fire in southern California.

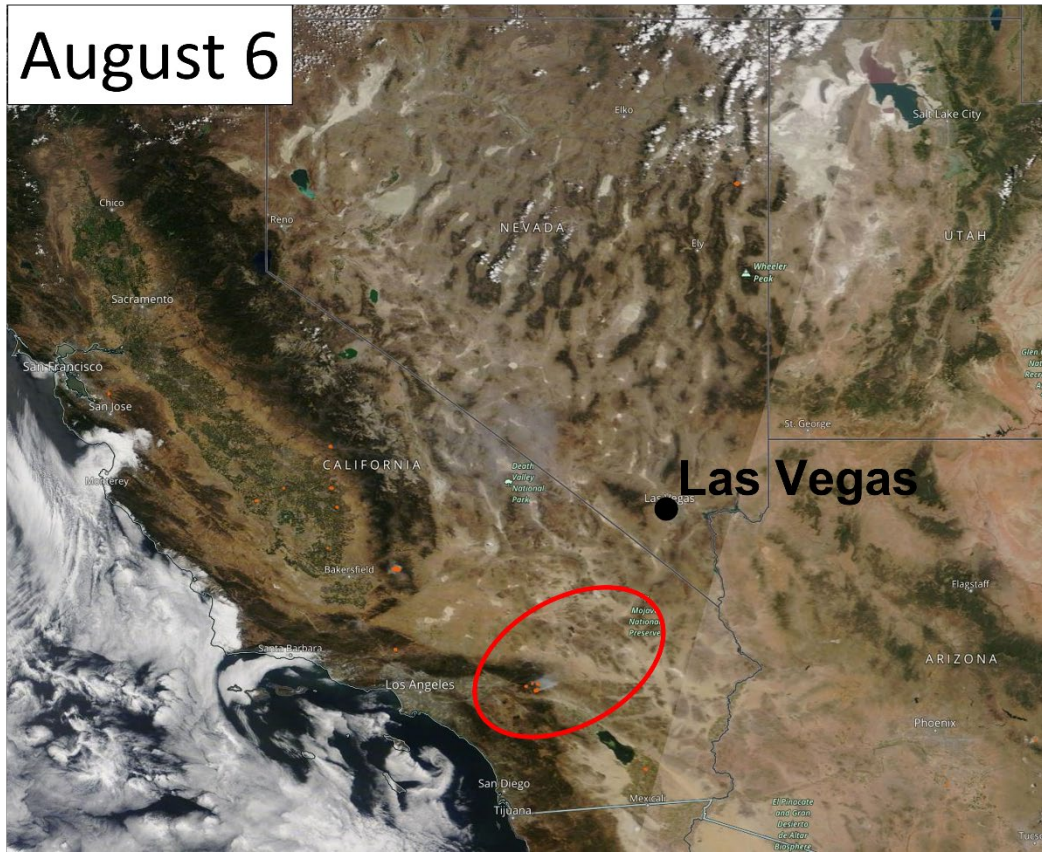


Figure 3-10. Visible satellite imagery over southern California, Nevada, and Arizona on August 6, 2020. Source: NASA Worldview. The red circle identifies the Apple Fire and associate smoke from this fire in southern California.

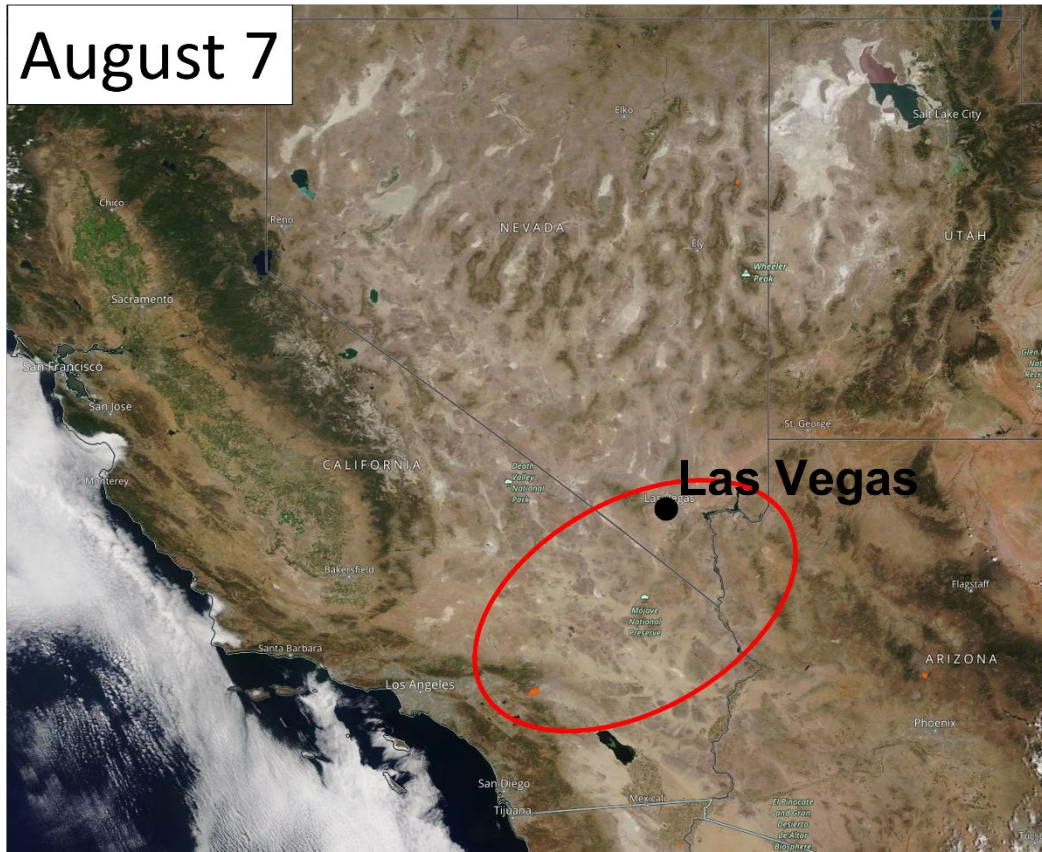


Figure 3-11. Visible satellite imagery over southern California, Nevada, and Arizona on August 7, 2020. Source: NASA Worldview. The red circle identifies the Apple Fire and associate smoke from this fire in southern California and Nevada.

3.1.3 HYSPLIT Trajectories

HYSPLIT trajectories were run to (1) demonstrate the transport of air parcels to Las Vegas from upwind areas, and (2) show transport of smoke-containing air parcels from wildfires toward the affected monitors. These trajectories show that air was transported from the Apple Fire in southern California to the Clark County area on the August 7, 2020, ozone event and the days leading up to it. Combined with satellite observations (described in Sections 3.1.2 and 3.2.3), the trajectories demonstrate that smoke was transported from southern California to Las Vegas.

NOAA’s online HYSPLIT model tool³ was used for the trajectory modeling. HYSPLIT is a commonly used model that calculates the path of a single air parcel from a specific location and height above the ground over a period of time. This path is the modeled trajectory. HYSPLIT trajectories can be used as evidence that fire emissions were transported to an air quality monitor. This type of analysis is important for meeting Tier 1 requirements and is required under Tier 3. The model options used

³ <http://ready.arl.noaa.gov/HYSPLIT.php>

for this study are summarized in [Table 3-2](#). The meteorological data from the North American Mesoscale Forecast System (NAM, 12-km resolution) and High-Resolution Rapid Refresh (HRRR, 3-km resolution) model were used.⁴ These data have high-spatial resolution, are readily available for HYSPLIT modeling over the desired lengths of time, and are expected to capture fine-scale meteorological variability. All backward trajectory start times were selected to align with peak ozone concentrations at a site where an exceedance occurred. The average hour of peak ozone concentration was chosen as the starting time for monitoring sites within the greater Las Vegas area (e.g., average hour of peak ozone concentrations at Walter Johnson and Joe Neal sites). Additionally, the backward trajectory matrix analysis was also initiated in the late morning and early afternoon (19:00 UTC or 11:00 a.m. local standard time and 21:00 UTC or 1:00 p.m. local standard time) to better understand the transport of ozone throughout the course of the full event day and the days leading up to it. As suggested in the EPA’s EE guidance (U.S. Environmental Protection Agency, 2016), a backward trajectory length of 72 hours was selected to assess whether smoke from the current day or previous two days may have been transported over a long distance to the monitoring sites. Further investigation showed that smoke from the Apple Fire was transported to Clark County within 24 to 48 hours. Therefore, 48-hour backward trajectory durations were used in this analysis. Trajectories were initiated at 50 m, 500 m, and 1,000 m above ground level to capture transport throughout the mixed boundary layer, as ozone precursors may be transported aloft and influence concentrations at the surface through vertical mixing. Three backward trajectory approaches available in the HYSPLIT model were used in this analysis: site-specific trajectories, trajectory matrix, and trajectory frequency. Site-specific back trajectories were run to show direct transport from the wildfire smoke to the affected site(s). This analysis is useful in linking smoke impacts at a single location (i.e., an air quality monitor) to wildfire smoke. Matrix back trajectories were run to show the general air parcel transport patterns from the Las Vegas area to the wildfire smoke plumes. Similarly, matrix forward trajectories were run to show air parcel transport patterns from the fires to the Las Vegas area. Matrix trajectories are useful in analyzing air transport over areas larger than a single air quality site. Trajectory frequency analysis show the frequency with which multiple trajectories initiated over multiple hours pass over a grid cell on a map. Trajectory frequencies are useful in estimating the temporal and spatial patterns of air transport from a source region to a specific air quality monitor. Additionally, a forward trajectory matrix was run for the southern California Apple Fire location to show transport in the direction of Clark County. Together, these trajectory analyses indicate the transport patterns into Clark County on August 7, 2020.

⁴ ready.noaa.gov/archives.php

Table 3-2. HYSPLIT run configurations for each analysis type, including meteorology data set, time period of run, starting location(s), trajectory time length, starting height(s), starting time(s), vertical motion methodology, and top of model height.

HYSPLIT Parameters	Backward Trajectory Analysis – Site-Specific	Back Trajectory Analysis – Matrix	Backward Trajectory Analysis – Frequency	Forward Trajectory Analysis – Matrix	Backward Trajectory Analysis – High Resolution
Meteorology	12-km NAM	12-km NAM	12-km NAM	12-km NAM	3-km HRRR
Time Period	August 7, 2020	August 7, 2020	August 7, 2020	August 6–8, 2020	August 7, 2020
Starting Location	36.2202 N, 115.2507 W	Evenly spaced grid covering Las Vegas, Nevada	36.2202 N, 115.2507 W	Evenly spaced grid covering fires in southern California	36.2202 N, 115.2507 W Indian Springs
Trajectory Time Length	48 hours	48 hours	48 hours	32 hours	48 hours
Starting Heights (AGL)	50 m, 500 m, 1,000 m	500 m, 1,000 m	500 m	500 m, 750 m, 1,000 m, 1,500 m	50 m, 500 m, 1,000 m
Starting Times	19:00 UTC	19:00 UTC	19:00 UTC	22:00 UTC	19:00 UTC, 21:00 UTC
Vertical Motion Method	Model Vertical Velocity	Model Vertical Velocity	Model Vertical Velocity	Model Vertical Velocity	Model Vertical Velocity
Top of Model	10,000 m	10,000 m	10,000 m	10,000 m	10,000 m

Site-specific backward trajectories were calculated from the Las Vegas Valley (36.1489 N, 115.2019 W) and the Indian Spring monitoring site on August 7, 2020. We chose to model all trajectories for sites within the Las Vegas metropolitan area using the Las Vegas Valley location. The Indian Springs monitoring site was far enough outside of the Las Vegas Valley to warrant initiating separate back trajectories. The hour of 19:00 UTC (i.e., 11:00 PST) was chosen as the model starting time for the Las Vegas Valley location to align with the peak hourly ozone concentration at the Walter Johnson site. The hour of peak ozone concentrations at the Indian Springs site (21:00 UTC or 13:00 PST) was chosen as the model starting time at this site to align with smoke impacts at the surface. The backward trajectories with overlaid HMS smoke plume and measured ozone (8-hour begin time average) from the Las Vegas Valley are shown in [Figure 3-12](#). All three trajectories, each at a different

height, follow a similar backward path from the Las Vegas Valley and passed either near or directly over the active fires and smoke plumes in southern California from the Apple Fire. Additionally, smoke reached Clark County directly on August 7, 2020, and enhanced ozone concentrations were observed at all sites in Las Vegas where smoke was present/nearby. Backward trajectories from the Las Vegas Valley location with overlaid HMS smoke from August 6 and 7 ([Figure 3-13](#)) show that the trajectory originating at 1000 m altitude passes directly over the smoke plume associated with the Apple Fire on August 6. On August 7, 500 m and 1000 m altitude back trajectories intersect the Apple Fire smoke plume during transport towards Clark County. [Figures 3-14 and 3-15](#) show the high-resolution (3 km) backward trajectories from the Las Vegas Valley and from Indian Springs on August 7. The results are consistent in that all six trajectories passed over southern California near or directly over the smoke plume of the Apple Fire.

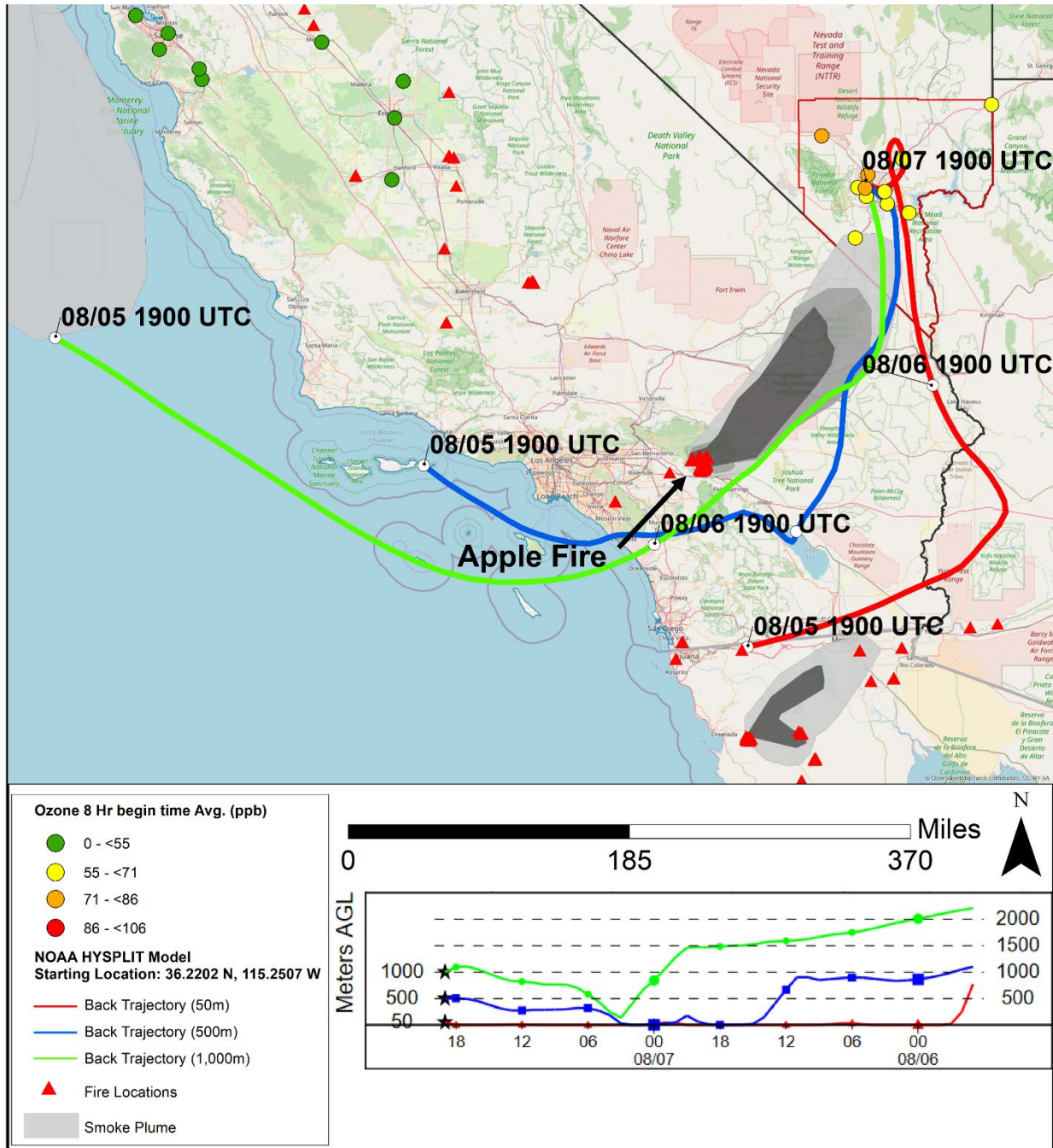


Figure 3-12. HYSPLIT back trajectories with HMS smoke from downtown Las Vegas, ending on August 7, 2020. 48-hour, NAM back trajectories are shown for 50 m (red), 500 m (blue), and 1,000 m (green) above ground level. The HMS smoke for August 7, 2020, is shown in shades of gray. Eight-hour ozone averages are shown as circles (green to red), and HMS fires are shown as red triangles.

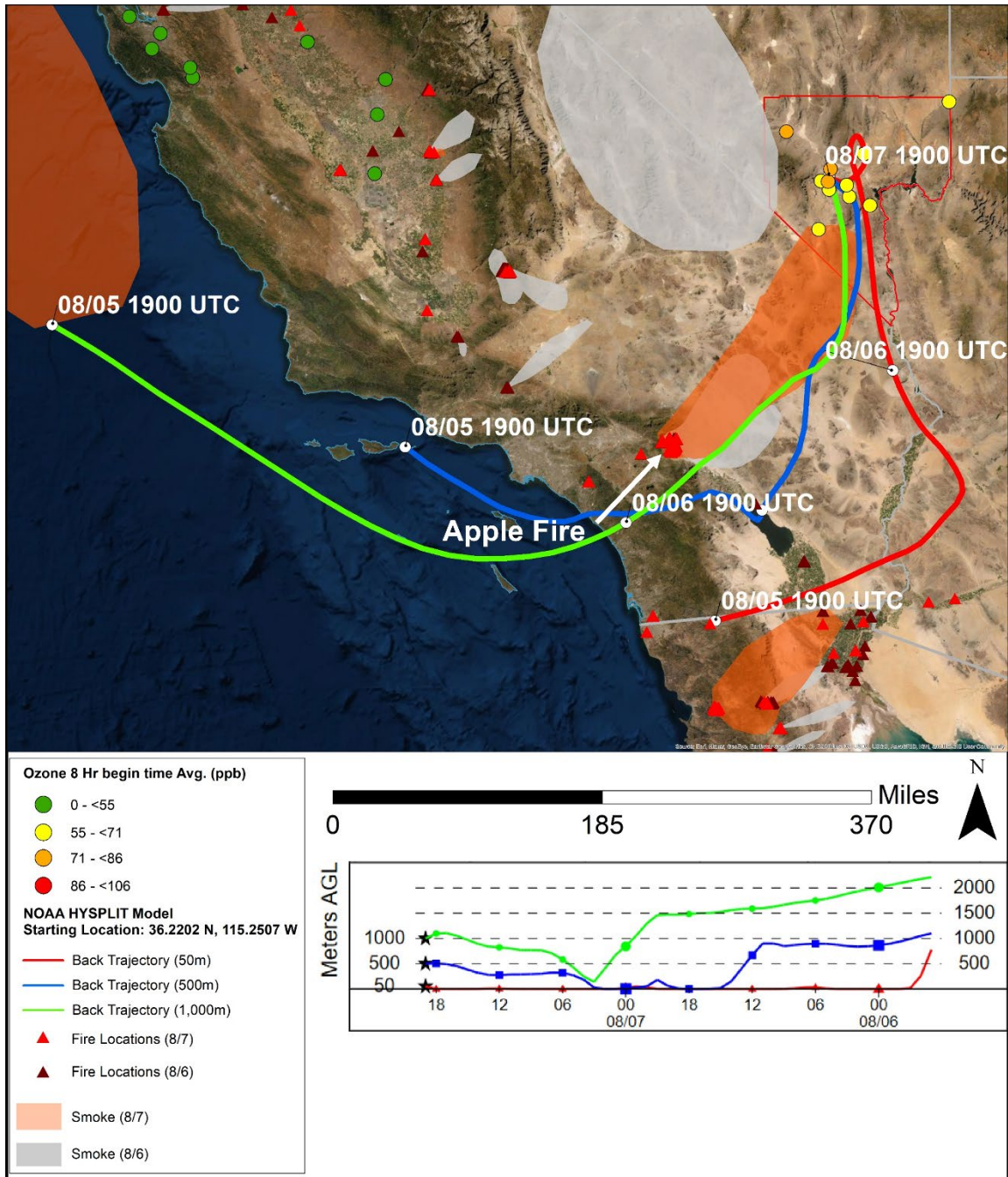


Figure 3-13. HYSPLIT back trajectories with HMS smoke on August 6 (grey) and August 7 (orange) from downtown Las Vegas, ending on August 7, 2020. 48-hour, NAM back trajectories are shown for 50 m (red), 500 m (blue), and 1,000 m (green) above ground level. Eight-hour ozone averages are shown as circles (green to red), and HMS fires are shown as red triangles.

NOAA HYSPLIT MODEL
 Backward trajectories ending at 1900 UTC 07 Aug 20
 HRRR Meteorological Data

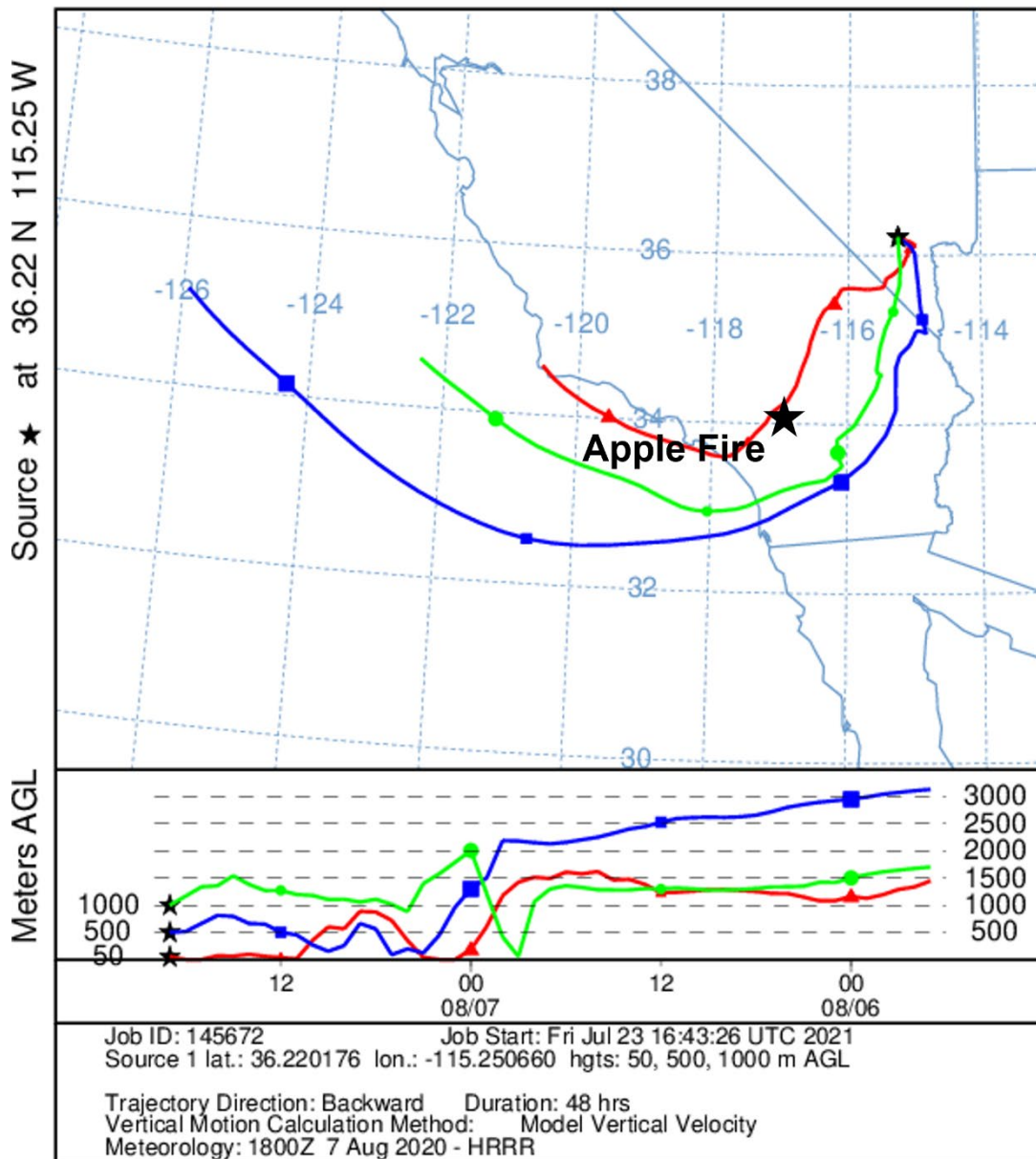


Figure 3-14. High-resolution HYSPLIT back trajectories from downtown Las Vegas. 48-hour, HRRR back trajectories initiated on August 7 are shown for 50 m (red), 500 m (blue), and 1,000 m (green) above ground level. The Apple Fire location is indicated by a black star.

NOAA HYSPLIT MODEL
 Backward trajectories ending at 2100 UTC 07 Aug 20
 HRRR Meteorological Data

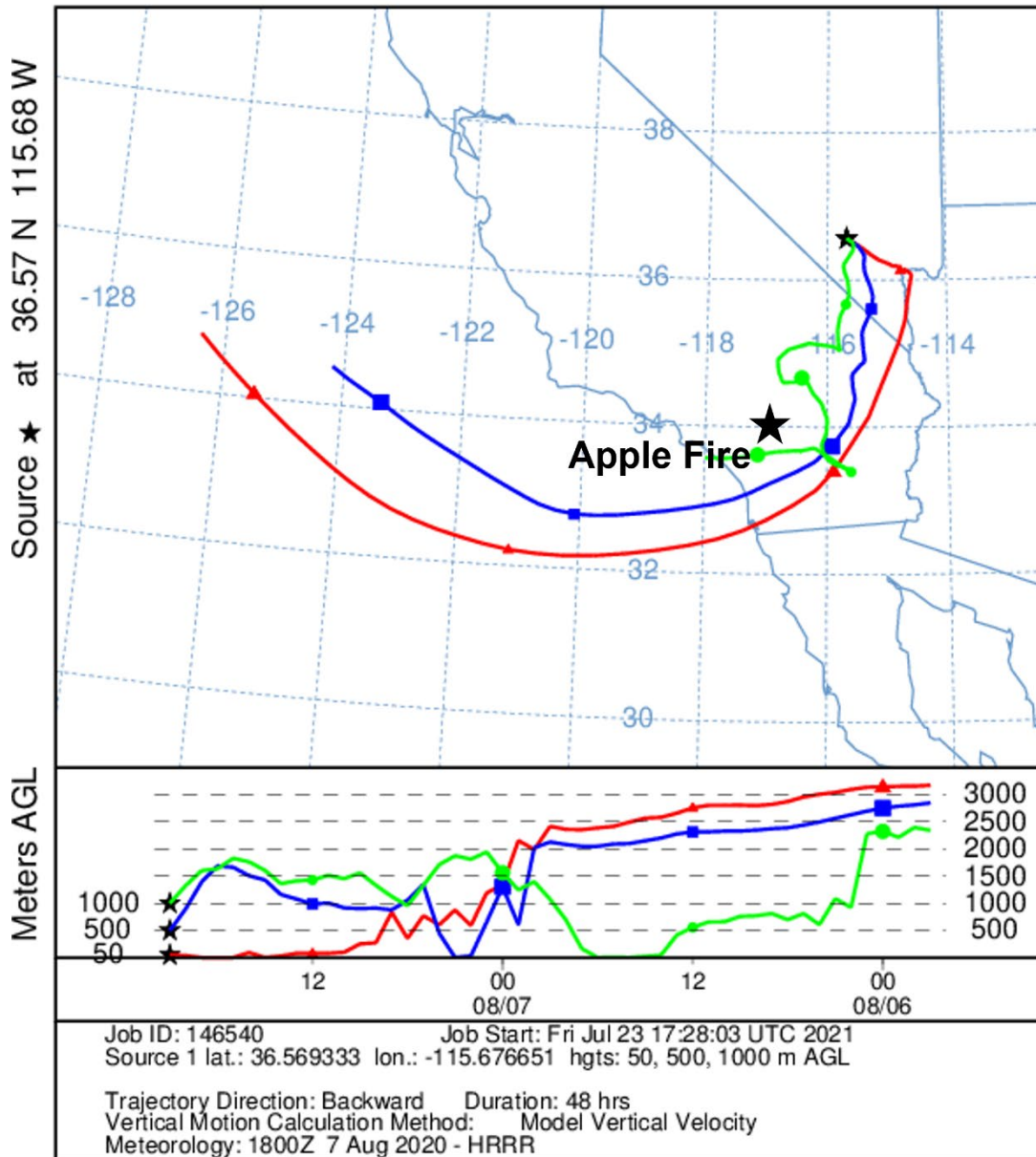


Figure 3-15. High-resolution HYSPLIT back trajectories from the Indian Springs site. 48-hour, HRRR back trajectories initiated on August 7 are shown for 50 m (red), 500 m (blue), and 1,000 m (green) above ground level. The Apple Fire location is indicated by a black star.

To identify variations in meteorological patterns of transported air to Las Vegas, we generated a HYSPLIT trajectory matrix. For this approach, trajectories are run in an evenly spaced grid of source locations. Figure 3-16 shows 48-hour backward trajectory matrices with source locations encompassing Las Vegas. The backward trajectories were initiated from the late morning (19:00 UTC

or 11:00 a.m. PST) at starting heights of 500 m and 1000 m above ground level (AGL) to capture transport into the lower boundary layer over the Las Vegas area. The air parcels that reached Las Vegas at 11 a.m. (PST) on the day of the event travelled from southern California (with some also intersecting the California/Mexico border). Consistent with the trajectories depicted in Figure 3-12, air was transported across southern California where the Apple Fire was burning and progressed northeastward where it intersected Las Vegas at 500 m and 1,000 m AGL.

The third trajectory approach used in this analysis was HYSPLIT trajectory frequency. In this option, a trajectory from a single location and height starts every three hours. Using a continuous 0.25-degree grid, the frequency of trajectories passing through each grid cell is totaled and then normalized by the total number of trajectories. Figures 3-17 and 3-18 show 48-hour backward trajectory frequency plots starting from the Las Vegas Valley and the Indian Springs site at 500 m AGL on August 7, 2020. The trajectory frequency plot yields similar results as those from the previous two approaches; transported air impacting the Las Vegas Valley on August 7, 2020, predominately came from southern California (and the California/Mexico border), near the Apple Fire.

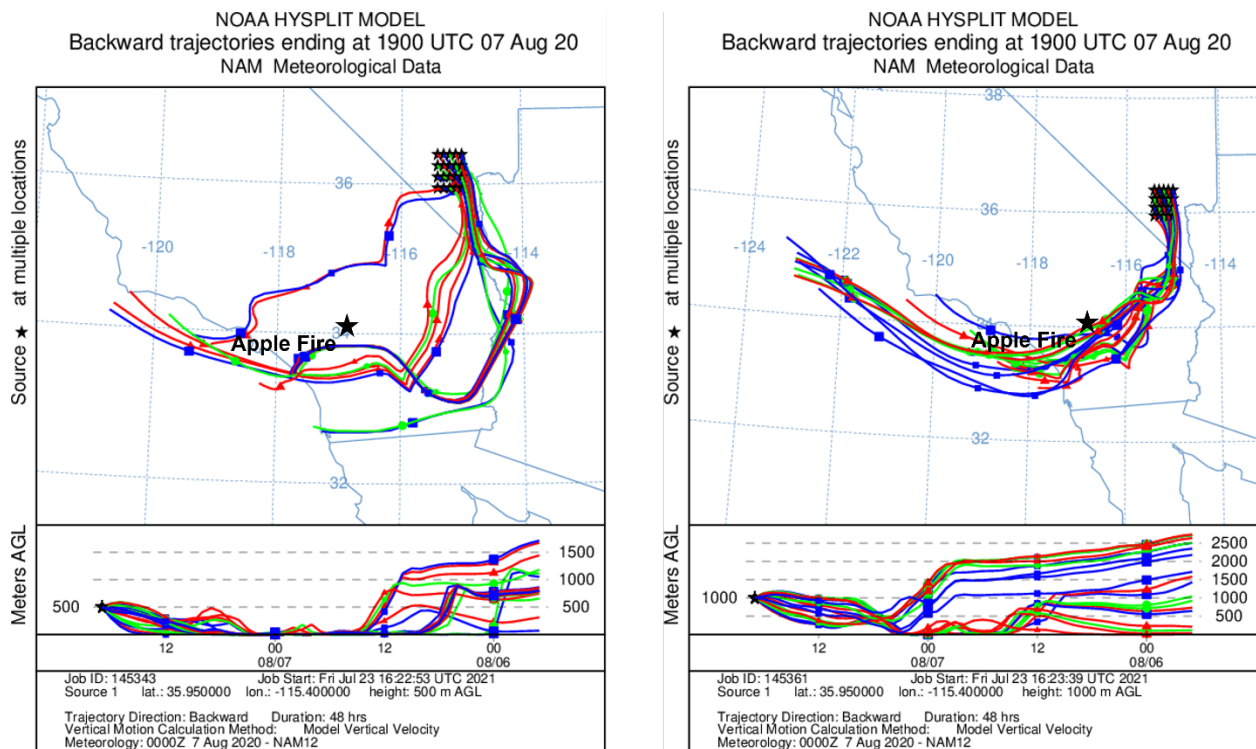
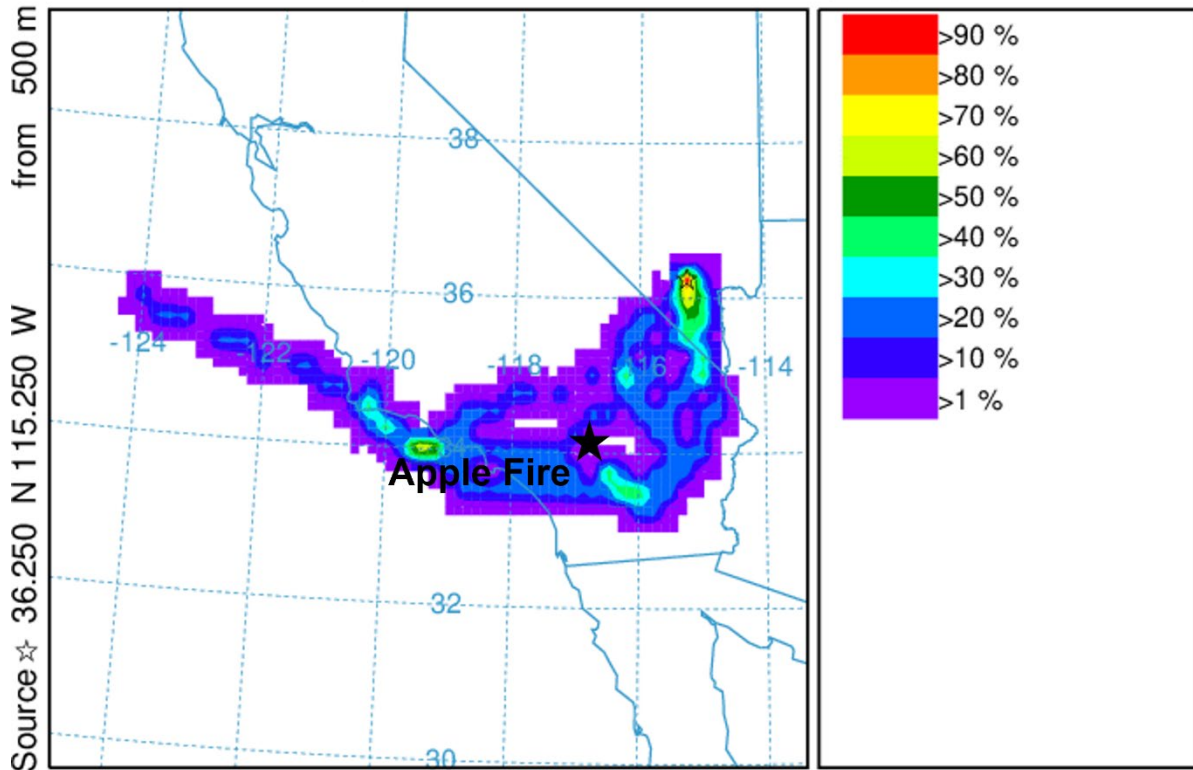


Figure 3-16. 48-hour, NAM HYSPLIT back trajectory matrix initiated on August 7 at 19:00 UTC (11:00 a.m. local time) from downtown Las Vegas at 500 m and 1,000 m above ground level. The Apple Fire location is indicated by a black star.

NOAA HYSPLIT MODEL - TRAJECTORY FREQUENCIES

trajs passing through grid sq./# trajectories (%) 0 m and 99999 m
 Integrated from 1900 07 Aug to 0100 05 Aug 20 (UTC) [backward]
 Freq Calculation started at 0000 00 00 (UTC)



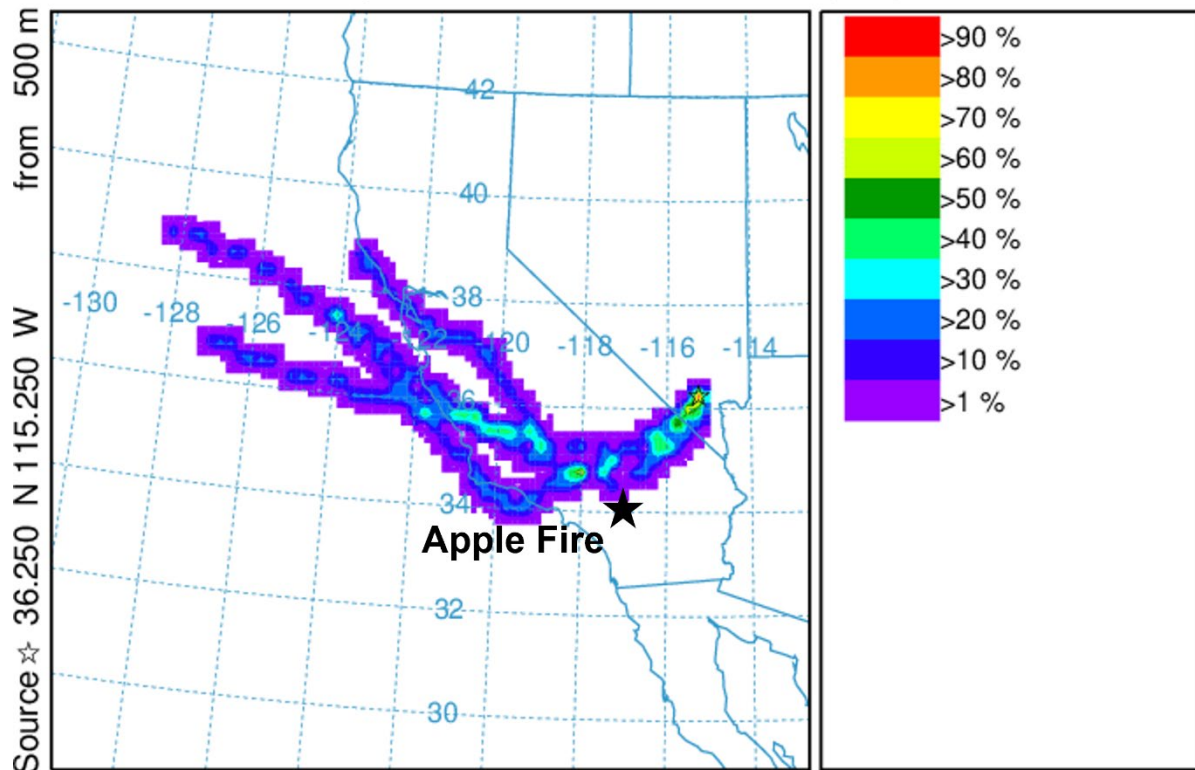
METEOROLOGICAL DATA

Job ID: 145031 Job Start: Fri Jul 23 16:10:03 UTC 2021
 Source 1 lat.: 36.220176 lon.: -115.250660 height: 500 m AGL
 Initial trajectory started: 1900Z 07 Aug 20
 Direction of trajectories: Backward Trajectory Duration: 48 hrs
 Frequency grid resolution: 0.25 x 0.25 degrees
 Endpoint output frequency: 60 per hour
 Number of trajectories used for this calculation: 4
 Meteorology: 0000Z 7 Aug 2020 - NAM12

Figure 3-17. 48-hour, NAM frequency HYSPLIT back trajectories initiated on August 7 at 19:00 UTC (11:00 a.m. local time) from downtown Las Vegas at 500 m above ground level. The colors within the frequency plot indicate the percent of trajectories that pass through a grid square. The Apple Fire location is indicated by a black star.

NOAA HYSPLIT MODEL - TRAJECTORY FREQUENCIES

trajs passing through grid sq./# trajectories (%) 0 m and 99999 m
 Integrated from 1900 06 Aug to 0100 04 Aug 20 (UTC) [backward]
 Freq Calculation started at 0000 00 00 (UTC)



METEOROLOGICAL DATA

Job ID: 145062 Job Start: Fri Jul 23 16:12:05 UTC 2021
 Source 1 lat.: 36.220176 lon.: -115.25066 height: 500 m AGL
 Initial trajectory started: 1900Z 06 Aug 20
 Direction of trajectories: Backward Trajectory Duration: 48 hrs
 Frequency grid resolution: 0.25 x 0.25 degrees
 Endpoint output frequency: 60 per hour
 Number of trajectories used for this calculation: 4
 Meteorology: 0000Z 6 Aug 2020 - NAM12

Figure 3-18. 48-hour, NAM frequency HYSPLIT back trajectories initiated for August 6 at 19:00 UTC (11:00 a.m. Local Time) from Indian Springs at 500 m above ground level. The colors within the frequency plot indicate the percent of trajectories that pass through a grid square.

Forward trajectories were run from fire locations in southern California starting at 22:00 UTC on August 6 (**Figure 3-19**), which corresponds with the time when the backward trajectories intersect the smoke plume of the Apple Fire. 500 m, 750 m, 1000 m, and 1500 m were chosen as the starting heights to capture transport at multiple heights within the lower troposphere and due to the uncertainty about the height of the smoke plumes from the Apple Fire. These trajectories show that smoke was transported from the Apple Fire in southern California to Clark County throughout the hours leading up to the ozone exceedances. These forward trajectories, combined with the back trajectories shown above, further support the transport of smoke from the southern California Apple Fire to Clark County, Nevada.

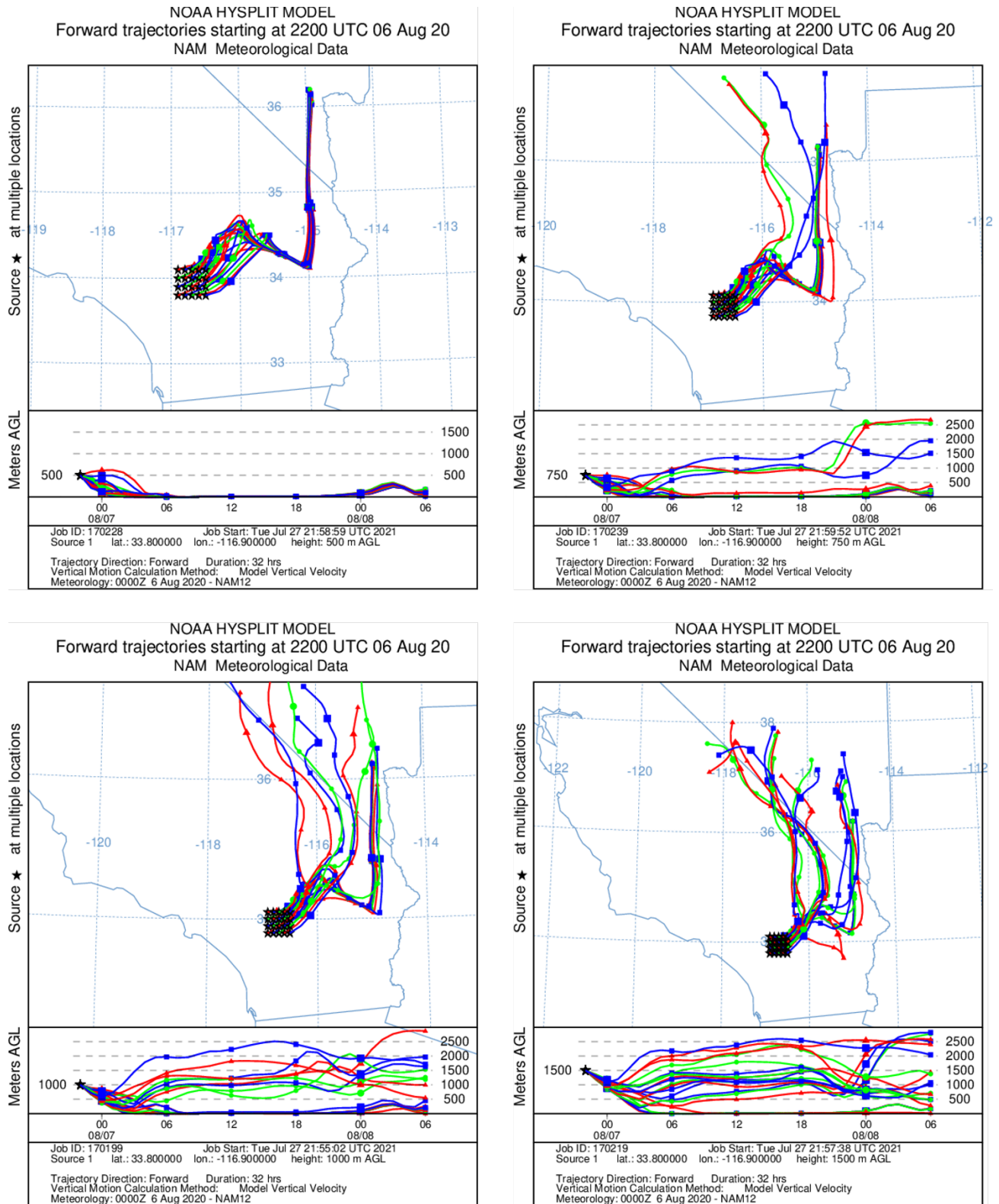


Figure 3-19. 32-hour, NAM forward HYSPLIT trajectory matrix initiated on August 6 at 22:00 UTC (August 6 2:00 p.m. local time) from the Apple Fire at 500 m, 750 m, and 1000 m, and 1500 m above ground level.

3.1.4 Media Coverage and Ground Images

News, weather, and environmental organizations provided widespread coverage of the effects of smoky conditions on air quality in Clark County. The multiple wildfires burning in California were cited as the source of the wildfire smoke impacting Clark County. On August 5, the Clark County Department of Environment and Sustainability (DES) released a Facebook post (Figure 3-20) that identified the Apple Fire and Stage Coach Fire as the cause of forecasted decreased air quality over the following days.⁵ The Clark County DES mentioned the lingering wildfire smoke in subsequent Facebook posts on August 6 and 7 that cautioned residents of elevated ozone levels. Additionally, 40 CFR 50.14(c)(1)(i) requires that air agencies must “notify the public promptly whenever an event occurs or is reasonably anticipated to occur which may result in the exceedance of an applicable air quality standard” in accordance with the mitigation requirement at 40 CFR 51.930(a)(1). Appendix A provides further details on Clark County Department of Environment and Sustainability’s public notification for the potential exceptional event on August 7, 2020.

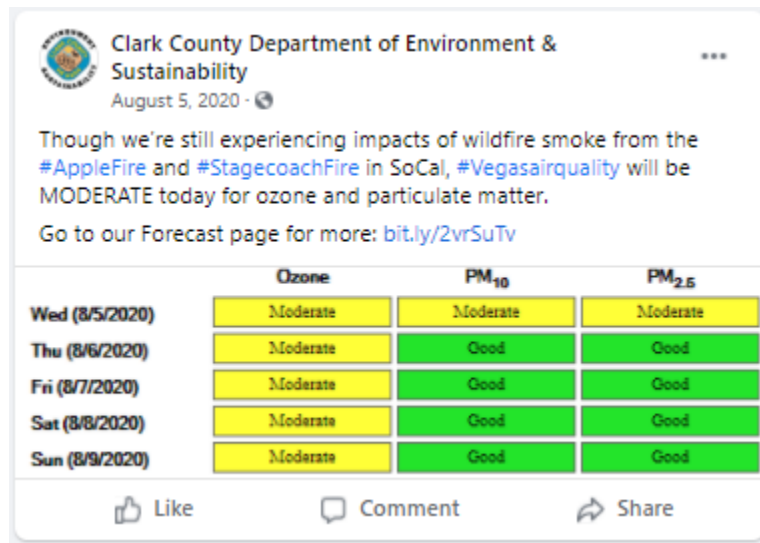


Figure 3-20 A Facebook post added by the Clark County Department of Environment and Sustainability on August 5, 2020, reporting lingering impacts of smoke from the Apple Fire on ozone levels in the Las Vegas area.

The *Las Vegas Review Journal* cited the National Weather Service in a story noting the influence of the Apple Fire on hazy conditions in Las Vegas, stating that “Smoke from fires in Southern California, especially the Apple Fire, will make skies hazy for a fourth straight day, according to the latest National Weather Service forecast,” and that “winds from the southwest are bringing the smoke toward Southern Nevada” (<https://www.reviewjournal.com/local/weather/hazy-skies-remain-as-las-vegas-high-dips-a-few-degrees-2089316/>).

⁵ <https://www.facebook.com/SustainClarkCounty/posts/1945916598871885>

Ground images from visibility cameras (operated by the Clark County DES, Division of Air Quality) located on the roof of the M Hotel in Las Vegas show the haze that persisted across the valley on August 7 (Figure 3-21). When compared to images taken on a clear day (Figure 3-22 shows images taken on May 21, 2020), the August 7 images show an opaque gray hue in every direction and reduced contrast to the outlines of distant landmarks due to wildfire smoke.

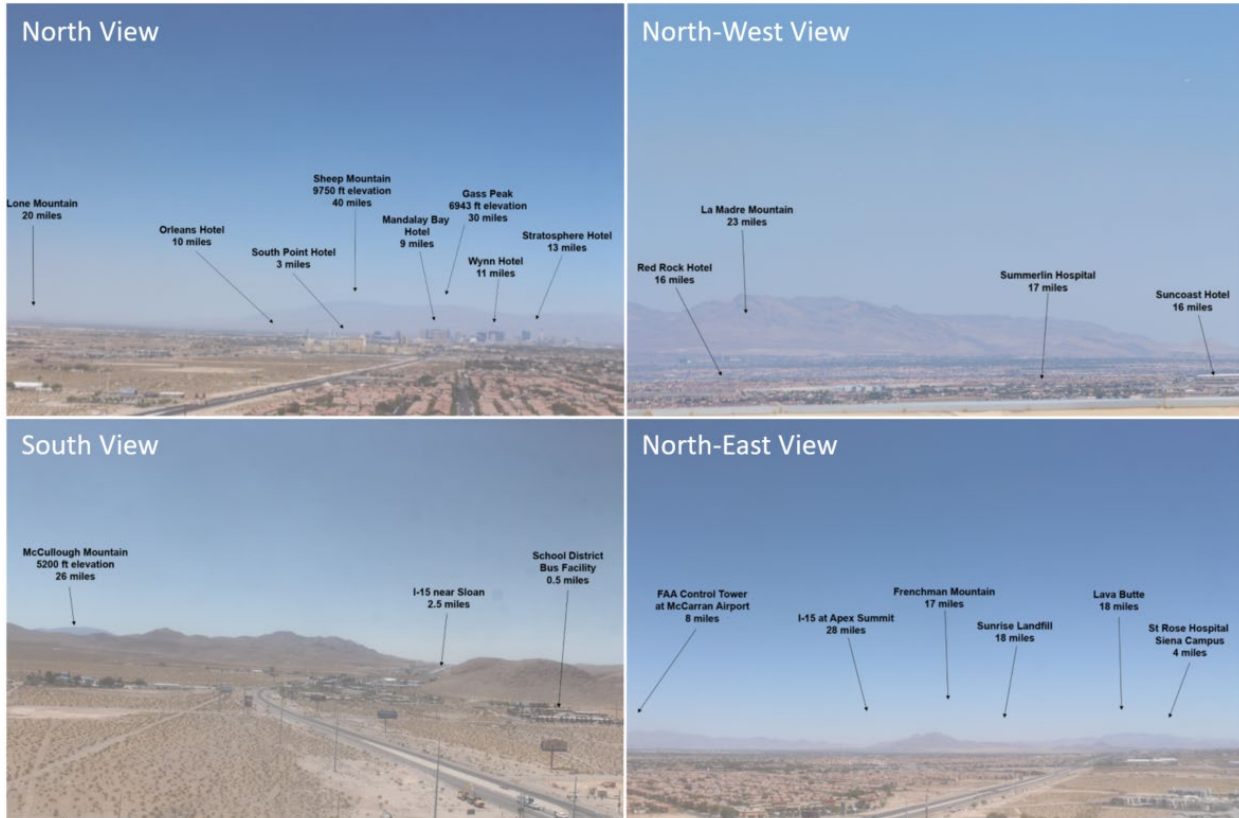


Figure 3-21. Clark County visibility images from August 7, 2020. Images taken from webcams set up in Clark County are shown for the EE on August 7. Each image is labeled with the viewing direction and landmarks.

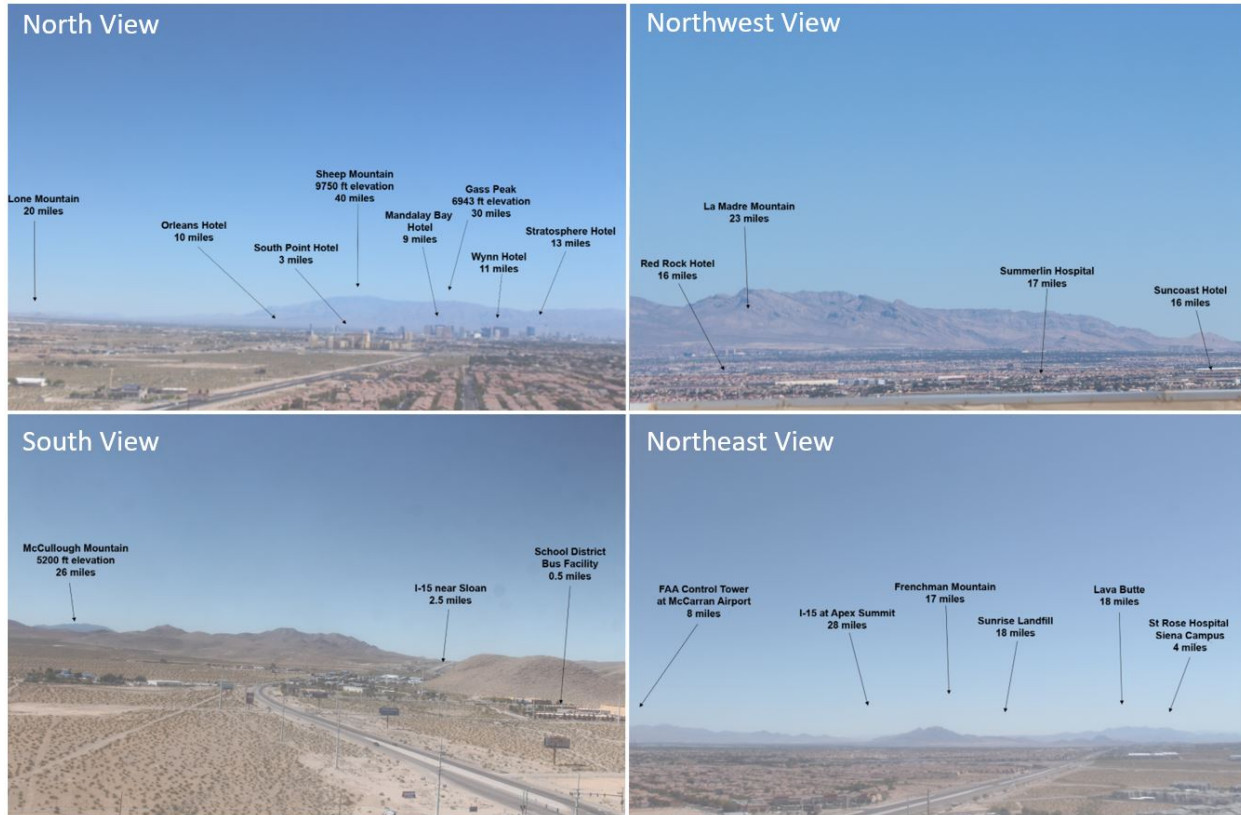


Figure 3-22. Visibility images taken from webcams set up in Clark County on a clear day (May 21, 2020). Each image is labeled with the viewing direction and landmarks.

3.2 Tier 2 Analyses

3.2.1 Key Factor #1: Q/d Analysis

The exceptional event guidance (U.S. Environmental Protection Agency, 2016) describes a method used to relate the quantity of smoke emissions and distance of the fire to an exceeding monitor. The resulting quantity, called Q/d, may be used to screen fires that meet a conservative threshold of air quality impacts.⁶ This section provides the results of the Q/d analyses for fires that were likely to have contributed to the August 7 ozone event in Clark County. Based on media coverage, transport analysis, and ground/satellite-based analyses in Section 3.1, the Apple Fire in southern California

⁶ Specifically, fires with a Q/d value meeting the 100 tons/km threshold may qualify for a tier 2 demonstration of a clear causal relationship. However, this threshold is insufficient to identify all cases where ozone impacts from smoke may have occurred. Pages 16-17 of the guidance state “To determine an appropriate and conservative value for the Q/d threshold (below which the EPA recommends Tier 3 analyses for the clear causal relationship), the EPA conducted a review. The reviews and analyses did not conclude that particular O₃ impacts will always occur above a particular value for Q/d. For this reason, a Q/d screening step alone is not sufficient to delineate conditions where sizable O₃ impacts are likely to occur.” (U.S. Environmental Protection Agency, 2016).

contributed to smoky conditions and high ozone concentrations in Clark County, Nevada, on August 7, 2020.

Figure 3-23 shows large fires burning in the vicinity of Clark County on August 7, 2020, including the Apple Fire in southern California. **Table 3-3** shows agency data available for the Apple Fire (as of December 2020). The Apple Fire started on July 31, 2020, as a result of a malfunctioning diesel engine and quickly turned into a large fire. It then ran uphill into steep, rugged wildland terrain that was inaccessible to most firefighting methods (<https://inciweb.nwcg.gov/incident/article/6902/53409>). By the end of August 7, 2020, the Apple Fire had burned approximately 32,412 acres, according to unified command morning updates available on InciWeb (<https://inciweb.nwcg.gov/incident/6902>). The total size of the fire amounted to 33,424 acres, with 100% containment declared by San Bernardino National Forest officials on November 16, 2020.

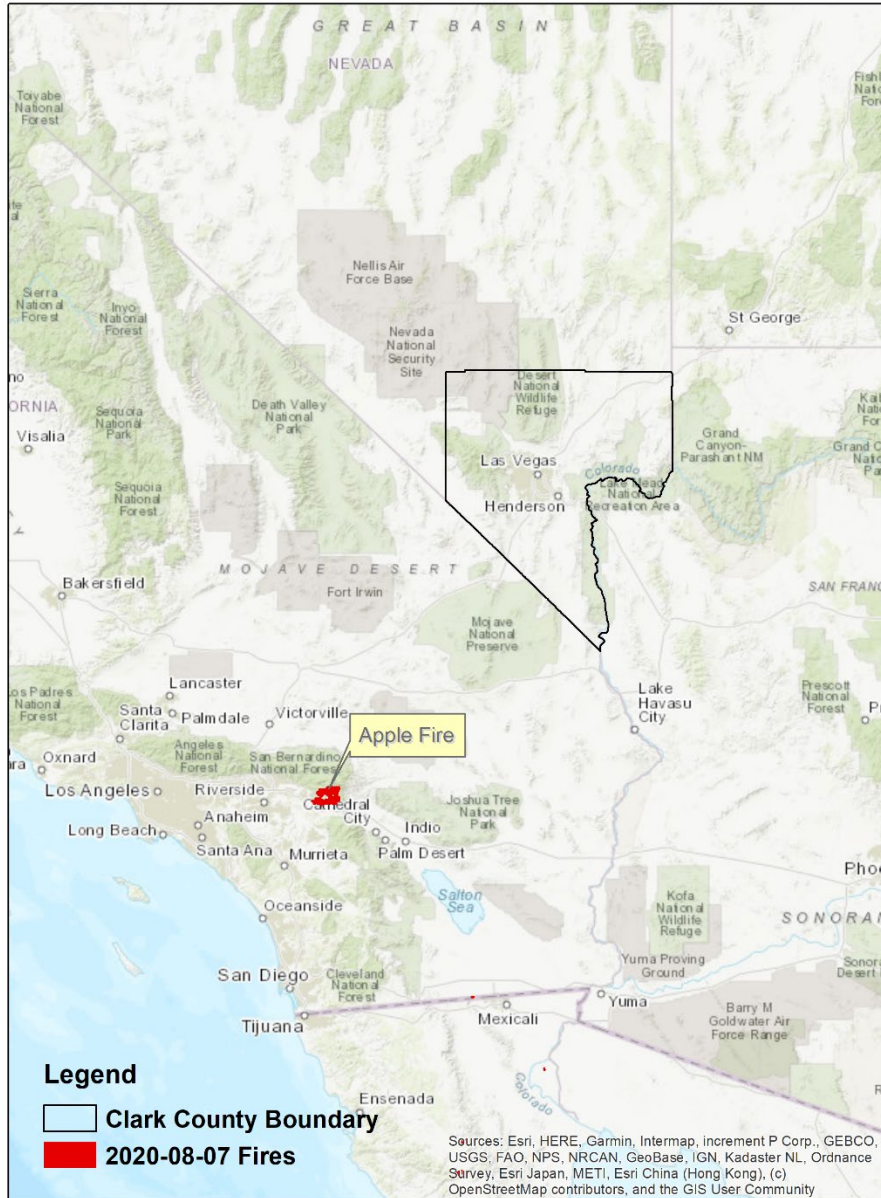


Figure 3-23. Large fires burning on August 7, 2020, in the vicinity of Clark County are shown in red. The Clark County boundary is shown in black.

Table 3-3. Fire data for the Apple Fire associated with the August 7 EE. Information includes start/containment date, cause of the fire, InciWeb estimates of the area burned by the EE date (August 7), and the total reported acres burned.

Fire Name	Start Date	Contained Date	Cause	Area Burned by EE Date (acres)	Total Area Burned (acres)
Apple Fire	7/31/2020	11/16/2020	Human	32,412	33,424

Key factor #1 for a Tier 2 demonstration requires an analysis of wildfire smoke emissions from a qualifying fire and the distance of the fire to the affected monitor or monitors. To identify qualifying fires, the guidance “recommends generating 24-hour back trajectories from the affected O₃ monitoring site(s) beginning at each hour of these two or three dates” (U.S. Environmental Protection Agency, 2016). Three dates would be used only if the 8-hour averaging period for the daily maximum 8-hour ozone data include hours falling on two dates (i.e., the 8-hour average includes at least 11 p.m. and midnight on two distinct calendar days). For this demonstration, 24-hour HYSPLIT back trajectories were generated from the monitor location starting on each hour of the day of the exceedance.

The guidance states that “...fires that are close to any of these back trajectories” may be used to calculate Q/d (U.S. Environmental Protection Agency, 2016). To identify fires that fall near the HYSPLIT trajectories, trajectories were buffered by a distance of 25% of the distance traveled by the trajectory, which is consistent with uncertainty reported for HYSPLIT trajectory modeling (Draxler, 1991). **Figure 3-24** shows the back trajectories and buffer of uncertainty from Clark County, Nevada. All fires falling within the uncertainty buffer of one or more trajectories were considered candidates for calculating Q/d.

To calculate Q/d for a qualifying fire, the total daily emissions of NO_x and reactive VOCs (rVOCs) in tons is divided by the distance from the fire to impacted monitors. BlueSky Playground Version 3.0.1 (<https://tools.airfire.org/playground/v3/>) was used to estimate emissions of NO_x and VOCs for the qualifying fire on a daily basis on August 7 and the two prior days. Daily fire growth was identified using agency reports directly or news reports that cited official sources. The fire’s location—as reported in InciWeb or by CAL FIRE—was used to identify the distance to the impacted monitors and fuelbed type. Emissions calculations were based on very dry conditions.

EPA guidance recommends that an event may qualify for a Tier 2 demonstration if the Q/d value for a fire, or the aggregate Q/d across multiple fires, exceeds a conservative value of 100 tons/km. Daily Q/d results indicate that significant emissions of NO_x and rVOCs occurred from the Apple Fire during the days leading up to and including the day of the exceedance (**Table 3-4**). However, due to the significant distance between the fire and the monitor location, the emissions were not large enough

to reach the Q/d threshold of 100 tons/km for a Tier 2 demonstration, and it was determined that Tier 3 analyses were needed to demonstrate a clear causal relationship.

The results of the Q/d analysis presented in this section agree with and further strengthen the conceptual model and Tier 3 weight of evidence of a clear causal relationship between the identified wildfires smoke emissions and the monitored ozone exceedance identified in this demonstration.

**Automated Smoke Exceptional Event Screening for Fire Report for August 07, 2020
Las Vegas Nevada**

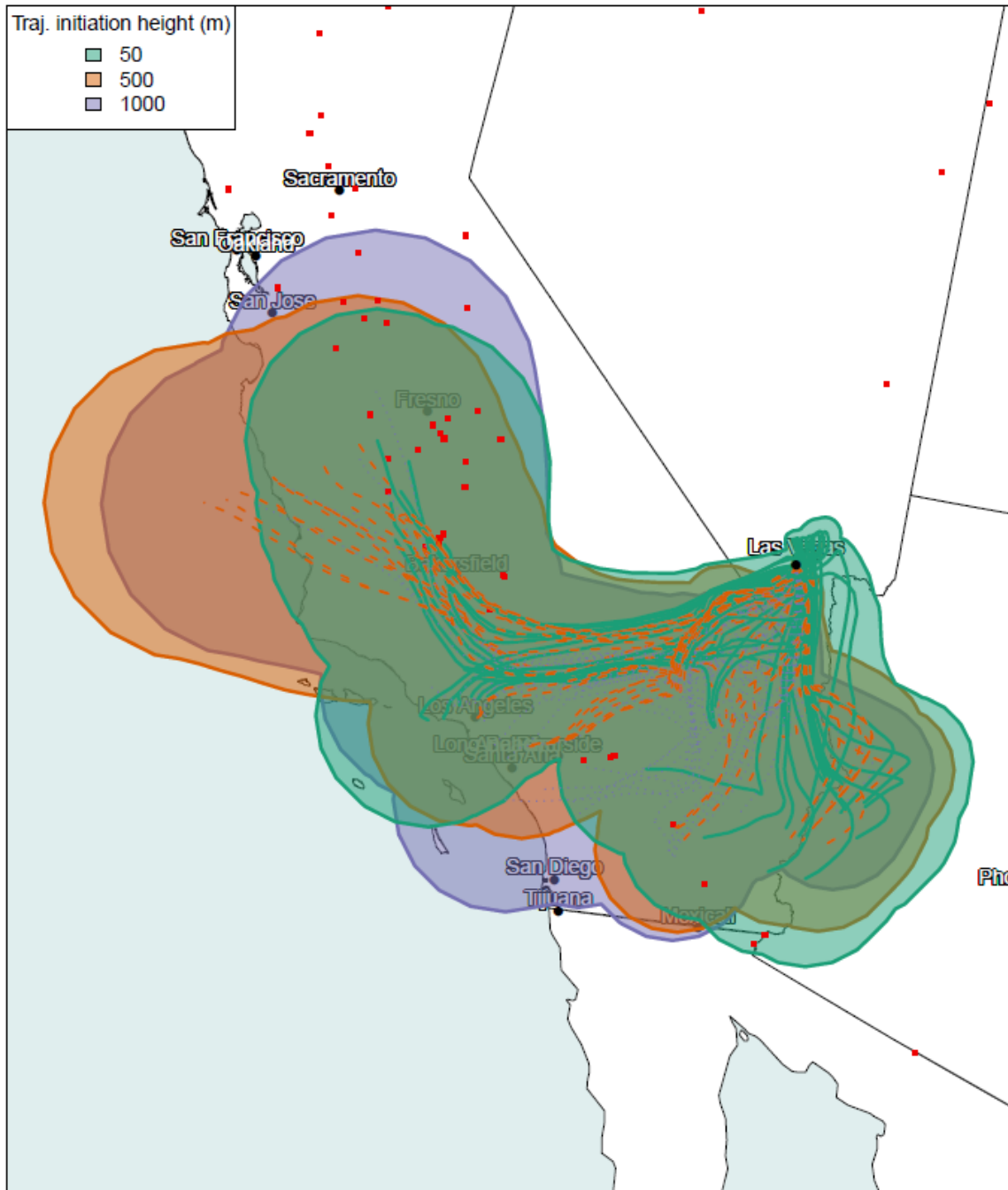


Figure 3-24. Q/d analysis. 24-hour back trajectories are shown as solid or dotted lines. The starting height of the back trajectory is indicated by the color. Uncertainty buffers, calculated as 25% of the distance traveled by the trajectory, are shown in colored polygons. Active fires on August 7 are shown as red squares. Fires falling within one or more uncertainty buffer(s) were considered candidates for calculation of individual or aggregate Q/d values.

Table 3-4. Daily growth, emissions, and Q/d for the Apple Fire. Growth for all dates shown were obtained from agency estimates available from the Incident Information System (InciWeb) at inciweb.nwcg.gov/incident/6902.

Date	Area (Acres)	Daily Growth (Acres)	NO _x (Tons)	VOCs (Tons)	Reactive VOCs (Tons)	Distance (Km)	Q/d (Tons/km)
8/7/2020	32,412	3,145	101.54	533.1	320	290	1.5
8/6/2020	29,267	1,182	38.16	200.36	120	290	0.5
8/5/2020	28,085	618	19.95	104.76	63	290	0.3

3.2.2 Key Factor #2: Comparison of Event Concentrations with Non-Event Concentrations

Another key factor in determining whether the August 7, 2020, exceedance event is exceptional is to compare event ozone concentrations with non-event concentrations via percentile and rank-order analysis. **Table 3-5** shows August 7, 2020, concentrations as a percentile in comparison with the last six years of data (with and without the other proposed 2018 and 2020 EE days included) at each site in Clark County. For the three monitoring sites (Walter Johnson, Joe Neal, and Indian Springs) that show a NAAQS standard exceedance on August 7, all of the exceedances are greater than or equal to the 98th percentile when compared to the last six years of data, even with all other proposed 2018 and 2020 EE days included. Without the other EE days included, the percentiles are slightly higher (≥99th percentile). To confirm that the calculated percentiles are not biased by non-ozone season data, **Table 3-6** shows the August 7 percentile ranks for all monitoring sites around Clark County in comparison with the last six years of ozone season (May to September) data. For Indian Springs, the August 7 percentile ranks above the 99th percentile (with all proposed 2018 and 2020 EE days included). The Walter Johnson and Joe Neal sites rank August 7 as above the 95th percentile when compared with the past six ozone seasons. When the other possible EE days are excluded, the percentile ranks for the Walter Johnson and Joe Neal sites increase to 97th percentile of ozone season concentrations. Although not all of the sites showed above the 99th percentile rank for August 7 compared with the last six ozone seasons, this analysis confirms that the August 7 EE included unusually high concentrations of ozone when compared with the last six years of data and the last six ozone seasons.

Table 3-5. Six-year percentile ozone. The August 7 EE ozone concentration at each site is calculated as a percentile of the last six years with and without other 2018 and 2020 EEs included in the historical record.

AQS Site Code	Site Name	6-Year Percentile	6-Year Percentile w/o EE Dates
320030071	Walter Johnson	97.9	98.7
320030075	Joe Neal	98.1	98.7
320037772	Indian Springs	99.4	99.5

Table 3-6. Six-year, ozone-season percentile ozone. The August 7 EE ozone concentration at each site is calculated as a percentile of the last six years' ozone season (May-September) with and without other 2018 and 2020 EEs included in the historical record.

AQS Site Code	Site Name	6-Year Percentile	6-Year Percentile w/o EE Dates
320030071	Walter Johnson	95.2	97.1
320030075	Joe Neal	95.7	97.0
320037772	Indian Springs	99.1	99.3

We also compared the rank-ordered concentrations at each site for 2020. As shown in Figures 2-3 through 2-5, ozone concentrations across 2020 were not atypically low, which might bias our rank-ordered analysis for August 7. **Tables 3-7 through 3-9** show the rank-ordered ozone concentrations for 2018 through 2020 and the design values for 2020, with the proposed 2018 and 2020 EEs included. Based on the concentration rankings, August 7 was the third highest ozone event for the Indian Springs site in 2020. However, for the Walter Johnson and Joe Neal sites, August 7 is not in the top five ozone concentrations of 2020 when including all other proposed EE events. Without other proposed EE events in 2020 included, all affected sites show August 7 ranked as the second highest ozone event in 2020.

Table 3-7. Site-specific ozone design values for the Walter Johnson monitoring site. The top five highest ozone concentrations for 2018-2020 at Walter Johnson are shown, and proposed EE days in 2018 and 2020 are included.

Walter Johnson Rank	2018	2019	2020
Highest	79	77	82
Second Highest	77	69	82
Third Highest	77	69	78
Fourth Highest	76	68	77
Fifth Highest	76	68	75
Design Value	73		

Table 3-8. Site-specific ozone design values for the Joe Neal monitoring site. The top five highest ozone concentrations for 2018-2020 at Joe Neal are shown, and proposed EE days in 2018 and 2020 are included.

Joe Neal Rank	2018	2019	2020
Highest	80	74	81
Second Highest	78	70	78
Third Highest	76	69	78
Fourth Highest	76	68	78
Fifth Highest	74	67	76
Design Value	74		

Table 3-9. Site-specific ozone design values for the Indian Springs monitoring site. The top five highest ozone concentrations for 2018-2020 at Indian Springs are shown, and proposed EE days in 2018 and 2020 are included.

Indian Springs Rank	2018	2019	2020
Highest	78	69	78
Second Highest	75	66	72
Third Highest	74	66	71
Fourth Highest	73	65	69
Fifth Highest	73	65	68
Design Value	69		

For further comparison with non-event ozone concentrations, **Table 3-10** shows five-year (2015-2019, proposed 2018 EE events included) MDA8 ozone statistics for the weeks before and after August 7. This two-week window analysis shows that each affected monitoring site shows MDA8 ozone concentrations on August 7, 2020, to be well above the average and above the 95th percentile of the last five years of data.

Table 3-10. Two-week non-event comparison. August 7, 2020, MDA8 ozone concentrations for each affected site are shown in the top row. Five-year (2015-2019) average MDA8 ozone statistics for July 31 through August 14 are shown for each affected site around Clark County to compare with the event ozone concentrations.

	Indian Springs 320037772	Joe Neal 320030075	Walter Johnson 320030071
Aug. 7	72	72	71
Mean	55	59	58
Median	55	59	58
Mode	52	51	57
St. Dev	7	9	9
Minimum	41	38	36
95 %ile	68	73	72
99 %ile	71	76	77
Maximum	72	81	82
Range	31	43	46
Count	96	96	96

The percentile, rank-ordered analyses, and the two-week window analysis, indicate that all affected monitoring sites on August 7 showed atypically high ozone concentrations compared with non-event concentrations. This conclusion supports a key factor, suggesting that August 7 was an EE in Clark County, Nevada.

3.2.3 Satellite Retrievals of Pollutant Concentrations

Satellite retrievals of pollutants associated with wildfire smoke, such as AOD, CO, and NO_x, can provide evidence that smoke was present at a monitoring site. We examined maps of Multi-Angle Implementation of Atmospheric Correction (MAIAC) AOD from the Moderate Resolution Imaging Spectroradiometer (MODIS) instrument onboard the Aqua and Terra satellites, CO retrievals from the

Atmospheric Infrared Sounder (AIRS) instrument onboard the Aqua satellite, and NO₂ retrievals from the Ozone Monitoring Instrument (OMI). These maps provide evidence to support the transport of smoke from the Apple Fire in southern California to Clark County, Nevada, as already demonstrated with visual imagery and trajectories in Sections 3.1 and 3.2. MODIS AOD measurements indicate the concentration of light-absorbing aerosols, including those emitted by wildfires, in the total atmospheric column. Between August 4 and 7, AOD measurements show the movement of a plume of aerosols originating from the Apple Fire (Figure 3-25). This plume spread from the Apple Fire northeastward towards southern Nevada, and western Arizona between August 4 and 7. MODIS AOD retrievals show a consistent picture of enhanced AOD near the Apple Fire, however AOD decreases as the plume moves toward the Clark County area on August 7 (Figure 3-26).

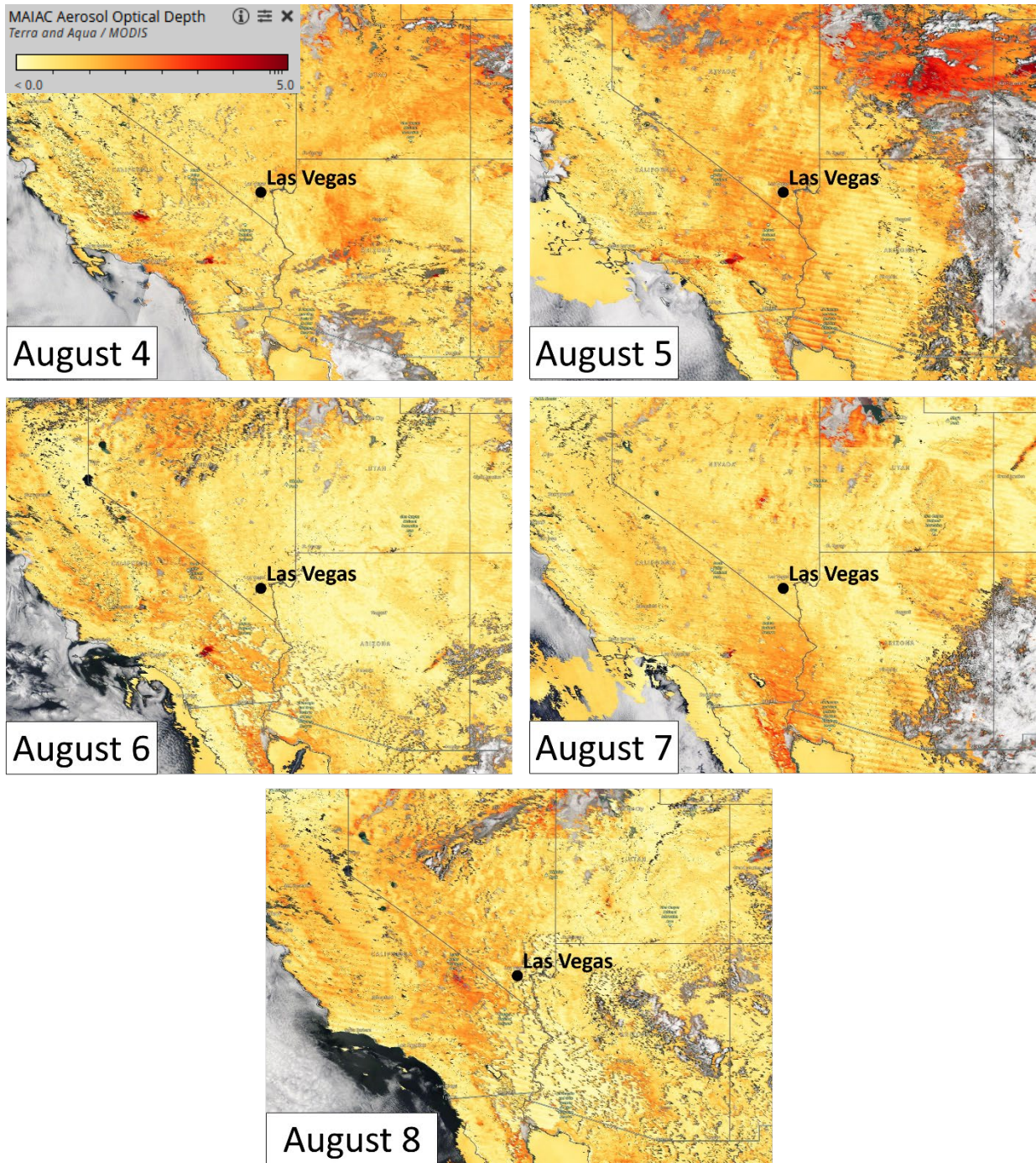


Figure 3-25. MAIAC MODIS Aqua/Terra combined AOD retrievals for the three days before the EE, during the EE on August 7, and the day after the EE.

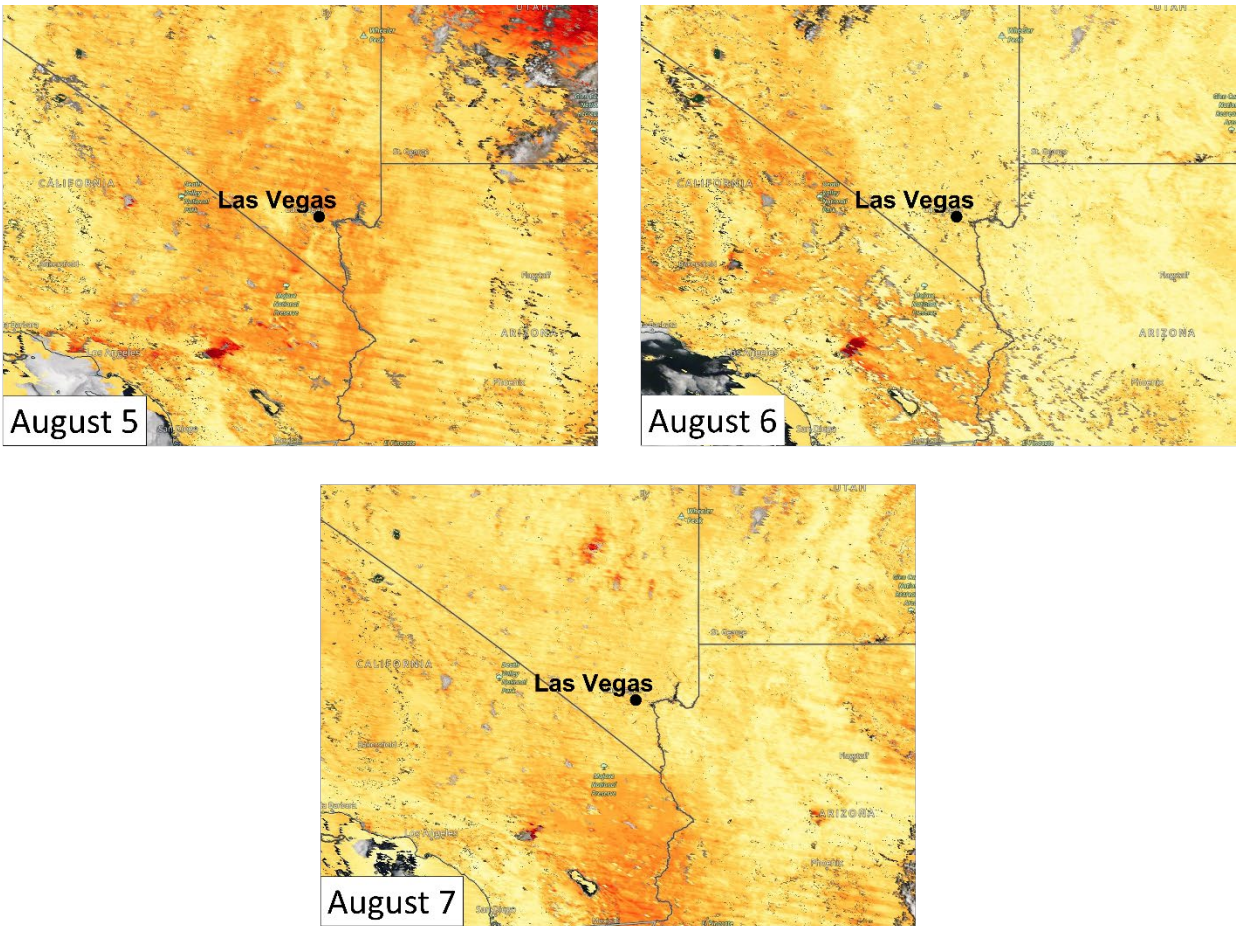


Figure 3-26. A zoomed-in view over Clark County and the Apple Fire of the MAIAC MODIS Aqua/Terra combined AOD retrieval two days before the EE and during the EE on August 7, 2020.

CO measurements at 500 hPa from AIRS show a similar pattern of smoke plume transport seen in the MODIS AOD data noted above. Unfortunately, CO measurements over and near the Clark County area were not captured by AIRS on August 7. CO satellite retrievals on the days before and after the August 7 event can be found in [Appendix B](#). Additionally, OMI NO₂ satellite retrievals were inconclusive for August 7 and were also moved to Appendix B.

3.2.4 Supporting Pollutant Trends and Diurnal Patterns

Ground measurements of wildfire plume components (e.g., PM_{2.5}, CO, NO_x, and VOCs) can be used to further demonstrate that smoke impacted ground-level air quality if enhanced concentrations or unusual diurnal patterns are observed. We examined concentrations of PM_{2.5}, CO, NO, NO₂, and TNMOC measured at all exceedance sites, as well as other nearby sites in Clark County. If PM_{2.5}, CO, NO_x, and VOC concentrations were enhanced at the time the smoke plume arrived in Clark County, these measurements would provide additional supporting evidence of smoke impacts in Clark County.

Figure 3-27 shows an overall view of the magnitude of pollutant concentrations measured around Clark County during the August 7 event. The night before August 7, each supporting pollutant shows a spike in concentration between 10 p.m. and 12 a.m. The close alignment of these increases is demonstrative of the buildup of pollutants from wildfire smoke in the days and hours leading up to the event. The rest of this section examines temporal abnormalities and site-specific trends for each supporting pollutant. Because less than one season's worth of data is available for TNMOC, this pollutant is excluded from detailed examination below.

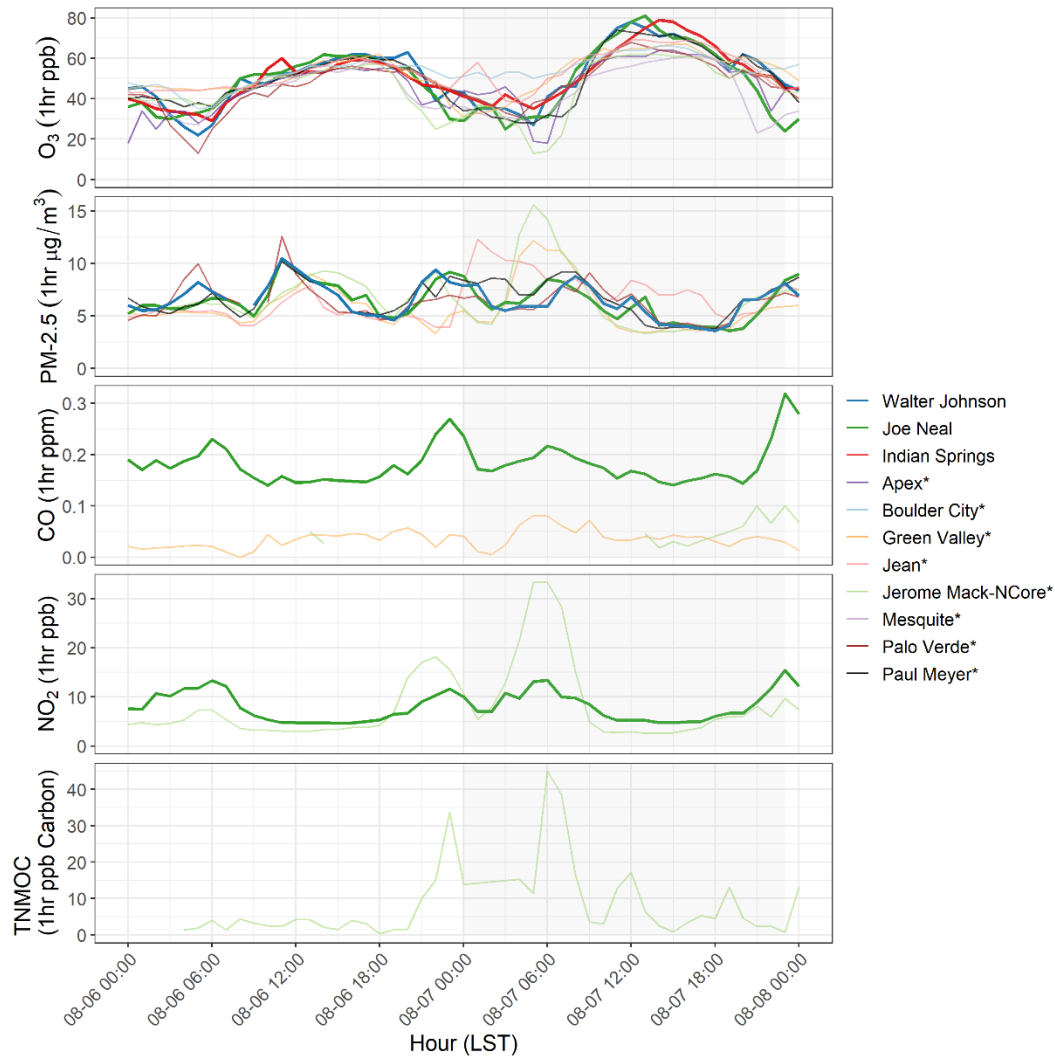


Figure 3-27. Hourly concentrations of ozone, PM_{2.5}, NO_x and TNMOC. Colored lines represent sites in exceedance on August 7. Gray lines represent supporting sites in Clark County. The gray bar represents August 7.

Unusual diurnal patterns of supporting measurements provide further evidence that smoke impacted Clark County air quality. **Figure 3-28** shows the diurnal profile for ozone and PM_{2.5} at the sites in Clark County that experienced an exceedance on August 7. Three years of PM_{2.5} data are available from Joe Neal, and one year of PM_{2.5} data is available from Walter Johnson. The seasonal (May to September) average ozone and PM_{2.5} concentrations are also shown. On a typical day, the diurnal profile of ozone shows a peak around midday and an overnight trough; the diurnal profile of PM_{2.5} exhibits the opposite behavior, with maximum levels overnight and a trough during the afternoon. On August 6, midday PM_{2.5} levels at both Walter Johnson and Joe Neal are elevated above average. This is demonstrative of an abnormal PM_{2.5} source impacting these sites and indicate that wildfire

emission plume buildup during the preceding day could have contributed to elevated ozone concentrations on the event date. Notably, a late-night spike in PM_{2.5} concentrations between August 6 and 7 (10 p.m. and 12 a.m.) is mirrored by other supporting pollutants examined below. Plots of PM₁₀/PM_{2.5} are included in [Appendix C](#), and indicate that the contribution of dust to abnormalities in PM_{2.5} concentration are minimal. Ozone was well above average at its peak at all sites on August 7.

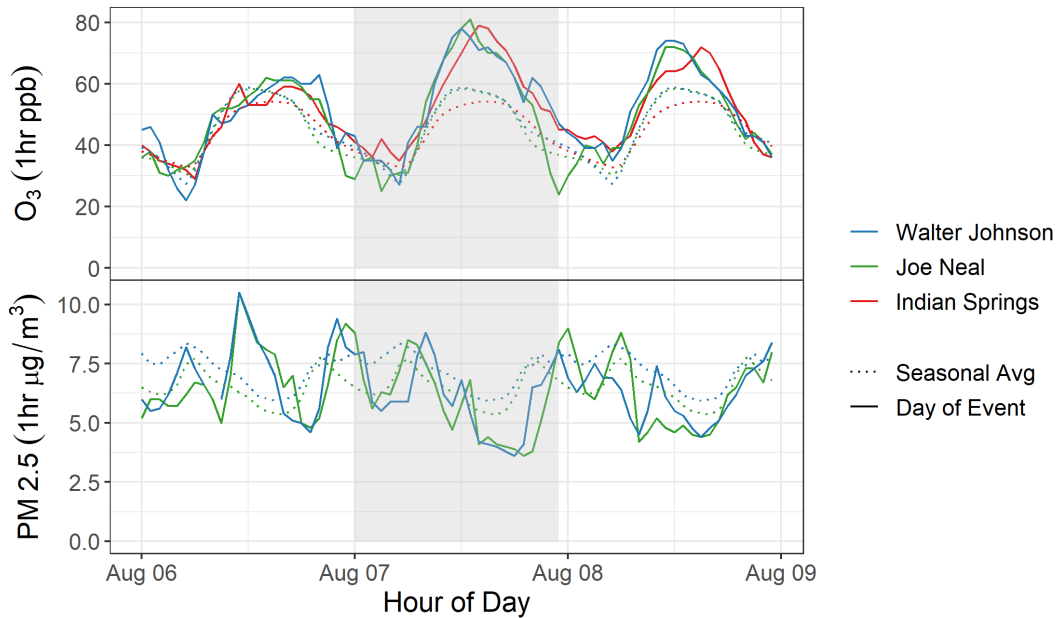


Figure 3-28. August 7 diurnal profile of ozone and PM_{2.5} (solid), and the five-year seasonal (May-Sept.) average (dotted) at sites in exceedance on August 7, 2020.

Figures 3-29 through 3-30 further display the diurnal profile and average seasonal diurnal profile of ozone and PM_{2.5} separated by event-affected monitoring site, along with the 5th-95th percentile range of historical values. On August 6, an abnormal midday peak in PM_{2.5} levels occurred at both sites during a time of day when, on average, PM_{2.5} levels are expected to decrease. An abnormal PM_{2.5} peak at 11 p.m. local time on August 6 was also observed at the Joel Neal site. All PM_{2.5} concentrations were below the 95th percentile of seasonal PM_{2.5} concentration diurnal profiles. Each site recorded a daily peak value for ozone above the 95th percentile of seasonal ozone concentrations.

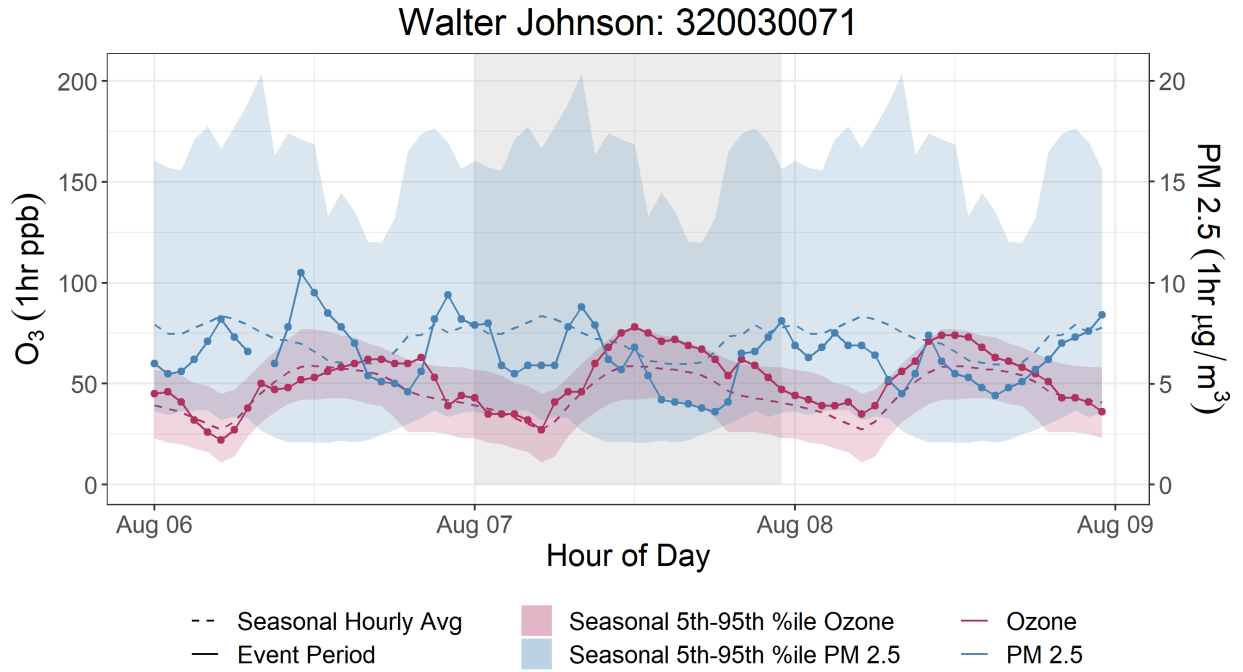


Figure 3-29. Diurnal profile of ozone (red) and PM_{2.5} (blue) concentrations at the Walter Johnson site, including concentrations on August 7 (solid) and the seasonal (May-Sept.) average (dotted). Shaded ribbons represent the 5th-95th percentile range.

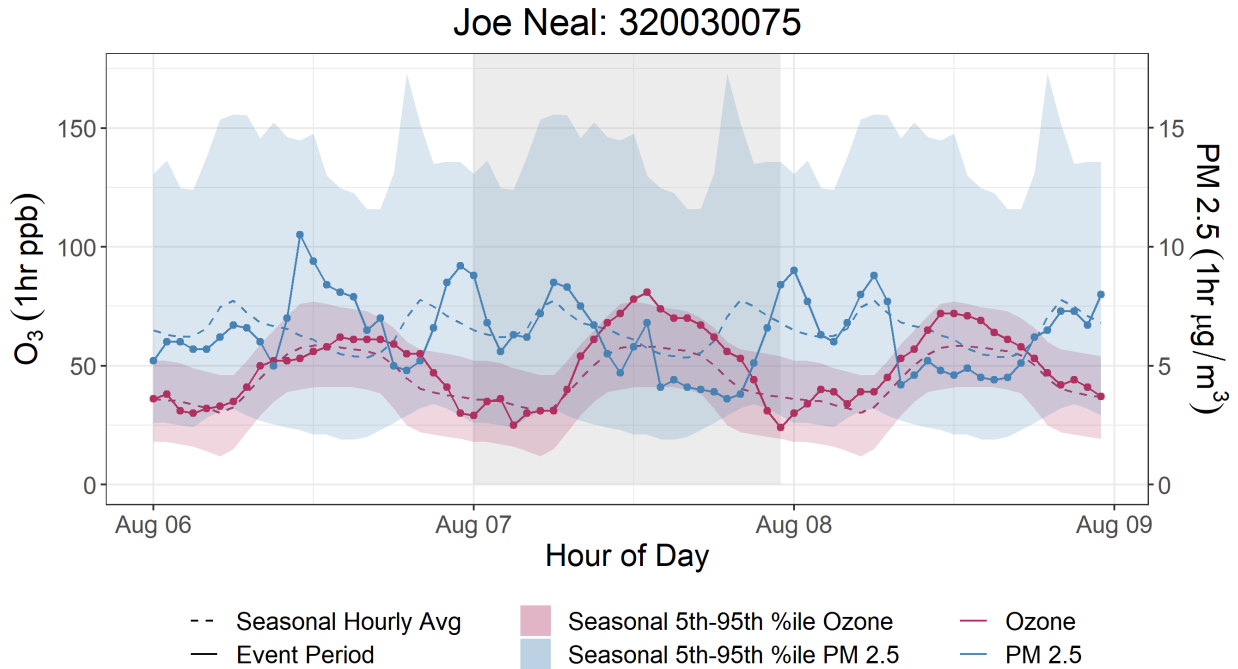


Figure 3-30. Diurnal profile of ozone (red) and PM_{2.5} (blue) concentrations at the Joe Neal site, including concentrations on August 7 (solid) and the seasonal (May-Sept.) average (dotted). Shaded ribbons represent the 5th-95th percentile range.

A diurnal profile of ozone and CO at Joe Neal, the only exceedance site at which CO data are available, on August 7 is displayed in [Figure 3-31](#). Two years of CO data are available from Joe Neal. There are deviations from the diurnal profile of CO concentrations on the night before the event date, aligning with a similar spike in PM_{2.5}, NO₂, and VOC concentrations noted above. However, all CO concentrations prior to and on the event date were at or below the 95th percentile of seasonal CO concentration diurnal profiles. These plots also display the five-year weekday and weekend average diurnal profile of CO, and the five-year 5th-95th percentile range. Where five years of CO data were not available for a site, data from the National Core (NCORE) reference site, Jerome Mack, were used. CO levels did not rise markedly with the peak in ozone on August 7 at the Joe Neal, Green Valley, or Jerome Mack (reference) sites.

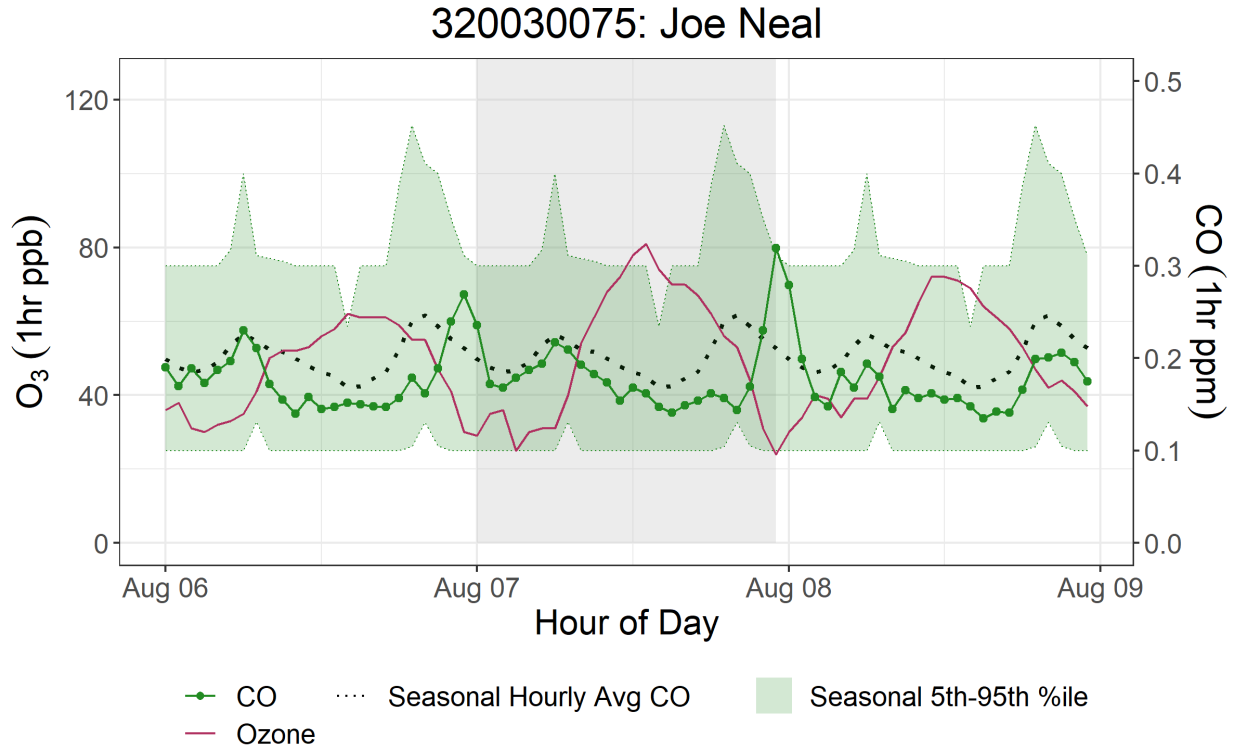


Figure 3-31. Ozone (red) and CO (green) concentrations for the Joe Neal site on August 7. The dotted line shows the seasonal (May to Sept) diurnal average. The green shaded area indicates the seasonal 5th-95th percentile values for statistical reference. The gray bar highlights the event date.

Lastly, concentrations of NO₂ were examined for the August 7 event in Clark County. NO₂ data are available only at the Joe Neal event site (five years of available data) and shown in [Figure 3-32](#). In comparison to the five-year average, NO₂ observations at the Joe Neal site were elevated in the late-night hours of August 6. This spike in NO₂ concentrations between 10 p.m. and 12 a.m. aligns closely with similar increases in CO, VOCs, and PM_{2.5} throughout Clark County, indicating an overnight buildup of wildfire smoke and accompanying ozone precursors in the region. However, all NO₂ concentrations prior to and on the event date were at or below the 95th percentile of seasonal NO₂ concentration diurnal profiles.

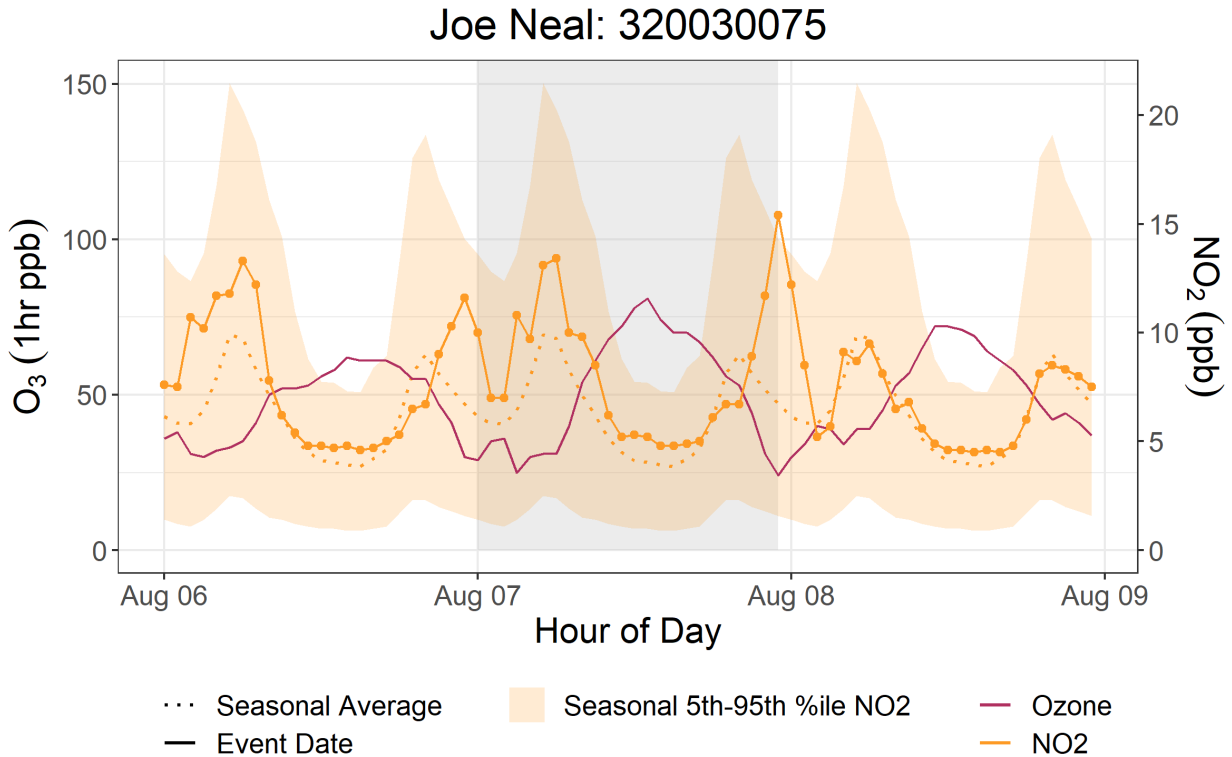


Figure 3-32. Ozone and NO₂ concentrations during the August 7 EE at Joe Neal. Ozone concentrations (red, solid lines), NO₂ concentrations (orange, solid lines), the five-year seasonal average of NO₂ (May – Sept.) (orange, dotted lines), and the seasonal 5th-95th percentile (orange, shaded area) for is shown for the August 7 EE period at Joe Neal.

The supporting pollutant trends and diurnal patterns, showing abnormal peaks in PM_{2.5}, CO and NO₂ the evening prior to the event date, and ozone concentrations outside of their normal seasonal or yearly historical averages, provide evidence of smoke impacts on the Clark County area throughout the day on August 7, 2020. Wildfires can generate the precursors needed to create ozone, NO_x, and VOCs. While ozone concentrations can be suppressed very near a fire due to NO_x titration, downwind areas are likely to see an increase in ozone concentrations due to the presence of both precursor gases and sufficient UV radiation (i.e., when an air mass leaves an area of very thick smoke that inhibited solar radiation) (Finlayson-Pitts and Pitts Jr, 1997; Jaffe et al., 2008; Bytnerowicz et al., 2010). Ozone precursors from wildfire smoke can also be transported a significant distance downwind, and if these compounds are mixed into an urban area (such as Las Vegas), the ozone concentrations produced can be significantly higher than they would be from either the smoke plume or the urban area alone (Jaffe et al., 2013; Wigder et al., 2013; Lu et al., 2016; Brey and Fischer, 2016). Since we find evidence of smoke impacts on August 7 in Clark County via supporting pollutant measurements and other analyses in Sections 3.1 and 3.2, we suggest that both the direct transport of ozone and the transport of ozone precursor gases likely caused the ozone exceedance.

Filter samples were also taken at the Jerome Mack monitoring site (including a collocated sample) in Clark County every three days during 2020. From these filter samples, concentrations of levoglucosan (a wildfire smoke tracer) were analyzed by the Desert Research Institute (DRI) using gas chromatography-mass spectroscopy (GC-MS). Levoglucosan is produced by the combustion of cellulose and can be emitted during large wildfire events at high concentrations that can be transported downwind (Simoneit et al., 1999; Simoneit, 2002; Bhattarai et al., 2019). Levoglucosan has an atmospheric lifetime of one to four days before it is lost due to atmospheric oxidation, and therefore can be used as a tracer of biomass burning (wildfires) far downwind from its source (Hoffmann et al., 2009; Hennigan et al., 2010; Bhattarai et al., 2019; Lai et al., 2014). In the Las Vegas region, residential wood combustion has historically not been a significant contributor to levoglucosan concentrations during the late summer time frame (Kimbrough et al., 2016). **Table 3-11** shows levoglucosan concentration, uncertainty, and positive/negative detection certainty during the August 7 event. Table 3-11 also shows the average levoglucosan concentration from 19 background days in 2018 and 2019 together with its standard deviation, and propagated uncertainty at the Jerome Mack site for comparison. On these background days, no ozone exceedance was observed, and fire/smoke influence was minimal according to HMS. When smoke from the Apple Fire reached Clark County on August 7, non-zero levoglucosan concentrations and positive detections are seen. The 16 and 20 ng/m³ detection of levoglucosan in Clark County at the Jerome Mack site and collocated measurement at Jerome Mack (respectively) is significantly higher than the background average of 2±3 ng/m³, providing certain evidence that wildfire smoke was affecting the area during the time period of the August 7 ozone exceedance.

Table 3-11. Levoglucosan concentrations at monitoring sites around Clark County, Nevada, before and after the August 7 ozone event. Positive or negative detection is also shown.

Sample Date	Sampling Site	Levoglucosan (ng/m ³)	Levoglucosan Uncertainty (ng/m ³)	Levoglucosan Detected?
Background days (2018-2019)	Jerome Mack	2±3	1	N/A
8/7/2020	Jerome Mack	16	1	Positive
	Collocated-Jerome Mack	20	1	Positive

3.3 Tier 3 Analyses

3.3.1 Total Column & Meteorological Conditions

Satellite analyses and HYSPLIT trajectories shown in Section 3.1 provide strong evidence that smoke was present over Clark County on August 7, 2020. However, the visible true color, AOD, and CO satellite data do not provide information about the vertical distribution of visible or measured smoke components. We examined ceilometer mixing height measurements to determine whether the smoke plume was present at or near the surface on August 7. Unfortunately, Cloud-Aerosol Light Detection and Ranging (LIDAR) and Infrared Pathfinder Satellite Observation (CALIPSO) data, which provide vertical profile measurements of atmospheric aerosols and clouds, were not available immediately before or during the August 7 event. CALIPSO data near (but upwind) of the Apple Fire are available in [Appendix D](#) for reference.

The mesoscale and local meteorological conditions from August 4 to 7 provide evidence for transport of smoke from the Apple Fire in southern California to Clark County, Nevada, as well as subsequent vertical mixing of smoke from aloft to the surface. Upper-level wind barbs at 500 hPa indicate that the persistent southwesterly wind directions caused smoke from the Apple Fire to move into the Clark County Area (Figure 3-33).

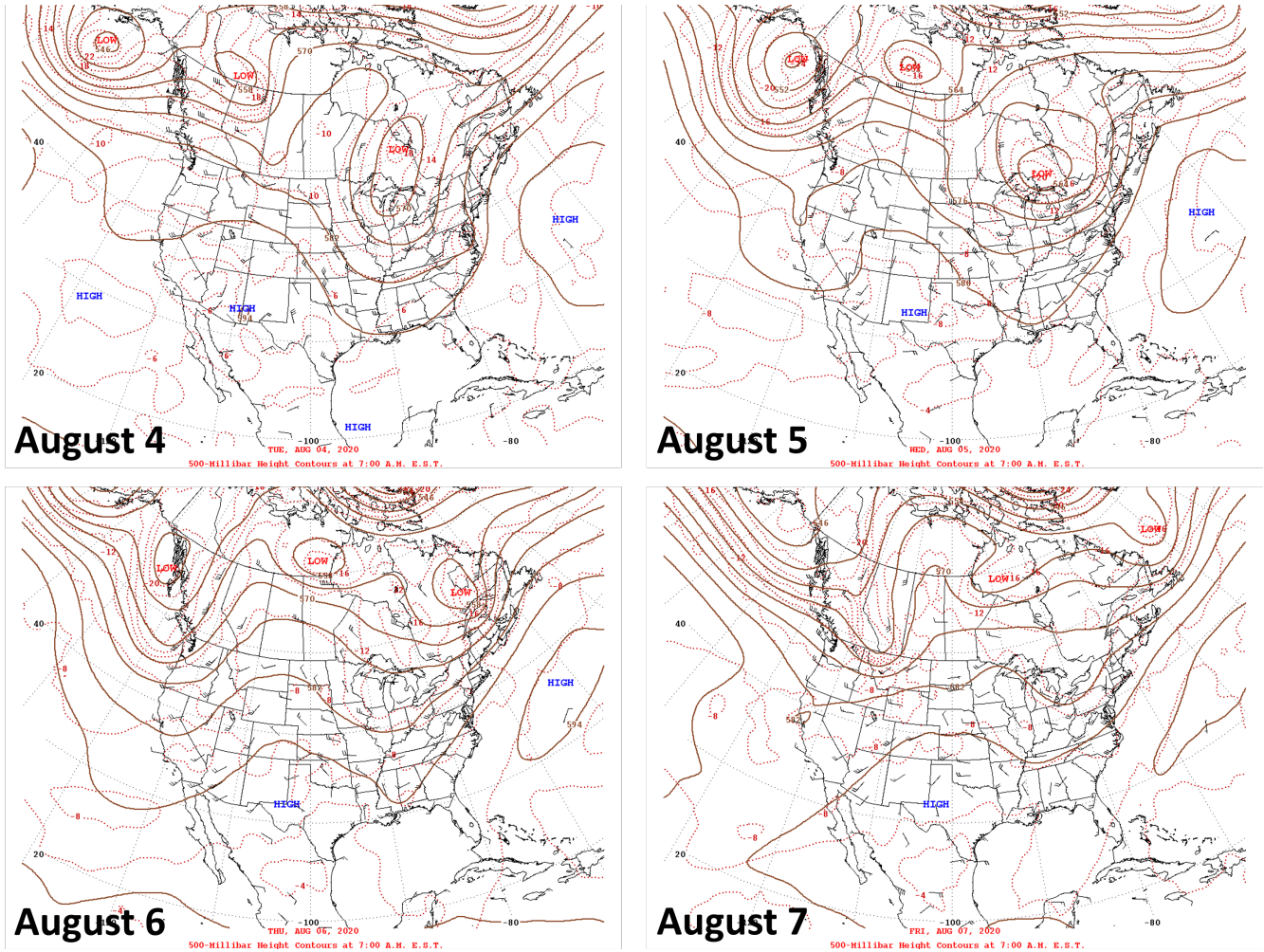


Figure 3-33. Daily upper-level meteorological maps for the three days leading up to the EE and during the August 7 EE.

Local observations of mixing heights in the Las Vegas area on August 6 and 7 suggest that smoke was likely mixed into the lower levels of the atmosphere. Ceilometer data from the Jerome Mack site on August 6 and 7 indicate mixing heights between approximately 2,000 and 3,000 m for several hours during the days (Figure 3-34). Furthermore, a surface low-pressure system was centered over the border of Nevada and California between August 4 and 7. Low pressure at the surface is often associated with enhanced vertical mixing in the lower troposphere (Figure 3-35). Mixing height data

from the ceilometer and the surface weather maps provide evidence of enhanced vertical mixing in the lower troposphere when smoke was present over Clark County.

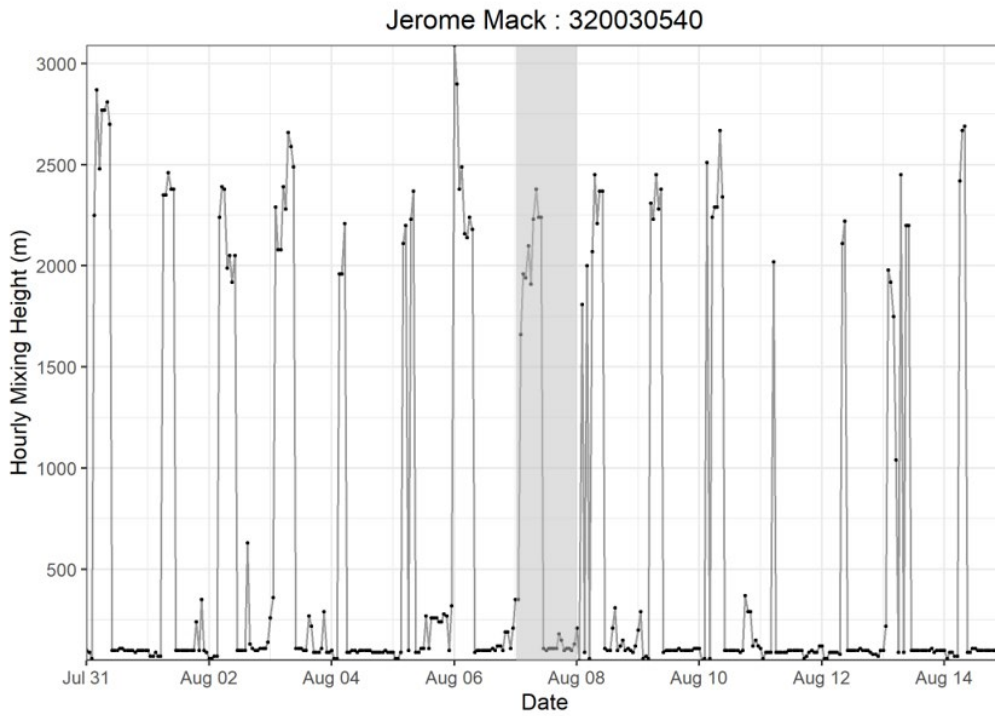


Figure 3-34. Time series of mixing heights taken from the Jerome Mack site (NCore site) for two weeks before and after the August 7 EE day. The shaded grey area highlights August 7, 2020.

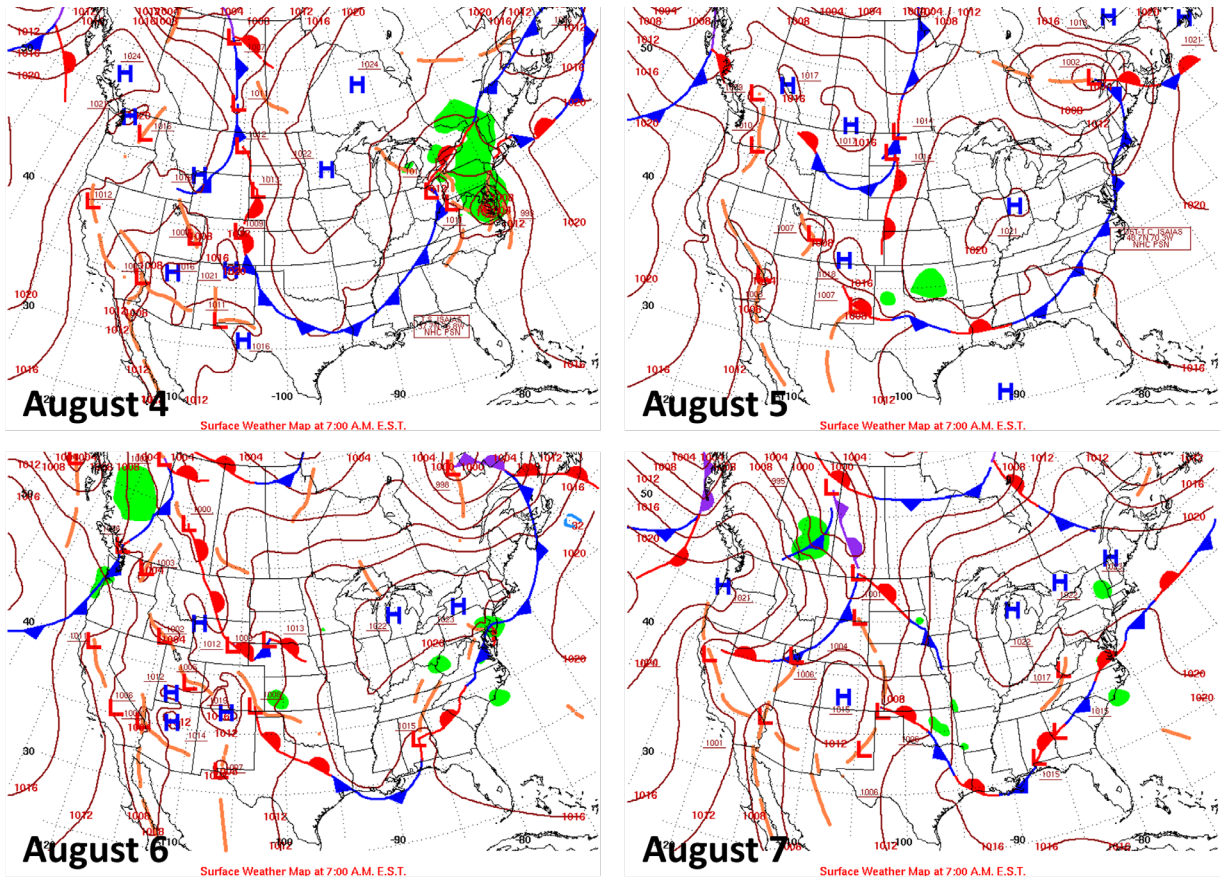


Figure 3-35. Daily surface meteorological maps for the three days leading up to the EE and during the August 7 EE.

In addition to the ceilometer-based measurements of mixing heights, vertical temperature profiles (Skew-T diagrams) can be used to estimate mixing heights. The vertical temperature profile at Las Vegas from August 4 to 7 shows the vertical atmospheric profile becoming drier in the lower troposphere—as shown by the widening between the temperature profile and the dewpoint profile—with wind directions consistently from the south and southwest (Figures 3-36 and 3-37), indicating smoke transport in the lower levels of the atmosphere from the Apple Fire into Clark County. Enhanced vertical mixing from August 4 and 5 to August 6 and 7 can be seen from a more pronounced, very large mixed layer—as indicated by temperatures decreasing with height roughly along the dry adiabat up to at least 600 hPa—with associated warm temperatures and very dry air. The upper-level and surface weather maps, ceilometer data, and the vertical temperature and wind profiles provide evidence that smoke from the Apple Fire was transported in the free troposphere and/or within the deep mixed layer and subsequently mixed down to the surface at Clark County.

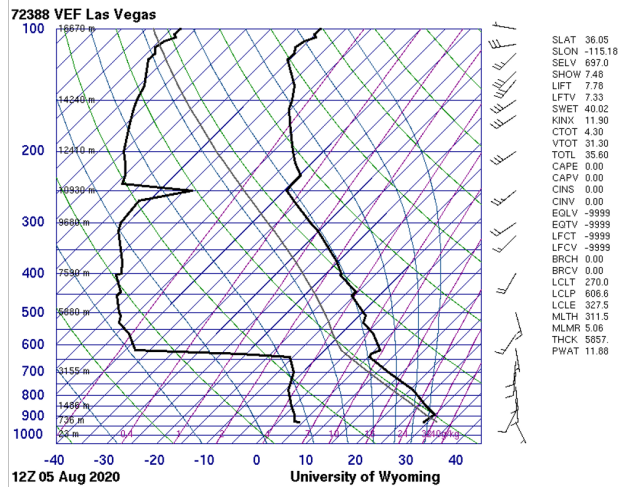
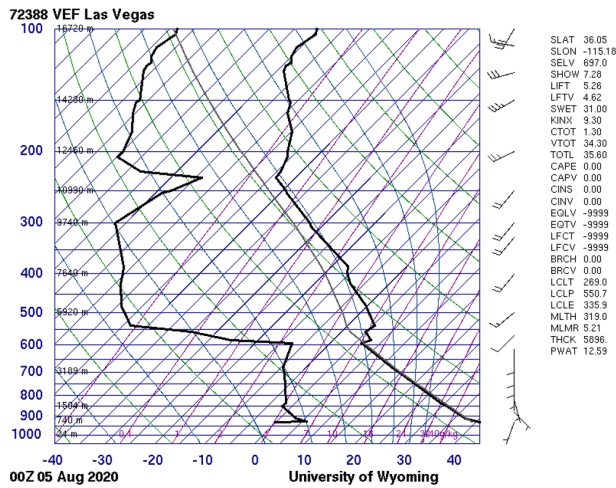
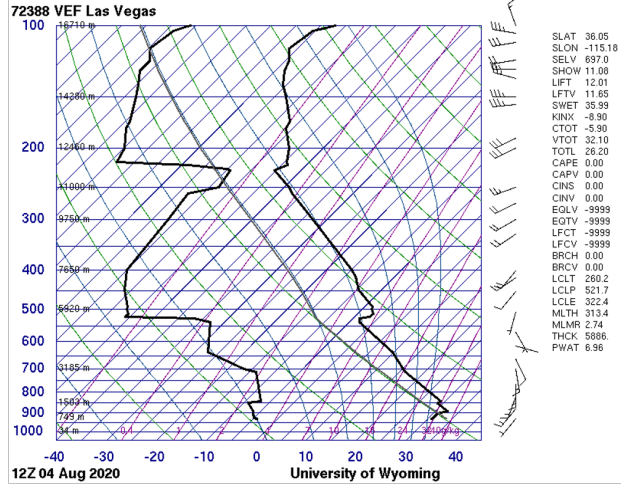
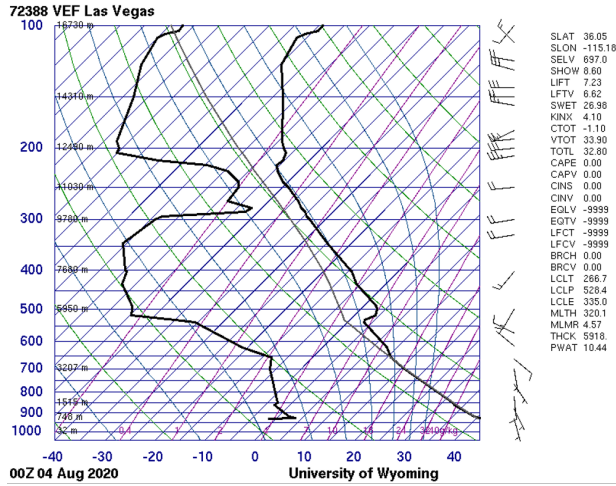


Figure 3-36. Skew-T diagrams from August 4 and 5, 2020, in Las Vegas, Nevada.

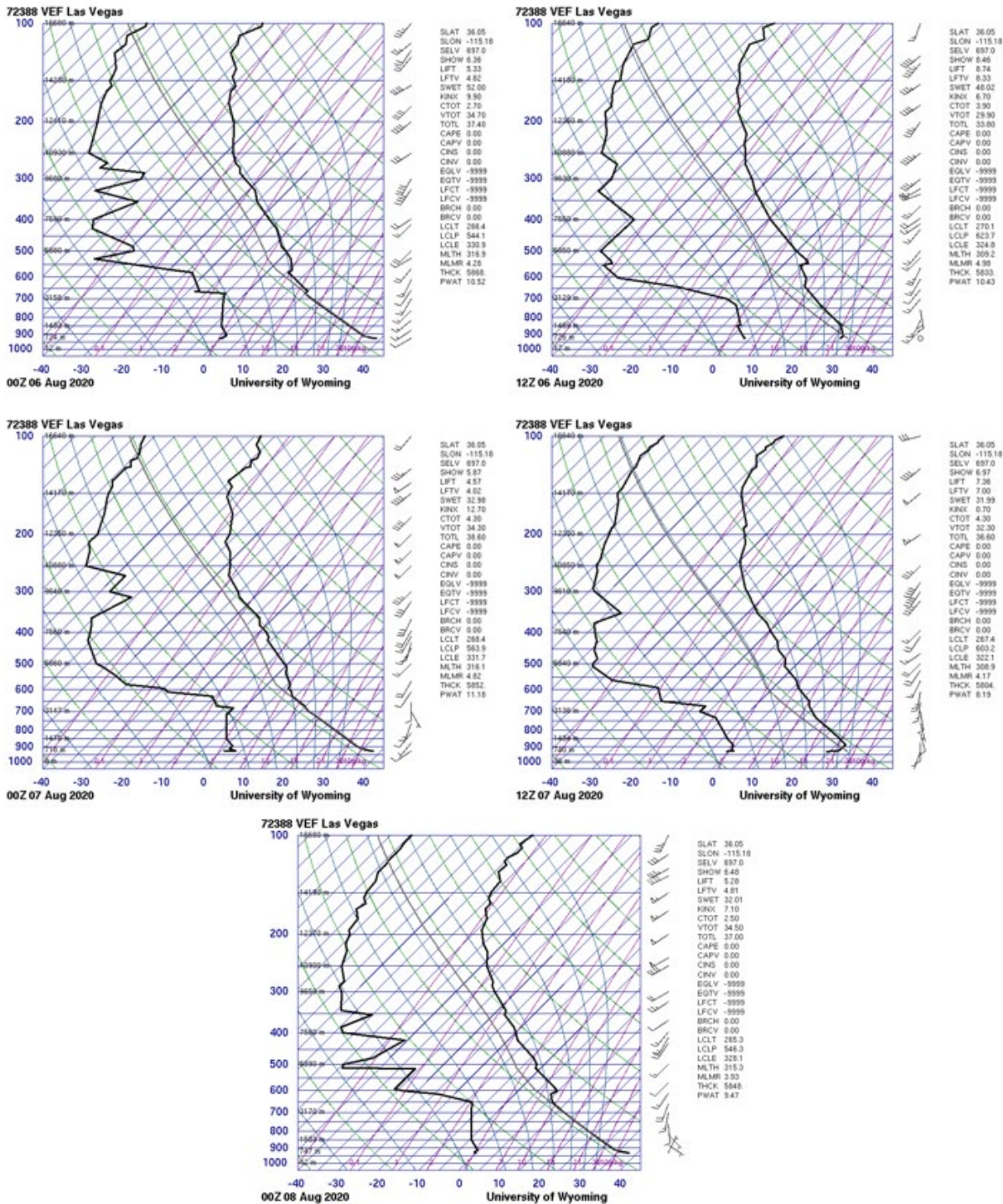


Figure 3-37. Skew-T diagrams from August 6 and 7, 2020 (local time), in Las Vegas, Nevada.

3.3.2 Matching Day Analysis

Ozone production and transport strongly depend on regional and local meteorological conditions. A comparison of ozone concentrations on suspected exceptional event days with non-event days that share similar meteorology can help identify periods when ozone production was affected by an atypical source. Given that similar meteorological days are likely to have similar ozone concentrations, noticeable differences in levels of ozone between the event date and meteorologically similar days can lend evidence to a clear causal relationship between wildfire smoke and elevated ozone concentration.

Identify Meteorologically Similar Days

In order to identify the best matching meteorological days, both synoptic and local conditions were examined from ozone-season days (April 1 through September 30) between 2014 and 2020. Excluded from this set are days with suspected EEs in the 2018 and 2020 seasons, as well as dates within 5 days of the event date, to ensure that lingering effects of smoke transport or stratospheric intrusion did not appear in the data.

To best represent similar air transport, twice daily HYSPLIT trajectories (initiated at 18:00 and 22:00 UTC) from Clark County for 2014-2020 were clustered by total spatial variance. The calculation, based on the difference between each point along a trajectory, provides seven distinct pathways of airflow into Clark County (see Section 3.3.3 for more details). The cluster that best represents the trajectory on the EE day was chosen, and ozone-season days within the cluster were then subset for regional meteorological comparison to the EE day.

For the meteorological comparison, a correlation score was assigned to each day from the cluster subset. The National Centers for Environmental Prediction (NCEP) reanalysis data were compiled for the ozone seasons in 2014-2020. Daily average wind speed, geopotential height, relative humidity, and temperature were considered at 1000 mb and 500 mb. At the surface, daily average atmospheric pressure, maximum temperature, and minimum temperature were utilized. Pearson product-moment coefficient of linear correlation (pattern correlation) was calculated between the EE date and each cluster-subset ozone-season day in 2014-2020 for each parameter. The pattern correlation calculates the similarity between two mapped variables at corresponding grid locations within the domain. The statistic was calculated using a regional domain of 30°N-45°N latitude and 125°W-105°W longitude. The correlation score for each day was defined as the average pattern correlation of all parameters at each height level. The correlation scores were then ranked by the highest correlation for 1000 mb, surface, and finally 500 mb. Dates within 5 days of the EE were removed from the similar day analysis to ensure the data are mutually exclusive. The 50 dates with the highest rank correlation scores were then chosen as candidate matching days for further analysis.

Local meteorological conditions for the subset of candidate matching days were then compared to conditions on August 7, 2020, and filtered to identify five or more days that best matched the event

date. Meteorological maps at the surface and 500 mb, and local meteorological data describing temperature, wind, moisture, instability, mixing layer height, and cloud cover were examined. The data source for each parameter is summarized in [Table 3-12](#).

Table 3-12. Local meteorological parameters and their data sources.

Meteorological Parameter	Data Source
Maximum daily temperature	Jerome Mack - NCore Monitoring Site
Average daily temperature	Jerome Mack - NCore Monitoring Site
Resultant daily wind direction	Jerome Mack - NCore Monitoring Site (calculated vector average)
Resultant daily wind speed	Jerome Mack - NCore Monitoring Site (calculated vector average)
Average daily wind speed	Jerome Mack - NCore Monitoring Site
Average daily relative humidity (RH)	Jerome Mack - NCore Monitoring Site
Precipitation	Jerome Mack - NCore Monitoring Site
Total daily global horizontal irradiance (GHI)	UNLV Measurement and Instrumentation Data Center (MIDC) in partnership with NREL (https://midcdmz.nrel.gov/apps/daily.pl?site=UNLV&start=20060318&yr=2021&mo=4&dy=29)
4:00 p.m. local standard time (LST) mixing layer mixing ratio	Upper air soundings from KVEF (http://weather.uwyo.edu/upperair/sounding.html)
4:00 p.m. LST lifted condensation level (LCL)	Upper air soundings from KVEF (http://weather.uwyo.edu/upperair/sounding.html)
4:00 p.m. LST convective available potential energy (CAPE)	Upper air soundings from KVEF (http://weather.uwyo.edu/upperair/sounding.html)
4:00 p.m. LST 1000-500 mb thickness	Upper air soundings from KVEF (http://weather.uwyo.edu/upperair/sounding.html)
Daily surface meteorological map	NOAA's Weather Prediction Center Daily Weather Maps (https://www.wpc.ncep.noaa.gov/dailywxmap/index.html)
Daily 500 mb meteorological map	NOAA's Weather Prediction Center Daily Weather Maps (https://www.wpc.ncep.noaa.gov/dailywxmap/index.html)

Matching Day Analysis

The meteorological conditions on August 7, 2020, were normal for the region at this time of year. [Table 3-13](#) displays that the percentile ranking of each examined meteorological parameter other than relative humidity at the Jerome Mack-NCORE site falls within the 5th-95th percentile range among 7 years of observations for the 30-day period surrounding August 7 (July 23 through August 22). Measurement summaries over this 30-day period best represent the expected conditions on the event date. The maximum temperature on August 7 was below the median for this time of year, though conditions were quite dry on this date. The relative humidity is at the 9th percentile and the mixing layer mixing ratio is at the 8th percentile. As is typical for Clark County during this period, there was no precipitation.

The subset of synoptically similar days identified according to the methodology above was further filtered based on parameters listed in [Table 3-12](#) to match local meteorological conditions that existed on the event date. [Table 3-14](#) shows the 19 days that best match the meteorological conditions that existed on August 7, 2020, as well as the MDA8 ozone concentration at each site that experienced an ozone exceedance on August 7, 2020. One matching day, June 19, 2015, was omitted from this analysis due to evidence of smoke impact in Clark County (see [Appendix E](#)). Surface maps for August 7, 2020, and each date listed in [Table 3-14](#), show consistent conditions with a surface low-pressure system over Clark County. In the upper atmosphere, a region of low-gradient, relatively high pressure sits over Clark County on most identified dates. Surface and upper-level maps are included in [Appendix E](#).

[Table 3-14](#) shows the average MDA8 ozone concentration across these 19 days with a range defined by one standard deviation, a conservative estimate given the small sample size. The expected MDA8 ozone concentration, given similar meteorological conditions to those on the event date, is well below the 70-ppb ozone standard at each site, ranging from 59 to 61 ppb. Further, the upper end of the provided range at each site also falls below the ozone standard. Only one date out of the 19, June 8, 2018, exceeds the 70-ppb ozone standard on a day when morning transport came directly from the Los Angeles basin and the HRRR model showed effects of smoke on this day (see [Appendix E](#)). However, because the HYSPLIT model did not intersect smoke and there were no fires immediately upwind, this date was not excluded from the analysis. Several similar dates with higher photochemical potential than August 7 (lower wind speeds, higher average temperatures, and greater solar irradiance) did not exceed the ozone standard. Thus, an ozone exceedance on August 7, 2020, was unexpected based on meteorological conditions alone. If meteorology were the sole cause of the ozone exceedance on August 7, 2020, we would expect to see similarly high ozone levels on each of the days with similar conditions listed in [Table 3-14](#), especially those with even warmer average temperatures than experienced on August 7.

Table 3-13. Percentile rank of meteorological parameters on May 6, 2020, compared to the 30-day period surrounding August 7 over seven years (July 23 through August 22, 2014-2020). The percentile ranking of precipitation is marked NA because a vast majority of observations are 0 in. The percentile ranking of a directional degree value is irrelevant and has been marked NA.

Date	Max Temp (°F)	Avg Temp (°F)	Resultant Wind Direction (°)	Resultant Wind Speed (mph)	Avg Wind Speed (mph)	Avg RH (%)	Precip (in)	Total GHI (kWh/m ²)	Mixing Layer Mixing Ratio (g/kg)	LCL (mb)	CAPE (J/kg)	500-1,000 mb Thickness (m)
2020-08-07	34	22	NA	41	35	9	NA	85	8	17	33	20

Table 3-14. Top 14 matching meteorological days to August 7, 2020. WJ, JN, and IS refer to monitoring sites Walter Johnson, Joe Neal, and Indian Springs respectively. Average MDA8 ozone concentration of meteorologically similar days is shown plus-or-minus one standard deviation rounded to the nearest ppb.

Date	Max Temp (°F)	Avg Temp (°F)	Resultant Wind Direction (°)	Resultant Wind Speed (mph)	Avg Wind Speed (mph)	Avg RH (%)	Precip (in)	Total GHI (kWh/m ²)	Mixing Layer Mixing Ratio (g/kg)	LCL (mb)	CAPE (J/kg)	500-1,000 mb Thickness (m)	MDA8 Ozone Concentration (ppb)		
													WJ	JN	IS
2020-08-07	103	91.62	132.87	2.11	3.15	8.54	0	8.2	3.93	546.35	0	5848	71	72	72
2017-08-15	99	89.42	156.74	4.41	5.52	19.21	0	7.5	6.65	626.35	0	5818	55	57	52
2018-06-08	103	90.62	140.86	1.4	3.1	8.83	0	8.83	4.58	564.05	0	5828	74	71	73
2018-06-15	102	92.71	192.03	7.38	7.99	14.38	0	7.43	5.09	576.91	0	5843	43	41	49
2018-08-25	105	92.96	199.12	3.37	4.31	16.17	0	7.14	6.73	604.54	78.47	5854	54	54	56
2018-08-26	104	94.17	193.19	5.43	6.28	17.42	0	7.33	5.88	583.05	167.48	5865	58	54	55
2018-08-31	102	91.83	201.06	4.88	5.39	7.38	0	7.35	3.15	519.51	0	5852	56	57	50
2019-07-03	100	91.96	195.09	8.57	8.81	9.67	0	8.46	3.94	547.75	0	5839	65	64	62
2019-07-04	102	91.62	202.29	6.05	6.22	8.92	0	9.08	1.96	476.95	0	5829	60	60	55
2019-08-17	107	96.08	193.57	5.16	5.88	8.71	0	8.11	3.42	511.13	0	5889	59	59	56
2020-06-02	103	91.21	131.12	0.47	1.25	13.04	0	6.07	5.22	580.2	29.24	5828	53	55	54
2020-06-21	108	96.38	125.64	2.14	2.84	8.42	0	8.76	4.73	538.65	0	5898	63	67	62
2020-07-06	109	97.5	158.73	1.69	3.32	6.08	0	8.79	4.8	533.86	0	5912	60	60	59
2020-07-10	110	97.29	115.69	1.14	2.44	6.46	0	8.62	6.13	565.7	0	5917	68	66	68
2020-08-04	107	96.25	143.24	3.1	4.29	5	0	8.03	5.21	550.72	0	5896	64	67	68
2020-08-05	105	94.46	192.71	3.35	4.44	9.12	0	8.13	4.28	544.19	0	5868	61	62	61
2020-08-06	103	93	160.51	4.96	5.26	10.67	0	8.16	4.82	563.92	0	5852	60	59	56
2020-08-08	105	93.38	121.46	1.46	2.94	7.04	0	8.15	4.04	539.5	0	5848	68	66	66
2020-08-09	106	94	122.97	1.28	2.11	7.96	0	8.13	3.79	527.5	0	5862	63	63	57
2020-09-25	101	87.46	148.59	1.53	3.12	13.96	0	5.82	4.25	553.54	0	5866	69	70	67
Average MDA8 Ozone Concentration of Meteorologically Similar Days													61 ± 7	61 ± 7	59 ± 7

These findings show that an external source of ozone contributed to the ozone exceedance on August 7, 2020. All examined meteorological parameters besides relative humidity fall between the 5th and 95th percentile. Our analysis expanded on methods shown in the EPA guidance and a previously concurred EE to identify 19 days that are meteorologically similar to August 7, 2020 (Arizona Department of Environmental Quality, 2018). The expected MDA8 ozone concentration at each site is over 10 ppb below the concentrations measured at each site on August 7, 2020. Based on this evidence, it is unlikely that meteorology alone enhanced photochemical production of ozone enough to cause an exceedance on August 7, 2020. This validates the existence of an extrinsic ozone source on the EE date.

3.3.3 GAM Statistical Modeling

Generalized additive models (GAM) are a type of statistical model that allows the user to predict a response based on linear and non-linear effects from multiple variables (Wood, 2017). These models tend to provide a more robust prediction than Eulerian photochemical models or simple comparisons of similar events (Simon et al., 2012; Jaffe et al., 2013; U.S. Environmental Protection Agency, 2016). Camalier et al. (2007) successfully used GAM modeling to predict ozone concentrations across the eastern United States using meteorological variables with r^2 values of up to 0.8. Additionally, previous concurred exceptional event demonstrations and associated literature, i.e., Sacramento Metropolitan Air Quality Management District (2011), Alvarado et al. (2015), Louisiana Department of Environmental Quality (2018), Arizona Department of Environmental Quality (2016), and Pernak et al. (2019) used GAM modeling to predict ozone events that exceed the NAAQS standards, some in EE cases. By comparing the GAM-predicted ozone values to the actual measured ozone concentrations (i.e., residuals), we can determine the effect of outside influences, such as wildfires or stratospheric intrusions, on ozone concentrations each day (Jaffe et al., 2004). High, positive residuals suggest a non-typical source of ozone in the area but cannot specifically identify a source. Gong et al. (2017) and McClure and Jaffe (2018) used GAM modeling, in addition to ground and satellite measurements of wildfire pollutants, to estimate the enhancement of ozone during wildfire smoke events. Similar to other concurred EE demonstrations, we used GAM modeling of meteorological and transport variables to estimate the MDA8 ozone concentrations at multiple sites across Clark County for 2014-2020. To estimate the effect of wildfire smoke on ozone concentrations, we can couple the GAM residual results (observed MDA8 ozone–GAM-predicted MDA8 ozone) with the other analyses to confirm that the non-typical enhancement of ozone is due to wildfires on August 7, 2020.

Using the same GAM methodology as prior concurred EE demonstrations and the studies mentioned above, we examined more than 30 meteorological and transport predictor variables, and through testing, compiled the 16 most important variables to estimate MDA8 ozone each day at eight monitoring sites across Clark County, Nevada (Paul Meyer, Walter Johnson, Joe Neal, Green Valley, Boulder City, Jean, Indian Springs, and Jerome Mack). As suggested by EPA guidance (U.S. Environmental Protection Agency, 2016), we used meteorological variables measured at each station

(the previous day's MDA8 ozone, daily min/max temperature, average temperature, temperature range, wind speed, wind direction, or pressure), if available (see Table 2-1). If meteorological variables were not available at a specific site, we supplemented the data with National Centers for Environmental Prediction (NCEP) reanalysis meteorological data to fill any data gaps. We also tested filling data gaps with Jerome Mack meteorological data and found results had no statistical difference. We used sounding data from KVEF (Las Vegas Airport) to provide vertical meteorological components; soundings are released at 00:00 and 12:00 UTC daily. Variables such as temperature, relative humidity, wind speed, and wind direction were averaged over the first 1000 m above the surface to provide near-surface, vertical meteorological parameters. Other sounding variables, such as Convective Available Potential Energy (CAPE), Lifting Condensation Level (LCL) pressure, mixing layer potential temperature, mixed layer mixing ratio, and 500-1,000 hPa thickness provided additional meteorological information about the vertical column above Clark County. We also initiated HYSPLIT GDAS 1°x1° 24-hour back trajectories from downtown Las Vegas (36.173°N, -115.155°W, 500 m AGL) at 18:00 and 22:00 UTC (10:00 a.m. and 2:00 p.m. local standard time) each day to provide information on morning and afternoon transport during critical ozone production hours. We clustered the twice-per-day back trajectories from 2014-2020 into seven clusters. [Figure 3-38](#) shows the clusters, percentage of trajectories per cluster, and heights of each trajectory cluster. We identified a general source region for each cluster: (1) Northwest U.S., (2) Stagnant Las Vegas, (3) Central California, (4) Long-Range Transport, (5) Northern California, (6) Southern California, and (7) Baja Mexico. Within the GAM, we use the cluster value to provide a factor for the distance traveled by each back trajectory. Additionally, day of year (DOY) was used in the GAM to provide information on season and weekly processes. The year (2014, 2015, etc.) was used a factor for the DOY parameter to distinguish interannual variability.

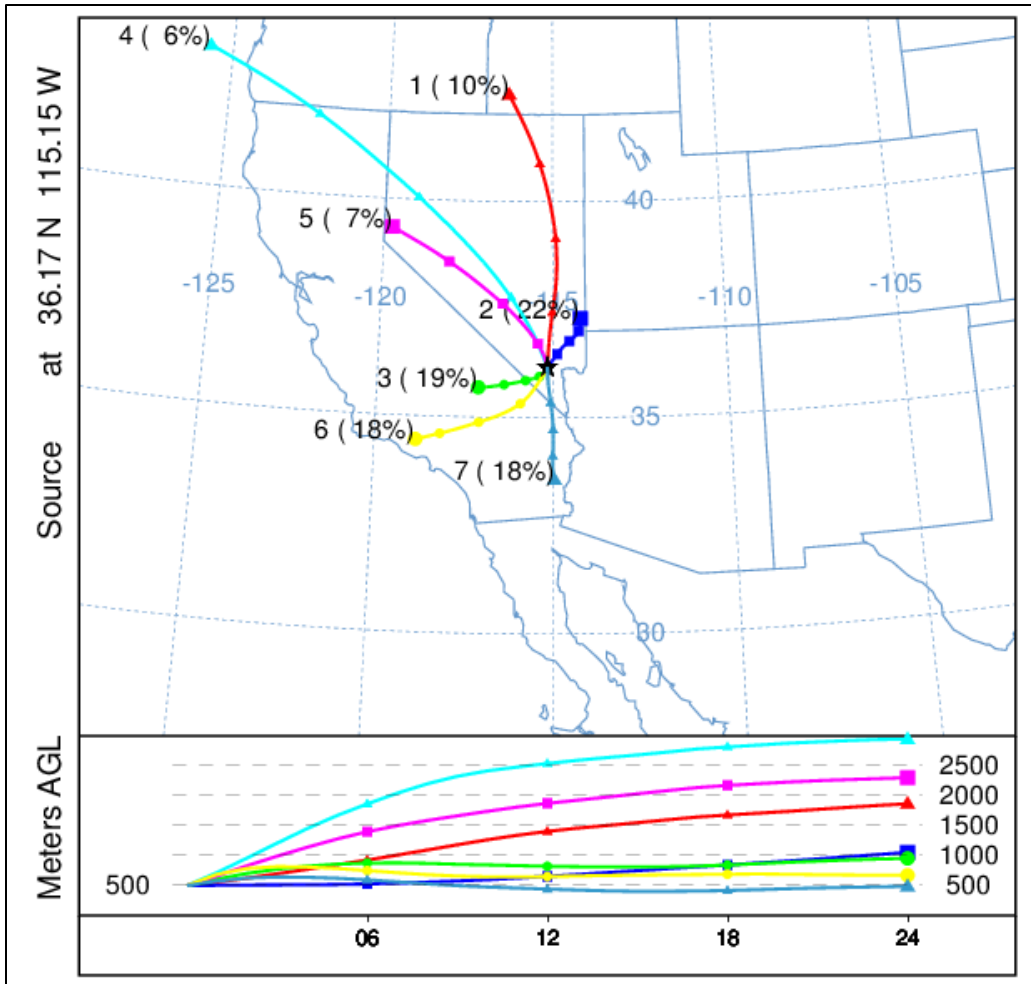


Figure 3-38. Clusters for 2014-2020 back trajectories. Seven unique clusters were identified for the twice daily (18:00 and 22:00 UTC) back-trajectories for 2014-2020 initiated in the middle of the Las Vegas Valley. The percentage of trajectories per cluster is shown next to the cluster number, and the height of each cluster is shown below the map.

Once all the meteorological and transport variables were compiled, we inserted them into the GAM equation to predict MDA8 ozone:

$$g(MDA8 O_{3,i}) = f_1(V1_i) + f_2(V2_i) + f_3(V3_i) + \dots + residual_i$$

where f_i are fit functions calculated from penalized cubic regression splines of observations (allowing non-linearity in the fit), V_i are the variables, and i is the daily observation. All variables were given a cubic spline basis except for wind direction, which used a cyclic cubic regression spline basis. For DOY and back trajectory distances, we used year factors (i.e., 2014-2020) and cluster factors (i.e., 1-7) to distinguish interannual variability and source region differences. The factors provide a different smooth function for each category (Wood, 2017). For example, the GAM smooth of DOY for 2014 can

be different than 2015, 2016, etc. In order to optimize the GAM, we first must adjust knots or remove any variables that are over-fitting or under-performing. We used the “mgcv” R package to summarize and check each variable for each monitoring site (Wood, 2020). A single GAM equation (using the same variables) was used for each monitoring site for consistency. During the initial optimization process, we removed the proposed 2018 and 2020 EE days from the dataset. We also ran 10 cross-validation tests by randomly splitting data 80/20 between training/testing for each monitoring site to ensure consistent results. All cross-validation tests showed statistically similar results with no large deviations for different data splits. We used data from each site during the April -September ozone seasons for 2014 through 2020, which is consistent with other papers modeling urban ozone (e.g., Pernak et al., 2019; McClure and Jaffe, 2018; Solberg et al., 2019; Solberg et al., 2018) and ozone concentrations during the periods with exceptional events are within the representative range of ozone in the GAM model.

Table 3-15 shows the variables used in the GAM and their F-value. The F-value suggests how important each variable is (higher value = more important) when predicting MDA8 ozone. Any bolded F-values had a statistically significant correlation ($p < 0.05$). R^2 , the positive 95th quantile of residuals, and normalized mean square residual values for each monitoring site are listed at the bottom of the table.

Table 3-15. GAM variable results. F-values per parameter used in the GAM model are shown for each site. Units and data sources for each parameter in the GAM model are shown on the right of the table. The 95th quantile, R², and normalized mean square residual information are shown at the bottom of the table.

Parameters	Paul Meyer	Walter Johnson	Joe Neal	Green Valley	Jerome Mack	Boulder City	Jean	Indian Springs	Unit	Source
Day of Year (DOY) factored by Year (2014-2020)	8.11	7.09	7.65	11.8	7.94	7.11	8.68	7.53	--	--
Previous Day MDA8 Ozone	37.9	22.7	41.5	18.1	27.9	31.3	105.5	123.8	ppb	Monitor Data
Average Daily Temperature	1.92	2.90	4.80	0.05	1.83	2.13	0.12	1.83	K	Monitor Data/NCEP Reanalysis
Maximum Daily Temperature	1.37	2.74	2.48	0.16	0.38	0.02	1.30	1.52	K	
Temperature Range (TMax - TMin)	4.12	2.13	1.38	1.74	1.77	1.51	0.50	0.54	K	
Average Daily Pressure	5.54	6.42	6.74	4.64	2.94	0.22	2.17	0.24	hPa	
Average Daily Wind Speed	11.1	5.03	7.49	5.02	15.3	0.07	0.49	2.19	knots	
Average Daily Wind Direction	0.47	1.04	0.24	1.35	2.43	0.69	0.11	2.48	deg	
18 UTC HYSPLIT Distance factored by Cluster	1.70	1.82	1.69	0.92	2.52	2.97	1.66	1.03	km	HYSPLIT Back-Trajectories
22 UTC HYSPLIT Distance factored by Cluster	1.03	0.74	1.47	1.47	1.20	1.26	1.19	0.50	km	
00 UTC Convective Available Potential Energy	3.50	0.13	0.37	1.17	1.16	0.57	5.71	6.49	J/kg	Sounding Data
00 UTC Lifting Condensation Level Pressure	1.36	2.78	2.29	2.41	3.76	0.38	1.43	0.38	hPa	
00 UTC Mixing Layer Potential Temperature	0.65	0.79	1.72	0.10	1.23	0.97	1.09	2.53	K	
00 UTC Mixed Layer Mixing Ratio	2.10	2.76	2.85	3.09	3.07	2.42	0.69	1.04	g/kg	
00 UTC 500-1000 hPa Thickness	2.91	0.43	1.70	1.60	1.69	4.11	2.18	1.83	m	
12 UTC 1km Average Relative Humidity	12.4	14.6	17.8	21.3	37.5	26.0	11.1	2.18	%	
95 th Quantile of Positive Residuals (ppb)	10	10	10	10	9	9	9	10		
R ²	0.55	0.58	0.60	0.58	0.61	0.58	0.57	0.55		
Normalized Mean Square Residual	3.6E-06	7.3E-04	6.1E-05	1.3E-04	3.1E-05	1.3E-04	1.2E-04	1.5E-04		

Table 3-16 provides GAM residual and fit results for all sites for the ozone seasons of 2014 through 2020. Overall, the residuals are low for all data points, and similarly low for all non-EE days. However, the 2018 and 2020 EE day residuals are significantly higher than the non-EE day results, meaning there are large, atypical influences on these days. **Figure 3-39** shows non-EE vs EE median residuals with the 95th confidence intervals denoted as notches in the boxplots. We show the data in both ways to provide specific values, as well as illustrate the difference in non-EE vs EE residuals. Since the 95th confidence intervals for median EE residuals are above and do not overlap with those for non-EE residuals at any site in Clark County, we can state that the median residuals are higher and statistically different ($p < 0.025$). The R^2 for each site ranged between 0.55 and 0.61, suggesting a good fit for each monitoring site, and similar to the results in prior studies and EE demonstrations mentioned previously (r^2 range of 0.4-0.8). We also provide the positive 95th quantile MDA8 ozone concentration, which is used to estimate a “No Fire” MDA8 ozone value based on the EPA guidance (U.S. Environmental Protection Agency, 2016). We also provide the median residuals (and confidence interval) for all non-EE days with observed MDA8 at or above 60 ppb; this threshold was needed to build a sufficient sample size with a representative distribution, and derive the median and 95% confidence interval. It should be noted that four out of the seven years modeled by the GAM were high wildfire years, and these values likely include a significant amount of wildfire days. We were not able to systematically remove wildfire influence by subsetting the Clark County ozone data based on HMS smoke, HMS smoke and $PM_{2.5}$ concentrations, and low wildfire years. These methods produced a significant number of false positives and negatives, and yielded datasets that were still affected by wildfire smoke. Therefore, these values should be considered an upper estimate of residuals for high ozone days. We see that the median residuals for 2018 and 2020 EE days are significantly higher than those on non-EE high observed ozone days since their confidence intervals do not overlap (or are comparable for the Jerome Mack station). The non-EE day residuals on days where observed MDA8 was at or above 60 ppb were determined to be normally distributed with a slight positive skew (median skewness = 0.39).

Table 3-16. Overall 2014-2020 GAM median residuals and 95% confidence interval range in square brackets for each site modeled. Sample size is shown in parentheses below the residual statistics. For sample sizes of less than ten, we include a range of residuals in square brackets instead of the 95% confidence interval. Residual results are split by non-EE days and the 2018 and 2020 EE days. R² for each site is also shown along with the positive 95th quantile result.

Site Name	All Residuals (ppb)	Non-EE Day Residuals (ppb)	2018 & 2020 EE Day Residuals (ppb)	R ²	Positive 95th Quantile (ppb)	Non-EE Day Residuals when MDA8 ≥ 60 ppb (ppb)
Boulder City	0.22 [-0.04, 0.48] (1,132)	0.22 [-0.04, 0.48] (1,130)	12.05 [10.38-13.72] (2)	0.58	9	4.05 [3.55, 4.55] (200)
Green Valley	0.17 [-0.15, 0.48] (948)	0.10 [-0.21, 0.41] (934)	7.38 [5.40, 9.36] (14)	0.58	10	3.76 [3.28, 4.23] (271)
Indian Springs	0.13 [-0.18, 0.44] (1,014)	0.08 [-0.22, 0.38] (1,010)	12.30 [9.37-17.19] (4)	0.55	10	4.79 [4.26, 5.32] (201)
Jean	0.21 [-0.06, 0.48] (1,149)	0.20 [-0.07, 0.47] (1,146)	12.57 [9.59-13.90] (3)	0.57	9	3.40 [2.94, 3.85] (290)
Jerome Mack	0.09 [-0.19, 0.36] (1,152)	0.05 [-0.22, 0.32] (1,141)	6.83 [4.21, 9.45] (11)	0.61	9	3.83 [3.32, 4.33] (242)
Joe Neal	0.23 [-0.08, 0.54] (1,113)	0.17 [-0.13, 0.47] (1,097)	7.77 [5.79, 9.75] (16)	0.60	10	3.32 [2.92, 3.71] (377)
Paul Meyer	0.21 [-0.08, 0.50] (1,159)	0.10 [-0.19, 0.39] (1,137)	8.11 [6.34, 9.88] (22)	0.55	10	3.58 [3.19, 3.97] (388)
Walter Johnson	0.27 [-0.03, 0.57] (1,163)	0.19 [-0.10, 0.48] (1,141)	7.16 [5.11, 9.21] (22)	0.58	10	3.53 [3.13, 3.93] (379)

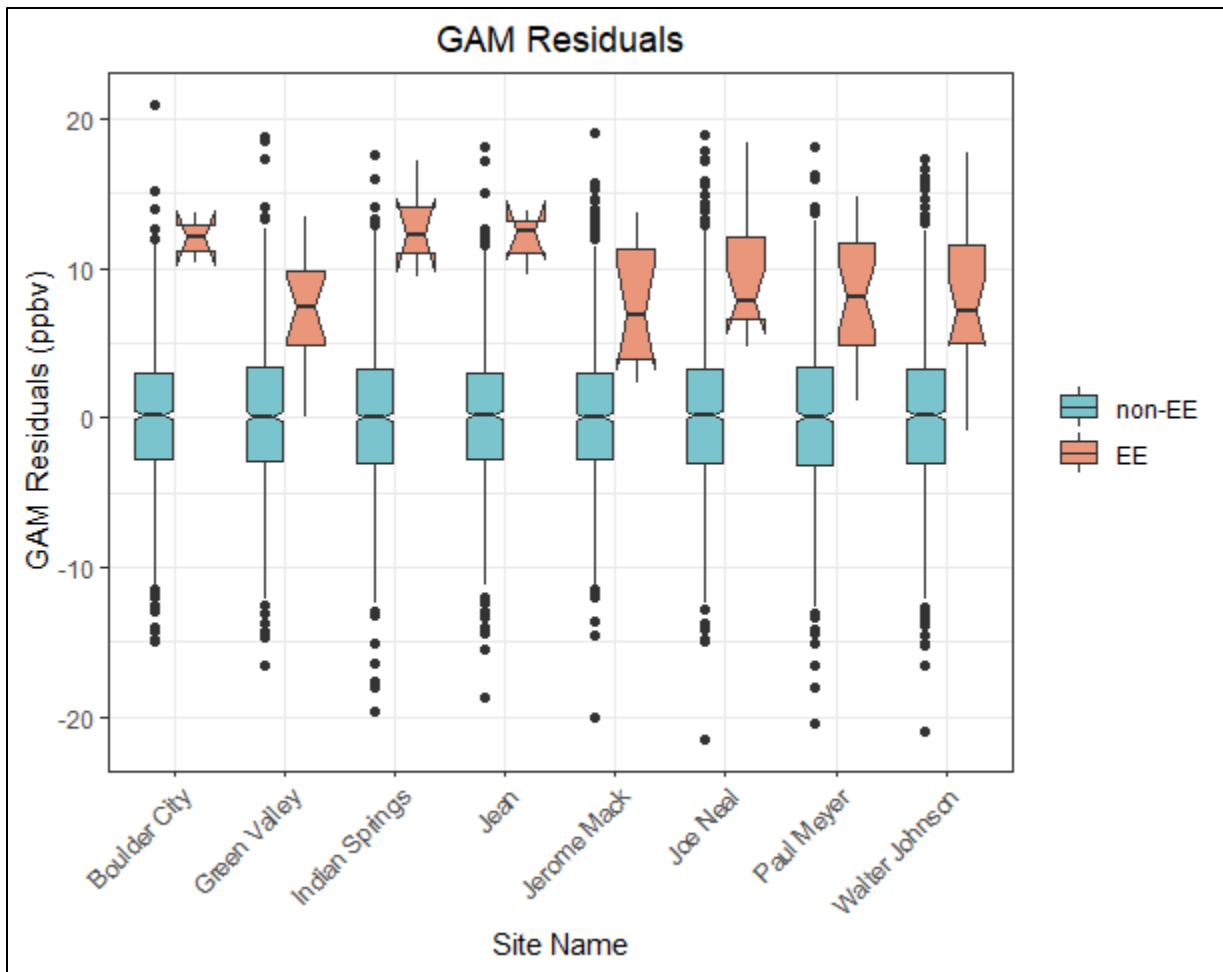


Figure 3-39. Exceptional event vs. non-exceptional event residuals. Non-exceptional events (non-EE in blue) and exceptional events (EE in orange) residuals are shown for each site modeled in Clark County. The notches for each box represent the 95th confidence interval. This figure illustrates the information in Table 3-16.

Overall, the GAM results show low bias and consistently significantly higher residuals on EE days compared with non-EE days. We also evaluated the GAM performance on verified high ozone, non-smoke days by looking at specific case studies. This was done to assess whether high-ozone days, such as the EE days, have a consistent bias that is not evident in the overall or high ozone day GAM performance. Out of the seven years used in the GAM model, four were high wildfire years in California (2015, 2017, 2018, and 2020). Since summer winds in Clark County are typically out of California (44% of trajectories originate in California according to the cluster analysis [not including transport through California in the Baja Mexico cluster]), wildfire smoke is likely to affect a large portion of summer days and influence ozone concentrations in Clark County. We identified specific case studies where most monitoring sites in Clark County had an MDA8 ozone concentration greater than or equal to 60 ppb and had no wildfire influence; “no wildfire influence” was determined by

inspecting HMS smoke plumes and HYSPLIT back trajectories for each day and confirming no smoke was over, near, or transported to Clark County. We found one to two examples from each year used in the GAM modeling, and required that at least half of the case study days needed to include an exceedance of the ozone NAAQS. [Table 3-17](#) shows the results of these case studies. Most case study days, including NAAQS exceedance days, show positive and negative residuals even when median ozone is greater than or equal to 65 ppb in Clark County, similar to the results for the entire multi-year dataset. GAM residuals on non-EE days when MDA8 is at or above 60 ppb have a median of 3.69 [95% confidence interval: 3.47, 3.88] (see [Table 3-16](#)). The high ozone, non-smoke case study days all show median residuals within or below the confidence interval of the high ozone residuals (from [Table 3-16](#)), meaning that the GAM model is able to accurately predict high ozone, non-smoke days within a reasonable range of error. Two additional factors indicate the GAM has good performance on normal, high ozone days: (1) the median residuals for the case studies are mostly lower than the 95% confidence interval of high ozone residuals (i.e., includes non-EE wildfire days), and (2) the case study days were verified as non-smoke days. Thus, residuals above the 95th confidence interval of the median residuals, such as those on the EE days, are statistically higher than on days with comparable high ozone concentrations, and not biased high because of the high ozone concentrations on these days.

Table 3-17. GAM high ozone, non-smoke case study results. Median GAM residuals for ten days in 2014-2020 are shown where most monitoring sites had MDA8 ozone concentrations of 60 ppb or greater. Sites used to calculate the MDA8 and GAM residual median/range are listed in the Clark County AQS Site Number column by site number.

Date	Clark County AQS Site Number	Median (Range) of Observed MDA8 Ozone (ppb)	Median (Range) GAM Residual (ppb)
5/17/2014	0601, 0075, 1019, 0540, 0043, 0071	66 (64-71)	1.66 (-0.53-4.28)
6/4/2014	0601, 0075, 0540, 1019, 0043, 0071	69 (66-72)	3.46 (1.70-4.80)
6/3/2015	1019, 0043, 0075, 0540, 7772, 0601, 0071	71 (65-72)	3.01 (-0.34-5.77)
6/20/2015	0601, 0298, 7772, 1019, 0540, 0075, 0043, 0071	65 (63-70)	1.40 (-6.20-5.28)
6/3/2016	0298, 1019, 0075, 0540, 0043, 0071	65 (63-71)	3.89 (1.89-5.26)
7/28/2016	0075, 0071, 0298, 0540, 0043	70 (63-72)	0.24 (-5.95-3.67)
6/17/2017	0601, 0075, 0071, 1019, 0540, 0298, 0043	66 (63-72)	1.85 (-1.94-7.01)
6/4/2018	0601, 0298, 7772, 1019, 0540, 0075, 0043, 0071	65 (60-67)	3.06 (-0.91-3.60)
5/5/2019	0601, 0298, 7772, 1019, 0540, 0075, 0043, 0071	65 (62-67)	1.28 (-2.00-3.42)
5/15/2020	0298, 0043, 0075, 0071	63 (63-65)	1.52 (1.09-3.49)

We also evaluate the bias of GAM residuals versus predicted MDA8 ozone concentrations in [Figure 3-40](#). Residuals (i.e., observed ozone minus GAM-predicted MDA8 ozone) should be independent of the GAM-predicted ozone value, meaning that the difference between the actual ozone concentration on a given day and the GAM output should be due to outside influences and not well described by meteorological or seasonal values (i.e., variables used in the GAM prediction). Therefore, in a well-fit model, positive and negative residuals should be evenly distributed across all

GAM-predicted ozone concentrations and on average zero. In Figure 3-40, we see daily GAM residuals at all eight monitoring sites in Clark County from 2014-2020, the residuals are evenly distributed across all GAM-predicted ozone concentrations, with no pattern or bias at high or low MDA8 fit concentrations. This evaluation of bias in the model is consistent with established literature and other EE demonstrations (Gong et al., 2018; McVey et al., 2018; Texas Commission on Environmental Quality, 2021; Pernak et al., 2019), and indicate a well-fit model. In Figure 3-41, we also provide a histogram of the residuals at each monitoring site modeled in Clark County. This analysis shows that residuals at each site are distributed normally around a median near zero, and none of the distributions shows significant tails at high or low residuals (median skew = 0.05 with 95% confidence interval [-0.03, 0.12]). This analysis of error in the model and our results are consistent with previously concurred EE demonstrations (Arizona Department of Environmental Quality, 2016) and previous literature (Jaffe et al., 2013; Alvarado et al., 2015; Gong et al., 2017; McClure and Jaffe, 2018; Pernak et al., 2019). Appendix F provides GAM residual analysis from the concurred ADEQ and submitted TCEQ demonstrations that compare well with our GAM residual results. Based on these analysis methods, bias in the model is low throughout the range of MDA8 prediction values and confirms that the GAM can be used to predict MDA8 ozone concentrations in Clark County.

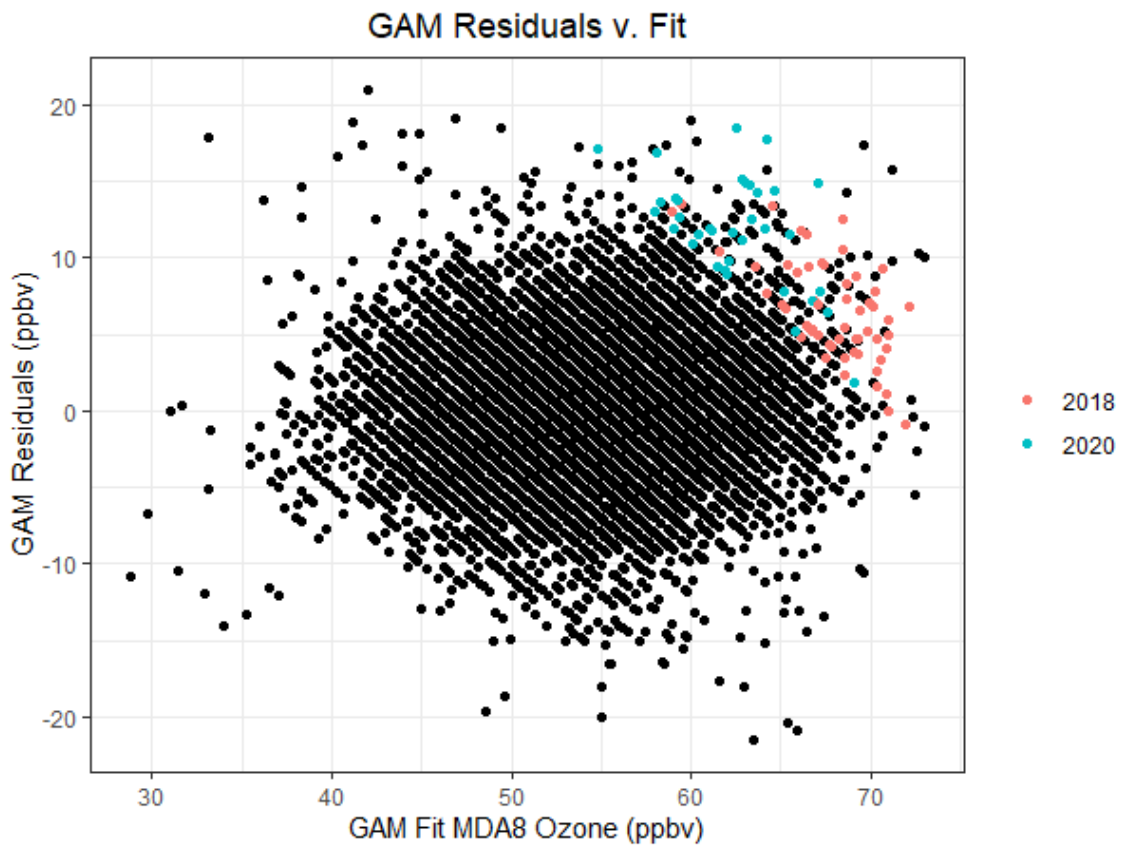


Figure 3-40. Daily GAM residuals for 2014-2020 vs GAM Fit (Predicted) MDA8 Ozone values. 2018 and 2020 exceptional events residuals are shown in red and blue.

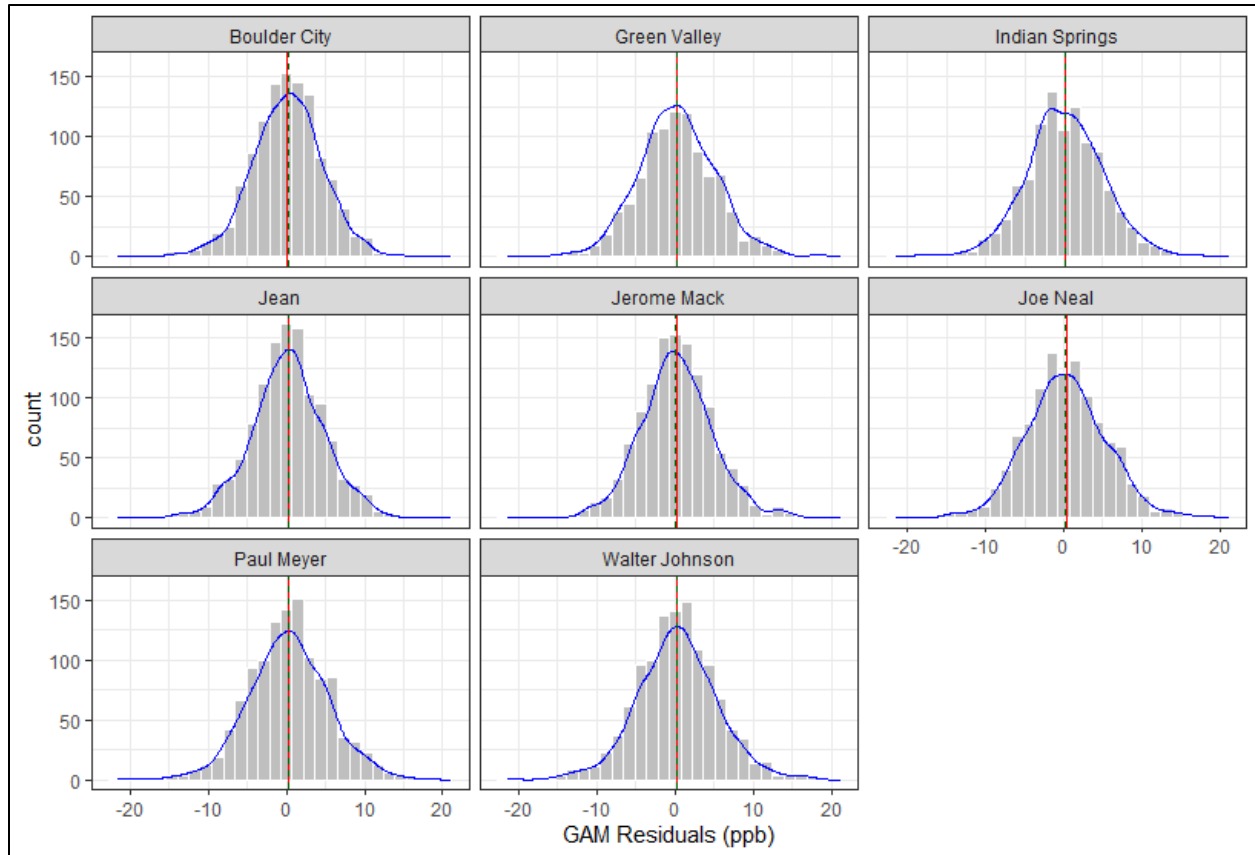


Figure 3-41. Histogram of GAM residuals at all modeled Clark County monitoring sites. The red line indicates the mean and the green dashed line indicates the median. The blue line provides the density distribution.

Within the GAM model, we include HYSPLIT 24-hour distance values, which are factored by cluster, to provide source region and stagnation information into the algorithm. A major upwind pollution source for Las Vegas is the Los Angeles Basin (see the Southern California cluster), which is around 400 km away. Since the GAM model uses source region and distance traveled information to help predict daily MDA8 ozone concentrations, contributions from LA should be accounted for in the algorithm. Based on this, we can assess whether GAM residuals on LA-source region days were significantly different from other source regions. In **Figures 3-42 and 3-43**, we subset the GAM results by removing any potential EE days. From these results, we find that both morning (18:00 UTC) and afternoon (22:00 UTC) trajectory data have similar distributions for all clusters. The notches in the box plots (representing the 95th confidence interval) provide an estimate of statistical difference, and show that the median of residuals is near zero for all clusters. The Northwest U.S. cluster at 18:00 UTC shows slightly negative residuals, while the Long-Range Transport cluster shows slightly positive residuals for both 18:00 and 22:00 UTC. The Southern California cluster shows a median residual of around zero for both 18:00 and 22:00 UTC trajectories, with significant overlap between the 95th confidence intervals of most other clusters (not statistically different). Additionally, the number of data points per cluster (bottom of each figure) corresponds well with transport from California being

dominant for the April through September time frame. Overall, this analysis provides evidence that even when the Los Angeles Basin (Southern California cluster) is upwind of Las Vegas, the GAM model performs well (low median residuals), and the results are statistically similar to most of the other clusters. This implies that when residuals are large, the Los Angeles Basin’s influence is unlikely to be the only contributor to enhancements in MDA8 ozone.

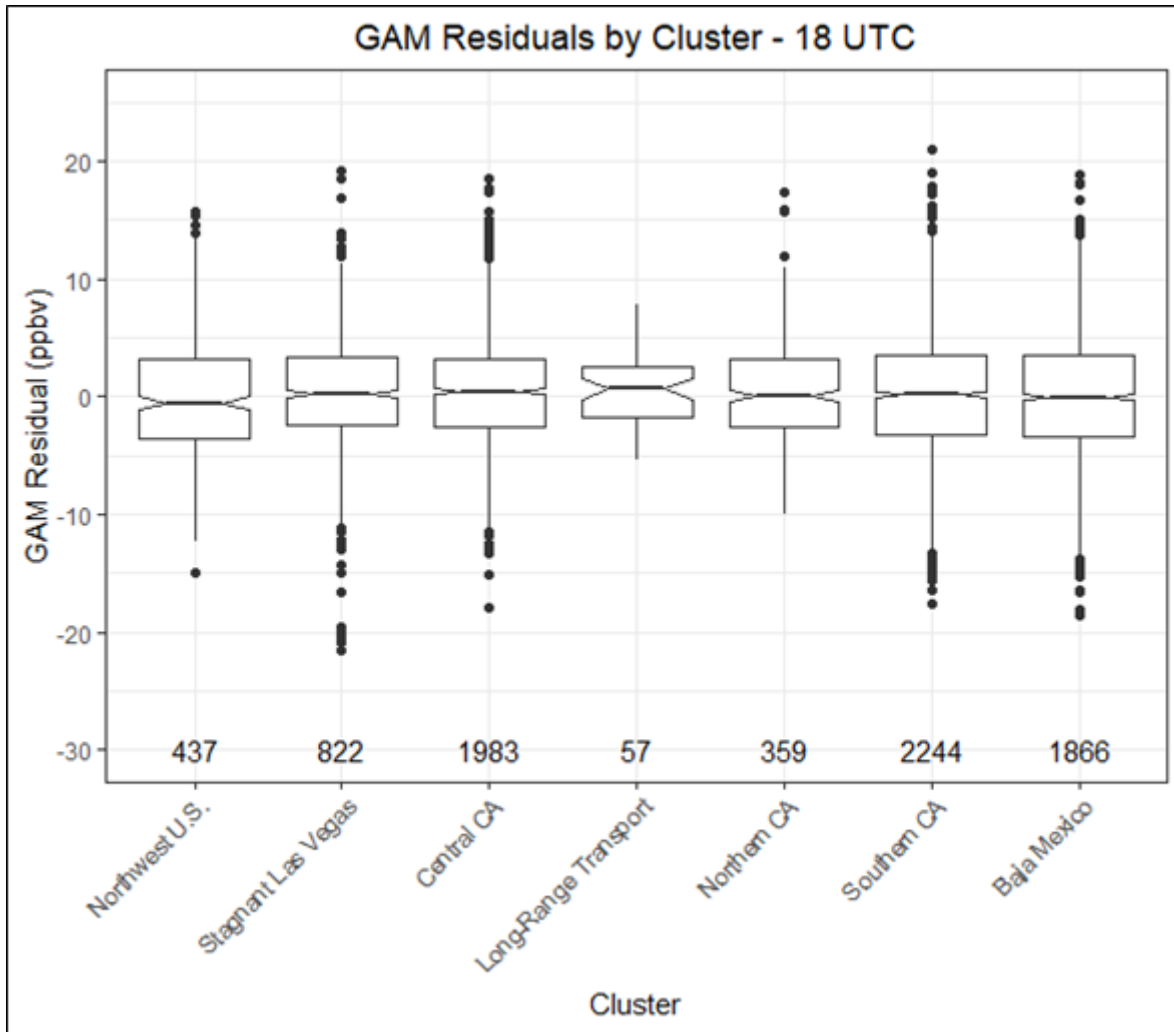


Figure 3-42. GAM cluster residual results for 18:00 UTC. The cluster is determined by grouping 24-hour back trajectories from Las Vegas based on their path. Clusters were created by using back trajectory results from Clark County between 2014 and 2020 (EE days were removed).

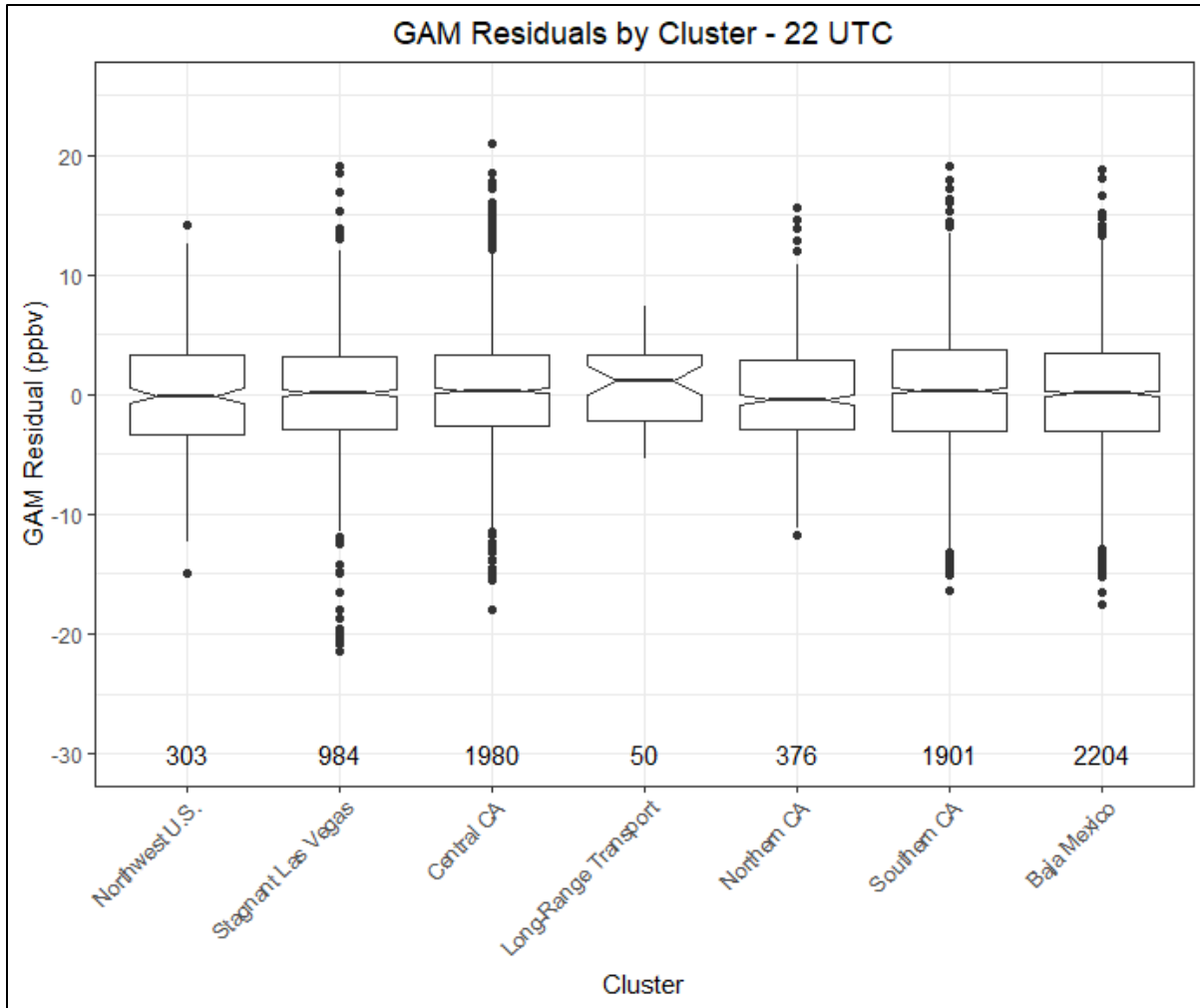


Figure 3-43. GAM cluster residual results for 22:00 UTC. The cluster is determined by grouping 24-hour back trajectories from Las Vegas based on their path. Clusters were created by using back trajectory results from Clark County between 2014 and 2020 (EE days were removed).

Mobile emissions sources decreased throughout the U.S. after COVID restrictions went into place in March 2020. Based on emission inventories from Las Vegas, on-road emissions make up a significant portion of the NO_x emissions inventory (see Section 2.3 for more details). Based on traffic data from the Nevada Department of Transportation, on-road traffic in Clark County in 2020 was significantly different than 2019 through early to mid-June (depending on the area where traffic volume was measured; see [Appendix G](#) for more details). [Figure 3-44](#) provides a scatter plot of MDA8 ozone observed versus GAM fit for all eight monitoring sites, separated by year. The linear regression fit, slope, and intercept do not show large difference between 2020 and other modeled years. [Figure 3-45](#) provides a more in-depth look at the most heavily affected months due to COVID restrictions and traffic changes (April – May 2020). The 95th confidence interval (shown as a notch in the box plots) show overlap between 2020 and most other years (except 2015 and 2016). The May 6, 9, and 28 EE days are included in the 2020 box. This analysis shows that there was not a statistically different GAM

response in 2020 compared with other years; this is confirmed in the COVID analysis section (Appendix G), where we show that MDA8 ozone during April – May 2020 in Las Vegas was not statistically different from previous years. While the reduction in traffic emissions due to COVID restrictions did not affect the August 7 event, we thought it was important to address the effects of COVID restrictions on the 2020 GAM results. Overall, ozone in Clark County did not change significantly and, similarly, GAM results were not significantly affected.

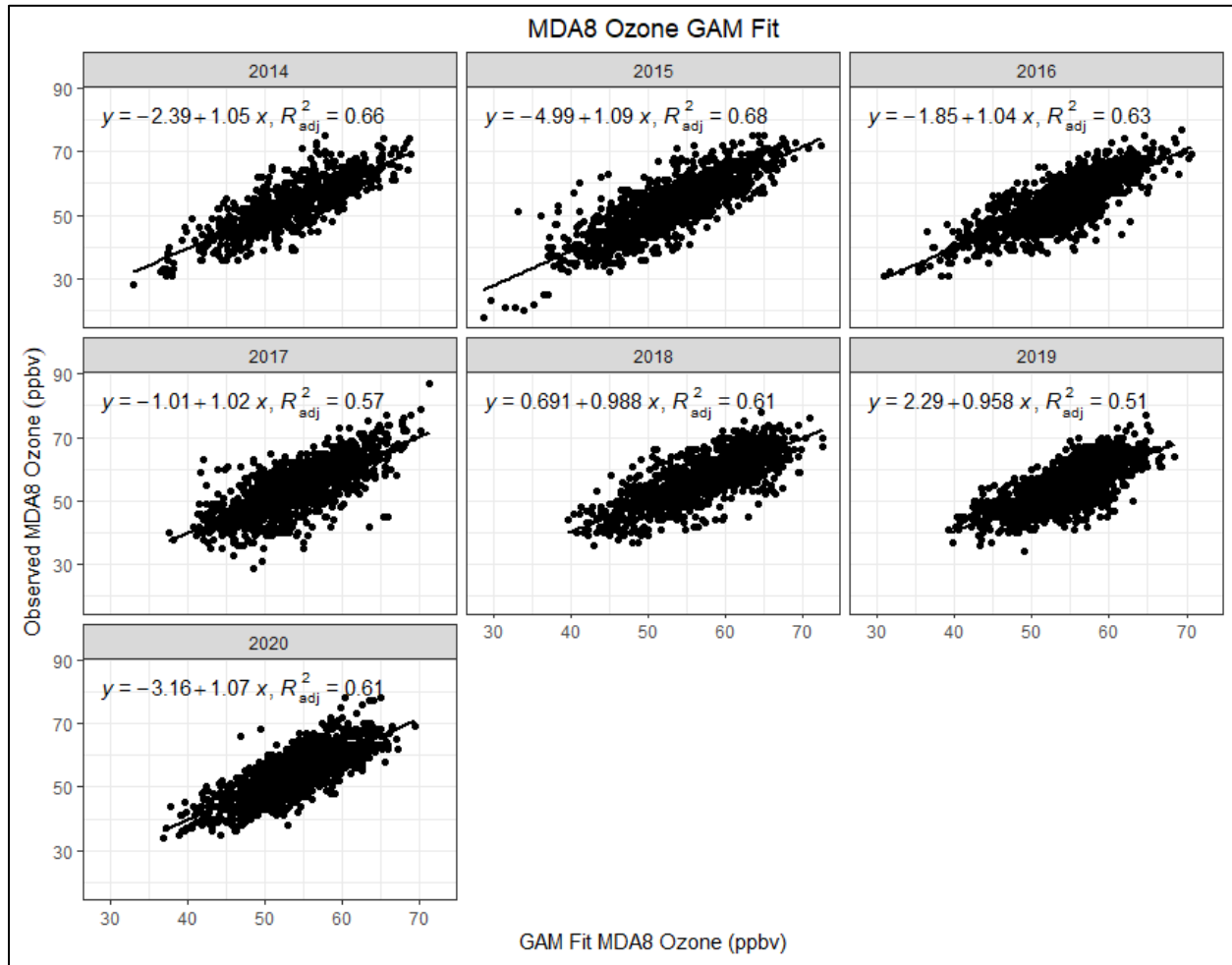


Figure 3-44. Observed MDA8 ozone vs. GAM fit ozone by year. The relationship between observed MDA8 ozone and GAM fit ozone at all eight modeled monitoring sites in Clark County is broken out by year, with linear regression and fit statistics shown (slope, intercept, and r^2). EE days are not included in the regression equations.

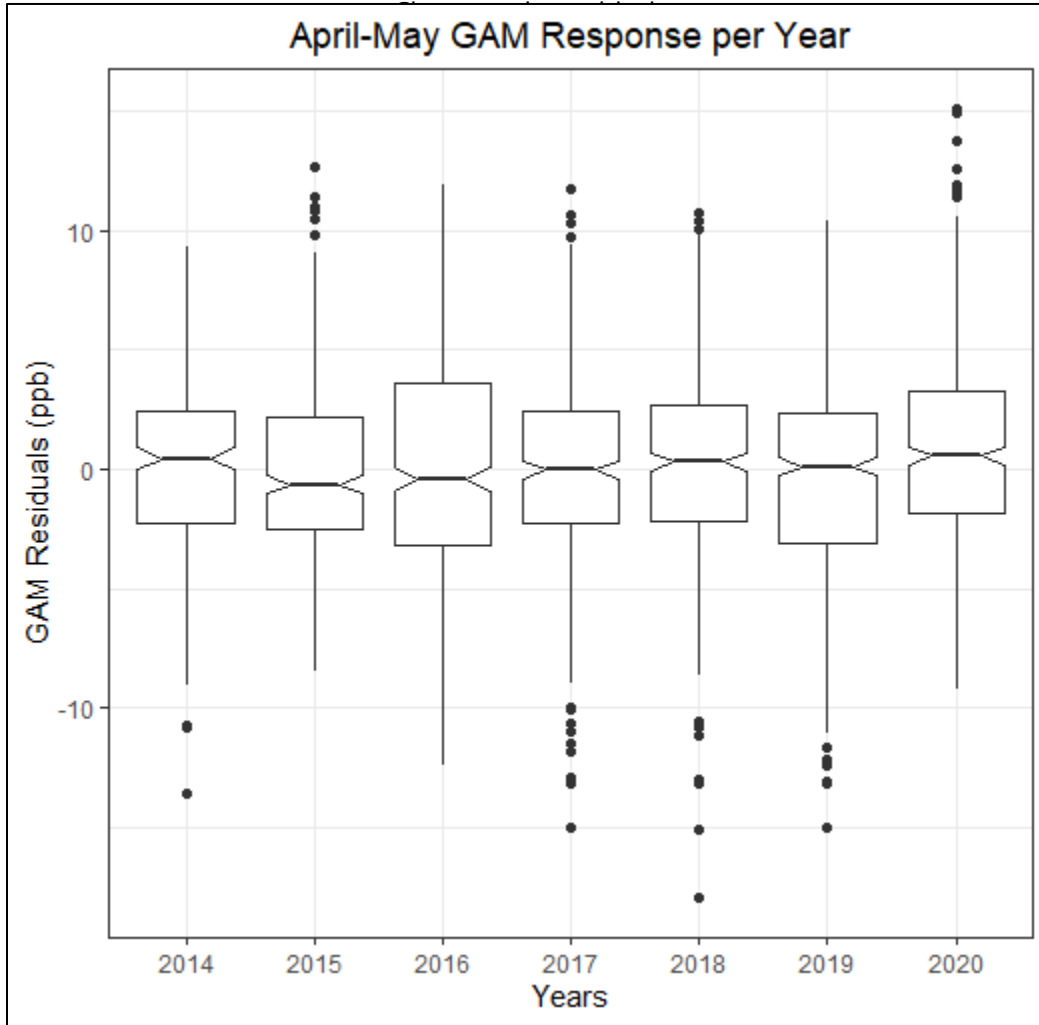


Figure 3-45. April–May Interannual GAM Response. April–May residuals per year from 2014–2020 are plotted for all eight modeled monitoring sites in Clark County. The potential EE days of May 6, 9, and 28 are included.

Figure 3-46 provides the observed MDA8 ozone versus GAM Fit MDA8 from 2014 through 2020 for the sites affected on August 7 (Indian Springs, Joe Neal, and Walter Johnson). We marked the possible 2020 (red), 2018 (blue), and other (purple) EE days to show that observed MDA8 ozone on these days is higher than those predicted by the GAM. The other (purple) points are from 2014–2016 and are suspected wildfire events, as indicated in EPA AQS record. We also highlight the August 7, 2020, EE day as a large red triangle in each figure. Linear regression statistics (slope, intercept, and r^2) are also provided for context. All linear regressions show a slope near unity, and a low intercept value (around 1-4 ppb) with a good fit r^2 value.

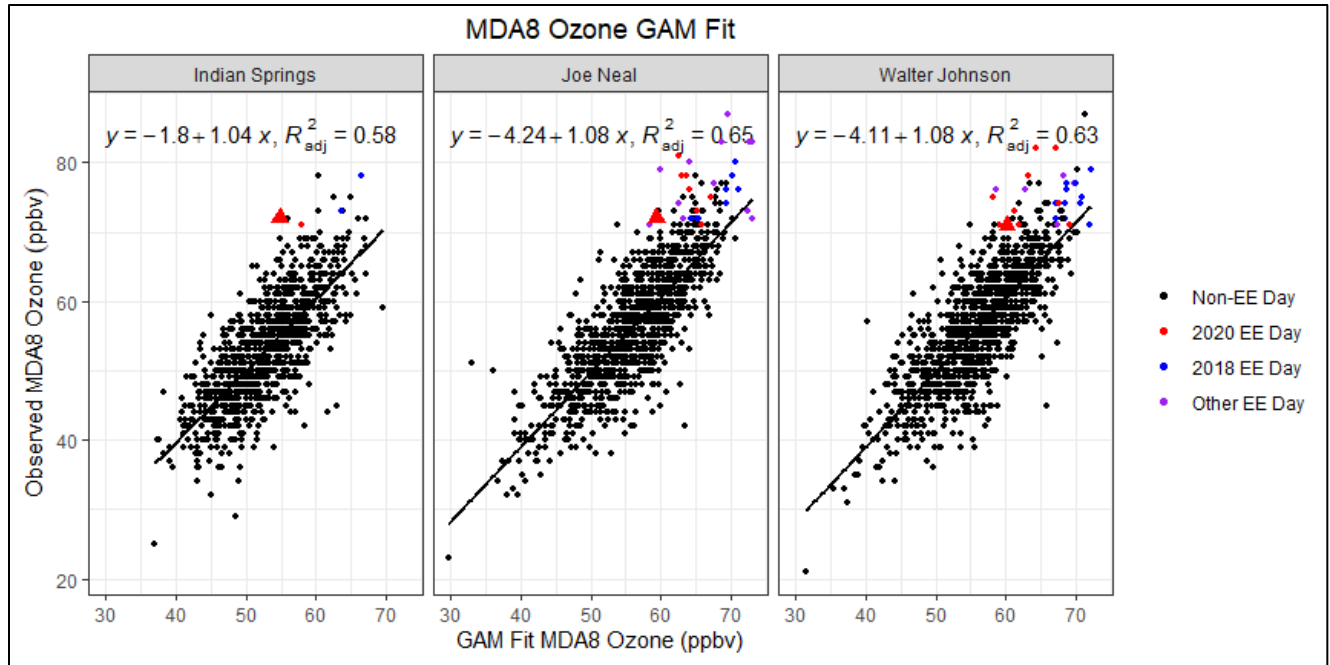


Figure 3-46. GAM MDA8 Fit versus Observed MDA8 ozone data from 2014 through 2020 for the EE affected sites on August 7, 2020. Black circles indicate data not associated with the 2018 or 2020 EE days, red circles indicate 2020 EE days, blue circles indicate 2018 EE days, and purple circles indicate 2014-2016 EE days. August 7 is shown as a red triangle. The black line is the linear regression of the data, and statistics (equation and r^2 value) are shown in the top of each sub-figure.

Table 3-18 provides the GAM results for August 7, 2020, at each monitoring site affected by the EE. GAM residuals show a modeled wildfire impact between 11 and 18 ppb for all monitoring sites, with MDA8 GAM prediction values well below the 0.070 ppm standard. EPA guidance requires a further level of investigation. By adding the GAM MDA8 Prediction value and the Positive 95th quantile of residuals, we calculated the “No Fire” MDA8 ozone value. The difference between the observed and “No Fire” MDA8 ozone value (1 to 8 ppb) is a conservative estimate of the influence of wildfire smoke at each site. Due to the large number of wildfires affecting Clark County during the 7-year modeling period, we also calculated the “No Fire” and minimum predicted fire influence given the 75th percentile (7 to 13 ppb). This provides a range of minimum smoke enhancement (1 to 13 ppb). The actual enhancement due to wildfire smoke likely lies between the minimum smoke enhancement estimate and the GAM residual. Previous studies and concurred EE demonstrations show and discuss the limitations of the 95th positive percentile evaluation (Miller et al., 2014; Arizona Department of Environmental Quality, 2016). Additionally, production of ozone is an extremely complex process that can only be predicted by meteorological variables in a GAM model with a 50%-80% correlation based on previously cited papers (our GAM model shows a 55%-61% correlation). In our case, this leaves exceptional events, wildfire influence during high-wildfire years, stratospheric intrusions, non-normal emissions, non-normal meteorology, etc., which make up the other 39%-45%. Due to the large number of high-wildfire years used in the GAM model, we assert that the minimum predicted

fire influence value (as determined by the positive 95th quantile) should not be used as strict guideline for actual fire influence. Based on the values from the GAM model, we see a significant, non-typical enhancement in MDA8 ozone concentrations at the affected Clark County monitoring sites on August 7, 2020.

Table 3-18. August 7 GAM results and residuals for each site. The GAM residual is the difference between observed MDA8 ozone and the GAM Prediction. We also estimate the minimum predicted fire influence based on the positive 95th quantile and GAM prediction value.

Site Name	MDA8 Ozone Concentration ^a (ppm)	MDA8 GAM Prediction ^b (ppm)	GAM Residual (ppm)	Positive 75th-95th Quantile ^c (ppm)	"No Fire" MDA8 ^{b+c} (ppm)	Minimum Predicted Fire Influence ^{a-(b+c)} (ppm)
Walter Johnson	0.071	0.060	0.011	0.005-0.010	0.065-0.070	0.001-0.006
Joe Neal	0.072	0.059	0.013	0.006-0.010	0.065-0.069	0.003-0.007
Indian Springs	0.072	0.054	0.018	0.005-0.010	0.059-0.064	0.008-0.013

Finally, **Figure 3-47** shows a 2-week time series of observed MDA8 ozone values across Clark County and the GAM prediction values at those sites. August 7, 2020 (and August 3, 2020 – another EE date), shows the large gap between observed MDA8 ozone and the GAM-predicted values. Outside of the possible EE day, the GAM prediction values are very close to the observed values, suggesting that immediately before and after the event, we are able to accurately predict typical fluctuations in ozone on non-event days.

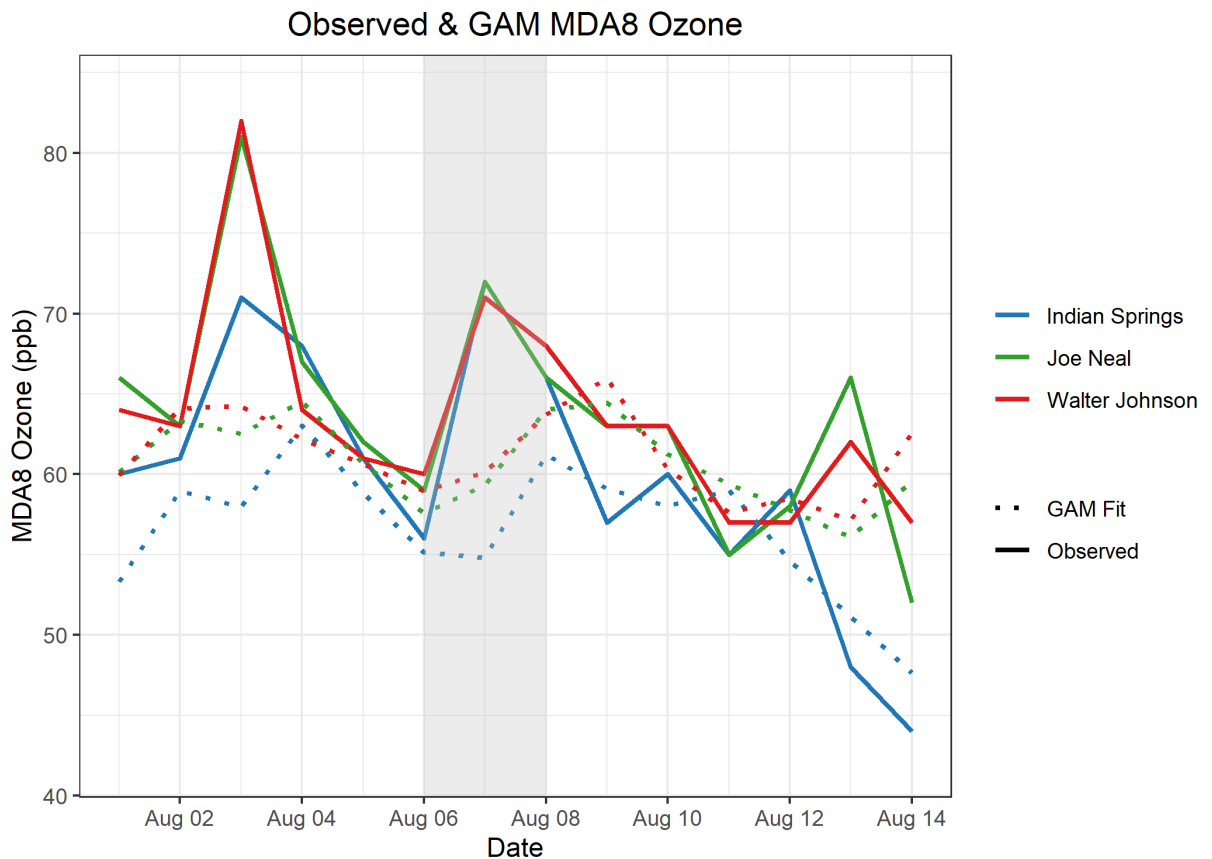


Figure 3-47. GAM time series showing observed MDA8 ozone for two weeks before and after the August 7 EE (solid lines). The GAM MDA8 ozone fit value is also shown for two weeks before and after September 2 (dotted line).

Overall, the GAM evidence clearly demonstrates that a non-typical source of ozone significantly impacted concentrations at all EE-affected Clark County sites on August 7, 2020. Coupled with wildfire smoke evidence from all other tiers of analyses, we can conclude by weight of evidence that the enhancement in ozone concentration was due to smoke from the Apple Fire in southern California that was transported to Clark County, Nevada.

3.4 Clear Causal Relationship Conclusions

The analyses conducted in this report support the impact of smoke from the Apple Fire in southern California on ozone concentrations in Clark County, Nevada, on August 7, 2020. We find that:

1. Visible satellite imagery, news articles, and back trajectories support the conclusion of smoke transport from the Apple Fire to Clark County.
2. A large mixing layer, back trajectories starting aloft near the fire and ending at the surface in Clark County, and surface enhancements of wildfire-related pollutants (particularly the wood smoke tracer, levoglucosan) in Clark County support the conclusion that smoke was mixed down to the surface in Clark County.
3. Comparisons with non-event concentrations, meteorologically similar matching day analysis, and GAM statistical modeling support the conclusion that the ozone concentrations seen in Clark County were well above typical summer concentrations.

The analyses presented in this report fulfill the requirements for a Tier 3 EE demonstration, and all conclusions for each type of analysis are summarized in [Table 3-19](#). The effect of the Apple Fire in Clark County caused ozone exceedances at the Walter Johnson, Joe Neal, and Indian Springs monitoring stations. Based on the evidence shown that the Apple Fire was a natural event and unlikely to recur, as well as the clear causal relationship between the wildfire event and the monitored exceedances, we conclude that the ozone exceedance event on August 7, 2020, in Clark County was not reasonably controllable or preventable.

Table 3-19. Results for each tier analysis for the August 7 EE.

Tier	Requirements	Finding
1	<ul style="list-style-type: none"> • Comparison of fire-influenced exceedance with historical concentrations • Key factor: Evidence that fire and monitor meet one of the following criteria: <ul style="list-style-type: none"> – Seasonality differs from typical season, or – Ozone concentrations are 5-10 ppb higher than non-event related concentrations • Evidence of transport of fire emissions to monitor: <ul style="list-style-type: none"> – Trajectories of fire emissions (reaching ground level), or – Satellite images and supporting evidence from surface measurements – Media coverage and photographic evidence of smoke 	<ul style="list-style-type: none"> • The August 7, 2020 ozone exceedance occurred during a typical ozone season, but event concentrations were significantly higher than non-event concentrations. • Trajectories, satellite images, media coverage, and ground images support smoke transport from the Apple Fire into Clark County.
2	<ul style="list-style-type: none"> • All Tier 1 requirements • Key Factor #1: Fire emissions and distance of fires • Key Factor #2: Comparison of the event-related ozone concentration with non-event-related high ozone concentrations (high percentile rank over five years/seasons) <ul style="list-style-type: none"> – Annual and seasonal comparison • Evidence that fire emissions affected the monitor (at least one of the following): <ul style="list-style-type: none"> – Visibility impacts – Changes in supporting measurements – Satellite enhancements of fire-related species (i.e., NO_x, CO, AOD, etc.) – Fire-related enhancement ratios and/or tracer species – Differences in spatial/temporal patterns 	<ul style="list-style-type: none"> • Q/d values for the Apple Fire were well below 100. • Ozone concentrations at all sites showed high percentile rank over the past five years and past five ozone seasons. • Surface concentrations of supporting pollutants show enhanced concentrations and changes in typical diurnal profiles, consistent with smoke. • Satellite measurements also show enhanced levels of fire-related species. • Levoglucosan, a wildfire tracer, showed a positive detection during this event.
3	<ul style="list-style-type: none"> • All Tier 2 requirements • Evidence of fire emissions effects on monitor: <ul style="list-style-type: none"> – Multiple analyses from those listed for Tier 2 • Evidence of fire emissions transport to the monitor: <ul style="list-style-type: none"> – Trajectory or satellite plume analysis, and – Additional discussion of meteorological conditions • Additional evidence such as: <ul style="list-style-type: none"> – Comparison to ozone concentrations on matching (meteorologically similar) days – Statistical regression modeling – Photochemical modeling of smoke contributions to ozone concentrations 	<ul style="list-style-type: none"> • Meteorology patterns during this event show transport from the Apple Fire area to Clark County. • Vertical profiles show the potential for vertical mixing and transport to the surface. • Meteorologically similar day analysis shows that average MDA8 ozone across similar days was well below the ozone NAAQS and 10 ppb lower than the August 7 exceedance at all affected sites. • GAM statistical modeling predicts ozone concentrations lower than observed, suggesting an impact from non-typical sources on ozone concentrations in Clark County during this event.

4. Natural Event Unlikely to Recur

A wildfire is defined in 40 CFR 50.1(n) as “any fire started by an unplanned ignition caused by lightning; volcanoes; other acts of nature; unauthorized activity; or accidental, human-caused actions, or a prescribed fire that has developed into a wildfire. A wildfire that predominantly occurs on wildland is a natural event.” Furthermore, a “wildland” is “an area in which human activity and development are essentially non-existent, except for roads, railroads, power lines, and similar transportation facilities. Structures, if any, are widely scattered.” 40 CFR 50.1(o). As shown in Table 3-3, the fire that contributed to this event was caused by human-caused actions, and therefore meets the definition of wildfire. Based on the documentation provided in Section 3.2.1 of this submittal, the Apple Fire in California, which contributed to wildfire smoke in Clark County, predominately took place on wildlands designated as National Forests, as seen in Figure 3-23. Therefore, under 40 CFR §50.1, the fire listed in Table 3-3 can be classified as natural event that is unlikely to recur. Accordingly, the Clark County Department of Environment and Sustainability has shown in this submittal that smoke from California wildfires, which led to an ozone exceedance in Clark County of August 7, 2020, may be considered for treatment as an EE.

5. Not Reasonably Controllable or Preventable

As shown by the documentation provided in Section 3.2.1 of this submittal, each wildfire listed in Table 3-3 burned predominantly on wildland. The Exceptional Events rule stated in 40 CFR 50.1(j) indicates that a wildfire that occurs on wildland is not reasonably controllable or preventable. Previous sections of this report have shown that each fire referenced in this report was a wildfire that occurred on wildland. The InciWeb report for the Apple Fire indicates that this wildfire burned across vast areas in generally inaccessible land, limiting firefighting efforts in each event (<https://inciweb.nwcg.gov/incident/6902/>). The Clark County Department of Environment and Sustainability is not aware of any evidence clearly demonstrating that prevention or control efforts beyond those made would have been reasonable. Therefore, the emissions that caused exceedances at monitors in Clark County on August 7 are neither reasonably controllable or preventable.

6. Public Comment

This exceptional event demonstration will undergo a 30-day public comment period concurrent with EPA's review beginning September 3, 2021. A copy of the public notice, along with any comments received and responses to those comments, will be submitted to EPA after the comment period has closed, consistent with the requirements of 40 CFR 50.14(c)(3)(v). [Appendix H](#) contains documentation of the public comment process.

7. Conclusions and Recommendations

The analyses conducted in this report support the conclusion that smoke from the Apple Fire in southern California impacted ozone concentrations in Clark County, Nevada, on August 7, 2020. This EE demonstration has provided the following elements required by the EPA guidance for wildfire EEs (U.S. Environmental Protection Agency, 2016):

1. A narrative conceptual model that describes the Apple Fire in southern California and how the emissions from this wildfire led to ozone exceedances downwind in Clark County (Sections 1 and 2).
2. A clear causal relationship between the Apple Fire and the August 7 exceedance through ground and satellite-based measurements, trajectories, emission modeling, comparison with non-event concentrations, and statistical modeling (Section 3).
3. Event ozone concentrations at or above the 99th percentile when compared with the last six years of observations at each site and were atypically high ozone days at each site (excluding other 2018 and 2020 EE events – Section 3).
4. The Apple Fire was a human-caused accident due to a malfunctioning diesel engine near a wildland interface; the fire grew rapidly and quickly beyond firefighting controls, which classifies this event as unlikely to recur (Section 4).
5. Demonstration that the emissions from the Apple Fire being transported to Clark County was neither reasonably controllable or preventable (Section 5).
6. This demonstration went through the public comment process via Clark County’s Department of Environment and Sustainability (Section 6).

The major conclusions and supporting analyses found in this report are:

1. Visible satellite imagery, news articles, and back trajectories support the conclusion of smoke transport from the Apple Fire to Clark County.
2. A large mixing layer, back trajectories starting aloft near the fire and ending at the surface in Clark County, and surface enhancements of wildfire-related pollutants in Clark County support the conclusion that smoke was mixed down to the surface in Clark County.
3. Comparisons with non-event concentrations, meteorologically similar matching day analysis, and GAM statistical modeling support the conclusion that the ozone concentrations seen in Clark County were well above typical summer concentrations.

The analyses presented in this report fulfill the requirements for a Tier 3 EE demonstration, and all conclusions for each type of analysis are summarized in Table 3-19. The effect of the Apple Fire in Clark County caused ozone exceedances at the Walter Johnson, Joe Neal, and Indian Springs monitoring stations. Based on the evidence shown that the Apple Fire was a natural event and

unlikely to recur, as well as the clear causal relationship between the wildfire event and the monitored exceedances, we conclude that the ozone exceedance event on August 7, 2020, in Clark County was not reasonably controllable or preventable.

8. References

- Alvarado M., Lonsdale C., Mountain M., and Hegarty J. (2015) Investigating the impact of meteorology on O₃ and PM_{2.5} trends, background levels, and NAAQS exceedances. Final report prepared for the Texas Commission on Environmental Quality, Austin, TX, by Atmospheric and Environmental Research, Inc., Lexington, MA, August 31.
- Arizona Department of Environmental Quality (2016) State of Arizona exceptional event documentation for wildfire-caused ozone exceedances on June 20, 2015 in the Maricopa nonattainment area. Final report, September. Available at https://static.azdeq.gov/pn/1609_ee_report.pdf.
- Arizona Department of Environmental Quality (2018) State of Arizona exceptional event documentation for wildfire-caused ozone exceedances on July 7, 2017 in the Maricopa Nonattainment Area. Final report, May. Available at https://static.azdeq.gov/pn/Ozone_2017ExceptionalEvent.pdf.
- Bhattarai H., Saikawa E., Wan X., Zhu H., Ram K., Gao S., Kang S., Zhang Q., Zhang Y., Wu G., Wang X., Kawamura K., Fu P., and Cong Z. (2019) Levoglucosan as a tracer of biomass burning: recent progress and perspectives. *Atmospheric Research*, 220, 20-33, doi: 10.1016/j.atmosres.2019.01.004. Available at <http://www.sciencedirect.com/science/article/pii/S0169809518311098>.
- Brey S.J. and Fischer E.V. (2016) Smoke in the city: how often and where does smoke impact summertime ozone in the United States? *Environ. Sci. Technol.*, 50(3), 1288-1294, doi: 10.1021/acs.est.5b05218, 2016/02/02.
- Bytnerowicz A., Cayan D., Riggan P., Schilling S., Dawson P., Tyree M., Wolden L., Tissell R., and Preisler H. (2010) Analysis of the effects of combustion emissions and Santa Ana winds on ambient ozone during the October 2007 southern California wildfires. *Atmospheric Environment*, 44, 678-687, doi: 10.1016/j.atmosenv.2009.11.014.
- Camalier L., Cox W., and Dolwick P. (2007) The effects of meteorology on ozone in urban areas and their use in assessing ozone trends. *Atmospheric Environment*, 41, 7127-7137, doi: 10.1016/j.atmosenv.2007.04.061.
- Clark County Department of Air Quality (2019) Ozone Advance program progress report update. August.
- Clark County Department of Environment and Sustainability (2020) Revision to the Nevada state implementation plan for the 2015 Ozone NAAQS: emissions inventory and emissions statement requirements. September. Available at https://files.clarkcountynv.gov/clarknv/Environmental%20Sustainability/SIP%20Related%20Documents/O3/20200901_2015_O3%20EI-ES_SIP_FINAL.pdf?t=1617690564073&t=1617690564073.
- Code of Federal Regulations (1997) Title 40, Part 58, Appendix D. Network design for SLAMS, NAMS, and PAMS.
- Draxler R.R. (1991) The accuracy of trajectories during ANATEX calculated using dynamic model analyses versus rawinsonde observations. *Journal of Applied Meteorology*, 30, 1446-1467, doi: 10.1175/1520-0450(1991)030<1446:TAOTDA>2.0.CO;2, February 25. Available at <https://journals.ametsoc.org/doi/abs/10.1175/1520-0450%281991%29030%3C1446%3ATAOTDA%3E2.0.CO%3B2>.
- Finlayson-Pitts B.J. and Pitts Jr J.N. (1997) Tropospheric air pollution: Ozone, airborne toxics, polycyclic aromatic hydrocarbons, and particles. *Science*, 276, 1045-1051, (5315).
- Gong X., Kaulfus A., Nair U., and Jaffe D.A. (2017) Quantifying O₃ impacts in urban areas due to wildfires using a generalized additive model. *Environ. Sci. Technol.*, 51(22), 13216-13223, doi: 10.1021/acs.est.7b03130.

- Gong X., Hong S., and Jaffe D.A. (2018) Ozone in China: spatial distribution and leading meteorological factors controlling O₃ in 16 Chinese cities. *Aerosol and Air Quality Research*, 18(9), 2287-2300. Available at <http://dx.doi.org/10.4209/aaqr.2017.10.0368>.
- Hennigan C.J., Sullivan A.P., Collett J.L., Jr., and Robinson A.L. (2010) Levoglucosan stability in biomass burning particles exposed to hydroxyl radicals. *Geophysical Research Letters*, 37(L09806), doi: 10.1029/2010GL043088. Available at https://www.firescience.gov/projects/09-1-03-1/project/09-1-03-1_hennigan_et_al_grl_2010.pdf.
- Hoffmann D., Tilgner A., Iinuma Y., and Herrmann H. (2009) Atmospheric stability of levoglucosan: a detailed laboratory and modeling study. *Environ. Sci. Technol.*, 44, 694-699.
- Jaffe D., Chand D., Hafner W., Westerling A., and Spracklen D. (2008) Influence of fires on O₃ concentrations in the western U.S. *Environ. Sci. Technol.*, 42(16), 5885-5891, doi: 10.1021/es800084k.
- Jaffe D.A., Bertschi I., Jaegle L., Novelli P., Reid J.S., Tanimoto H., Vingarzan R., and Westphal D.L. (2004) Long-range transport of Siberian biomass burning emissions and impact on surface ozone in western North America. *Geophys. Res. Lett.*, 31(L16106).
- Jaffe D.A., Wigder N., Downey N., Pfister G., Boynard A., and Reid S.B. (2013) Impact of wildfires on ozone exceptional events in the western U.S. *Environ. Sci. Technol.*, 47(19), 11065-11072, doi: 10.1021/es402164f, October 1. Available at <http://pubs.acs.org/doi/abs/10.1021/es402164f>.
- Kimbrough S., Hays M., Preston B., Vallero D.A., and Hagler G.S.W. (2016) Episodic impacts from California wildfires identified in Las Vegas near-road air quality monitoring. *Environ. Sci. Technol.*, 50(1), 18-24. Available at <https://doi.org/10.1021/acs.est.5b05038>.
- Lai C., Liu Y., Ma J., Ma Q., and He H. (2014) Degradation kinetics of levoglucosan initiated by hydroxyl radical under different environmental conditions. *Atmospheric Environment*, 91, 32-39, doi: 10.1016/j.atmosenv.2014.03.054, 2014/07/01/. Available at <http://www.sciencedirect.com/science/article/pii/S1352231014002398>.
- Langford A.O., Senff C.J., Alvarez R.J., Brioude J., Cooper O.R., Holloway J.S., Lin M.Y., Marchbanks R.D., Pierce R.B., Sandberg S.P., Weickmann A.M., and Williams E.J. (2015) An overview of the 2013 Las Vegas Ozone Study (LVOS): impact of stratospheric intrusions and long-range transport on surface air quality. *Atmospheric Environment*, 109, 305-322, doi: 10.1016/j.atmosenv.2014.08.040, 2015/05/01/. Available at <http://www.sciencedirect.com/science/article/pii/S1352231014006426>.
- Louisiana Department of Environmental Quality (2018) Louisiana exceptional event of September 14, 2017: analysis of atmospheric processes associated with the ozone exceedance and supporting data. Report submitted to the U.S. EPA Region 6, Dallas, TX, March. Available at https://www.epa.gov/sites/production/files/2018-08/documents/ldeq_ee_demonstration_final_w_appendices.pdf.
- Lu X., Zhang L., Yue X., Zhang J., Jaffe D., Stohl A., Zhao Y., and Shao J. (2016) Wildfire influences on the variability and trend of summer surface ozone in the mountainous western United States. *Atmospheric Chemistry & Physics*, 16, 14687-14702, doi: 10.5194/acp-16-14687-2016.
- McClure C.D. and Jaffe D.A. (2018) Investigation of high ozone events due to wildfire smoke in an urban area. *Atmospheric Environment*, 194, 146-157, doi: 10.1016/j.atmosenv.2018.09.021, 2018/12/01/. Available at <http://www.sciencedirect.com/science/article/pii/S1352231018306137>.
- McVey A., Pernak R., Hegarty J., and Alvarado M. (2018) El Paso ozone and PM_{2.5} background and totals trend analysis. Final report prepared for the Texas Commission on Environmental Quality, Austin, Texas, by Atmospheric and Environmental Research, Inc., Lexington, MA, June. Available at <https://www.tceq.texas.gov/assets/public/implementation/air/am/contracts/reports/da/582188176307-20180629-aer-ElPasoOzonePMBBackgroundTotalsTrends.pdf>.
- Miller D., DeWinter J., and Reid S. (2014) Documentation of data portal and case study to support analysis of fire impacts on ground-level ozone concentrations. Technical memorandum prepared for the

- U.S. Environmental Protection Agency, Research Triangle Park, NC by Sonoma Technology, Inc., Petaluma, CA, STI-910507-6062, September 5.
- National Weather Service Forecast Office (2020) Las Vegas, NV: general climatic summary. Available at <https://www.wrh.noaa.gov/vef/lassum.php>.
- Pernak R., Alvarado M., Lonsdale C., Mountain M., Hegarty J., and Nehr Korn T. (2019) Forecasting surface O₃ in Texas urban areas using random forest and generalized additive models. *Aerosol and Air Quality Research*, 19, 2815-2826, doi: 10.4209/aaqr.2018.12.0464.
- Sacramento Metropolitan Air Quality Management District (2011) Exceptional events demonstration for 1-hour ozone exceedances in the Sacramento regional nonattainment area due to 2008 wildfires. Report to the U.S. Environmental Protection Agency, March 30.
- Simon H., Baker K.R., and Phillips S. (2012) Compilation and interpretation of photochemical model performance statistics published between 2006 and 2012. *Atmospheric Environment*, 61, 124-139, doi: 10.1016/j.atmosenv.2012.07.012.
- Simoneit B.R.T., Schauer J.J., Nolte C.G., Oros D.R., Elias V.O., Fraser M.P., Rogge W.F., and Cass G.R. (1999) Levoglucosan, a tracer for cellulose in biomass burning and atmospheric particles. *Atmospheric Environment*, 33, 173-182.
- Simoneit B.R.T. (2002) Biomass burning - a review of organic tracers for smoke from incomplete combustion. *Applied Geochemistry*, 17, 129-162.
- Solberg S., Walker S.-E., Schneider P., Guerreiro C., and Colette A. (2018) Discounting the effect of meteorology on trends in surface ozone: development of statistical tools. Technical paper by the European Topic Centre on Air Pollution and Climate Change Mitigation, Bilthoven, the Netherlands, ETC/ACM Technical Paper 2017/15, August. Available at https://www.eionet.europa.eu/etcs/etc-atni/products/etc-atni-reports/etcacm_tp_2017_15_discount_meteo_on_o3_trends.
- Solberg S., Walker S.-E., Guerreiro C., and Colette A. (2019) Statistical modelling for long-term trends of pollutants: use of a GAM model for the assessment of measurements of O₃, NO₂ and PM. Report by the European Topic Centre on Air pollution, transport, noise and industrial pollution, Kjeller, Norway, ETC/ATNI 2019/14, December. Available at <https://www.eionet.europa.eu/etcs/etc-atni/products/etc-atni-reports/etc-atni-report-14-2019-statistical-modelling-for-long-term-trends-of-pollutants-use-of-a-gam-model-for-the-assessment-of-measurements-of-o3-no2-and-pm-1>.
- Texas Commission on Environmental Quality (2021) Dallas-Fort Worth area exceptional event demonstration for ozone on August 16, 17, and 21, 2020. April. Available at <https://www.tceq.texas.gov/assets/public/airquality/airmod/docs/ozoneExceptionalEvent/2020-DFW-EE-Ozone.pdf>.
- U.S. Census Bureau (2010) State & County QuickFacts. Available at <http://quickfacts.census.gov/qfd/states/.html>.
- U.S. Environmental Protection Agency (2015) 40 CFR Part 50, Appendix U: interpretation of the primary and secondary National Ambient Air Quality Standards for ozone. Available at https://www.ecfr.gov/cgi-bin/text-idx?SID=43eb095cc6751633290941788ab4f3bd&mc=true&node=ap40.2.50_119.u.
- U.S. Environmental Protection Agency (2016) Guidance on the preparation of exceptional events demonstrations for wildfire events that may influence ozone concentrations. Final report, September. Available at www.epa.gov/sites/production/files/2016-09/documents/exceptional_events_guidance_9-16-16_final.pdf.
- U.S. Environmental Protection Agency (2020) Green Book: 8-hour ozone (2015) area information. Available at <https://www.epa.gov/green-book/green-book-8-hour-ozone-2015-area-information>.

- Wigder N.L., Jaffe D.A., and Saketa F.A. (2013) Ozone and particulate matter enhancements from regional wildfires observed at Mount Bachelor during 2004–2011. *Atmospheric Environment*, 75, 24–31, doi: 10.1016/j.atmosenv.2013.04.026, August. Available at <http://www.sciencedirect.com/science/article/pii/S1352231013002719>.
- Wood S. (2020) Mixed GAM computation vehicle with automatic smoothness estimation. Available at <https://cran.r-project.org/web/packages/mgcv/mgcv.pdf>.
- Wood S.N. (2017) *Generalized additive models: an introduction with R*, 2nd edition, CRC Press, Boca Raton, FL.
- Zhang L., Lin M., Langford A.O., Horowitz L.W., Senff C.J., Klovenski E., Wang Y., Alvarez R.J., II, Petropavlovskikh I., Cullis P., Sterling C.W., Peischl J., Ryerson T.B., Brown S.S., Decker Z.C.J., Kirgis G., and Conley S. (2020) Characterizing sources of high surface ozone events in the southwestern US with intensive field measurements and two global models. *Atmospheric Chemistry & Physics*, 20, 10379–10400, doi: 10.5194/acp-20-10379-2020. Available at <https://acp.copernicus.org/articles/20/10379/2020/acp-20-10379-2020.pdf>.